Journal of Advanced Ceramics
先进陶瓷
ISSN 2226-4108
CN 10-1154/TQ
清华大学出版社 Tsinghua University Press
SciOpen

J Adv Ceram 2026, **15**: 9221316

https://doi.org/10.26599/JAC.2026.9221316

Review

Advances in SiC aerogel materials for thermal insulation and electromagnetic wave absorption

Limeng Song[1], Feiyue Hu[2, *], Huagao Wang[3, *], Linan Wang[3], Yongqiang Chen[4, *], Haibin Wang[3], Dou Zhang[5], Xinglai Yuan[3, 4], Li Guan[1], Xiaoqin Guo[1], Kesong Yu[1], Duo Chen[1], Yabo Huang[1], Xinyue Zhang[1], Zhongyi Bai[1], Bozhen Song[1], Qilong Gao[6], Hailong Wang[4], Yanqiu Zhu[7], Rui Zhang[1, 3, 4, *], Bingbing Fan[4, *]

[1] *Henan Key Laboratory of Aeronautical Materials and Application Technology, Henan International Joint Laboratory of Aeronautical Function Materials and Advanced Processing Technology, School of Material Science and Engineering, Zhengzhou University of Aeronautics, Zhengzhou 450015, China*

[2] *State Key Laboratory of Engineering Materials for Major Infrastructure, School of Materials Science and Engineering, Southeast University, Nanjing 211189, China*

[3] *Institute of Advanced Ceramics, Henan Academy of Sciences, Zhengzhou 450046, PChina*

[4] *School of Materials Science and Engineering, Zhengzhou University, Zhengzhou 450001, China*

[5] *Department of Astronautical Science and Mechanics, Harbin Institute of Technology, Harbin 150001, China*

[6] *School of Physics, Zhengzhou University, Zhengzhou 450001, China*

[7] *Faculty of Environment, Science and Economy, University of Exeter, Exeter EX44QF, UK*

*Corresponding Authors:

E-mail: F. Hu, hufeiyue@seu.edu.cn;

H. Wang, huagaowang@163.com;

Y. Chen: chenyq@zzu.edu.cn;

R. Zhang: zhangray@zzu.edu.cn;

B. Fan: fanbingbing@zzu.edu.cn

Received: March 22, 2026; Revised: April 17, 2026; Accepted: May 2, 2026

清華大學出版社 Tsinghua University Press | SciOpen

Abstract

Silicon carbide (SiC) aerogels represent an emerging class of multifunctional materials that integrate a three-dimensional (3D) porous architecture with the intrinsically superior physicochemical properties, exhibiting considerable promise for thermal insulation and electromagnetic wave (EMW) absorption under extreme environments. This review systematically summarizes recent advances in the fabrication strategies, structure-property relationships, and functional performance of SiC aerogels. For thermal insulation, the highly porous framework effectively suppresses solid-state heat conduction and gas convection, while the wide bandgap semiconducting nature of SiC enables efficient thermal radiation attenuation, collectively ensuring excellent insulation stability at elevated temperatures. SiC aerogels deliver broadband and strong absorption through a combination of moderate electrical conductivity, abundant interfacial polarization, optimized impedance matching, and multiple scattering within the 3D porous network with respect to EMW absorption. Moreover, recent studies demonstrate that synergistic enhancement of thermal insulation and EMW absorption can be achieved via multicomponent compositional engineering, hierarchical structural design, and advanced fabrication techniques, thereby accelerating the deployment of SiC aerogels in frontier applications including aerospace, defense systems, and thermal management for emerging energy technologies.

Keywords: SiC aerogel; Thermal insulation; Electromagnetic wave absorption; Synergetic enhancement; Multifunctional integration

1. Introduction

The rapid advancement of frontier technologies such as aerospace, defense systems, and emerging energy platforms has generated an urgent demand for multifunctional materials capable of stable operation under extreme environments[1-5]. Among the key challenges, thermal management and electromagnetic wave (EMW) absorption are particularly critical. In application scenarios such as hypersonic vehicles, reusable spacecraft, and high-power-density electronic systems, materials are required to endure extreme aerodynamic heating or localized temperatures reaching several

thousand degrees Celsius, while also maintaining effective control over increasingly complex EMW environments[6, 7]. Conventional single-function materials are generally insufficient to meet the stringent requirements of functional integration, lightweight design, and long-term reliability. Aerogels, widely regarded as ultimate thermal insulation materials owing to their ultralow density and highly porous architectures, have therefore attracted considerable attention[8-10]. However, conventional oxide aerogels such as silicon dioxide (SiO_2) suffer from sintering and phase instability at elevated temperatures, whereas carbon-based aerogels exhibit inadequate oxidation resistance in oxygen-rich environments, which severely restricts their applicability under harsh conditions[11, 12]. To overcome these limitations, increasing research efforts have focused on silicon carbide (SiC), which is distinguished by outstanding thermal stability, robust mechanical properties, and unique semiconducting characteristics[13]. By integrating the intrinsic advantages of SiC with the three-dimensional (3D) nanoscale network characteristic of aerogels, a new class of porous solids known as SiC aerogels has emerged[14]. Rather than being merely porous SiC, these materials preserve and extend the essential features of aerogels and enable the integration of efficient thermal insulation with strong EMW absorption over a broad temperature window from ambient to ultra-high temperatures. Consequently, SiC aerogels represent a promising and rapidly developing direction in the interdisciplinary field of advanced ceramics and multifunctional porous materials[15, 16].

SiC aerogels exhibit a pronounced performance amplification that originates from the synergistic integration of intrinsic material characteristics and rational structural engineering. As an ultrahigh temperature ceramic, SiC possesses an exceptionally high melting point of approximately 2700°C and maintains structural stability above 1600°C in inert environments. Even under oxidative conditions, a dense and protective SiO_2 layer can form on the surface at temperatures between 1000 and 1200°C, thereby extending the maximum service temperature well beyond that of conventional SiO_2 aerogels, which is about 800°C, and carbon aerogels, which are limited to roughly 400°C in air[17-19]. In parallel, the continuous SiC framework endows the aerogel with markedly enhanced mechanical strength, elastic modulus, and fracture toughness,

effectively alleviating the intrinsic brittleness of oxide aerogels and improving operational reliability under severe thermal stresses[20]. Moreover, as a wide bandgap semiconductor, SiC introduces distinctive optoelectronic and thermal functionalities that further broaden its application potential[21]. Regarding thermal insulation, the 3D porous architecture of SiC aerogels effectively inhibits multiple heat transfer pathways. Nanoscale pores restrict the motion of gas molecules, thereby largely suppressing convective heat transfer in a manner similar to conventional aerogels. Meanwhile, the highly tortuous solid framework substantially hinders phonon transport, leading to a pronounced reduction in solid-state thermal conductivity (TC)[22]. At elevated temperatures above 800°C, where radiative heat transfer becomes dominant, the SiC framework itself functions as an intrinsic infrared attenuation network by strongly absorbing and scattering thermal radiation. This intrinsic radiative shielding capability enables excellent high temperature insulation without the incorporation of additional opacifying agents[23]. Beyond thermal management, SiC aerogels also display compelling EMW absorption behavior. The moderate electrical conductivity of semiconducting SiC resides in an optimal regime that enables effective electromagnetic coupling while simultaneously facilitating energy dissipation through conduction loss and interfacial polarization relaxation mechanisms[24]. The 3D porous architecture further amplifies these effects by improving impedance matching through graded pore structures, promoting wave penetration, and substantially extending propagation paths via multiple internal reflections and scattering. As a result, broadband and strong electromagnetic absorption can be achieved at ultralow densities[25, 26]. Collectively, these thermal insulation and electromagnetic attenuation mechanisms, which originate from porous networks and interfacial effects at the microstructural level, establish a robust physical foundation for the synergistic integration and simultaneous enhancement of both functionalities within a single lightweight material platform[27-29].

To realize these conceptual advantages in practical applications, extensive research has focused on the construction strategies, structural engineering, and property optimization of SiC aerogels. From a synthesis perspective, dominant approaches

include sol–gel processing coupled with carbothermal reduction, chemical vapor infiltration (CVI) or deposition, template-assisted fabrication, and precursor-derived conversion routes. These strategies are primarily aimed at establishing continuous, homogeneous, and nanoscale SiC skeletal networks that underpin multifunctional performance[30-32]. Recent researches have increasingly focused on the coordinated optimization of thermal insulation and EMW absorption through precise regulation of microstructural features and macroscopic architectures[33]. In the terms of thermal insulation, SiC based composite aerogels have been developed that combine ultralow TC with outstanding thermal stability across an exceptionally broad temperature range, from ambient conditions to 1800°C. This performance has been realized through structural design strategies including hierarchical pore architectures, biomimetic layered or interpenetrating network configurations, and the incorporation of high melting point secondary phases[34, 35]. Concurrently, continuous advances in mechanical reinforcement and multifunctional integration are accelerating the transition of these materials toward practical deployment under extreme environments[36]. In the field of EMW absorption, the incorporation of carbonaceous materials, two dimensional materials, magnetic components, or other ceramic phases into SiC allows effective regulation of the dielectric permittivity and magnetic permeability of the hybrid systems. Such compositional tuning facilitates the synergistic optimization of dielectric loss, magnetic loss, and impedance matching, which are essential for efficient electromagnetic attenuation[37-40]. Furthermore, rationally engineered core shell architectures, hollow configurations, and multidimensional ordered structures intensify loss mechanisms such as interfacial polarization and multiple internal reflections. As a result, these materials demonstrate efficient absorption and pronounced reflection loss (RL) within the X and Ku frequency bands[41, 42].

The growing demand for integrated thermal and electromagnetic protection has made SiC aerogels a focal point in the development of multifunctional materials that combine wave absorption with thermal insulation[43]. The underlying approach relies on exploiting a unified 3D porous nanonetwork that simultaneously serves as a platform

for suppressing heat transfer across solid, gas, and radiative pathways, while also enabling efficient dissipation of electromagnetic energy through impedance matching, multiple scattering, and interfacial polarization processes[44]. Recent studies demonstrate that lightweight multifunctional materials exhibiting both ultralow TC and ultrabroadband strong electromagnetic absorption can be realized through strategies such as constructing SiC at SiO_2 core shell nanocable architectures, designing biomimetic alternating multilayer structures, or incorporating magnetic nanoparticles to establish dielectric and magnetic synergistic networks[45-47]. Beyond intrinsic material integration, advanced macroscopic design strategies have enabled the spatial integration of multiple functionalities, including EMW absorption, thermal insulation, and low infrared emissivity. Representative examples include sandwich structured configurations and radar infrared compatible stealth metamaterials, which highlight substantial potential for application in high temperature thermal protection systems for stealth aircraft, as well as electromagnetic compatibility and thermal management in advanced electronic equipment[48, 49]. Although challenges persist in large scale fabrication, cost effectiveness, and long term environmental stability, SiC aerogels, owing to their highly tunable structures and properties, are emerging as a key materials platform for next generation multifunctional systems operating under extreme conditions[50].

Notably, although existing reviews have addressed SiC-based aerogels, a systematic and comprehensive evaluation of multifunctional composites that simultaneously integrate EMW absorption and thermal insulation remains lacking. To bridge this gap, as illustrated in Figure 1, this review systematically introduces the fundamental concepts of SiC aerogels and critically elucidates their underlying mechanisms for thermal insulation and EMW absorption. Emphasis is placed on recent advances, design strategies, and future development trends in thermal insulation, EMW absorption, and their integrated implementation, with the aim of providing a comprehensive reference for both fundamental research and practical applications in related fields.

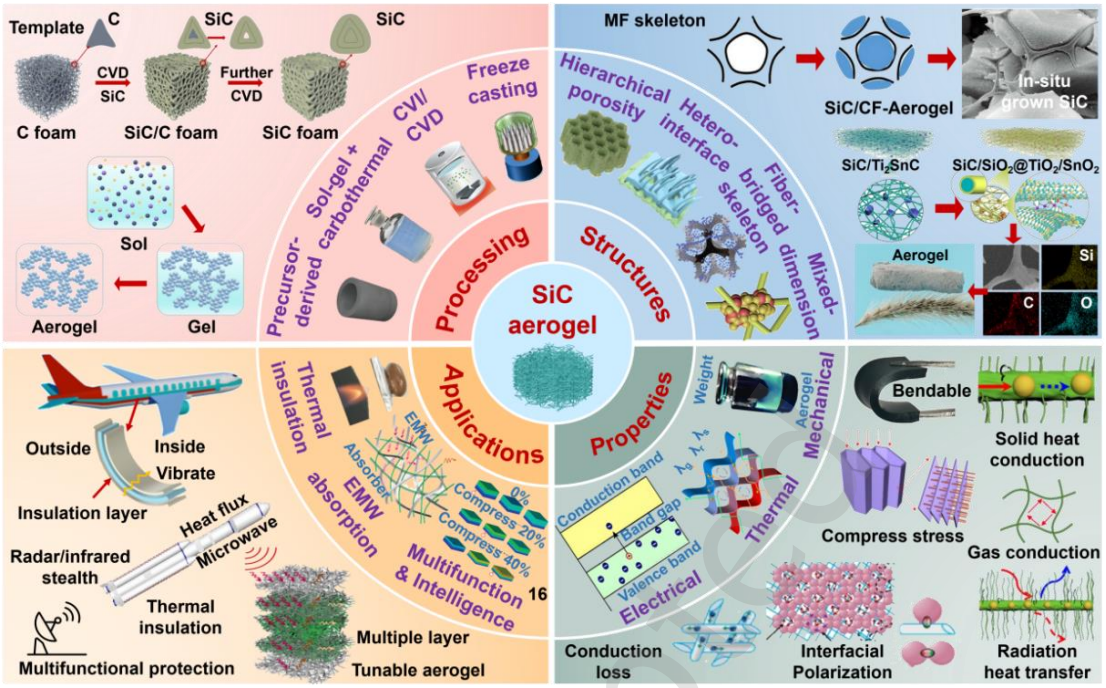

Figure 1. Schematic overview of the processing strategies, structural architectures, properties, and multifunctional application scenarios of SiC aerogels. Abbreviations: CVD: chemical vapor deposition; CVI: chemical vapor infiltration; EMW, electromagnetic wave; MF: melamine foam; CF: carbon foam. Parts of this Figure are reproduced or adapted from Refs.[9, 14, 16, 31, 34, 37, 40, 42, 43, 46]. Reproduced with permission:[9] Copyright 2025, American Chemical Society.[14] Copyright 2024, Elsevier.[16] Copyright 2022, Wiley-VCH.[31] Copyright 2019, Elsevier.[34] Copyright 2025, Elsevier.[37] Copyright 2017, American Chemical Society.[40] Copyright 2021, Springer Nature.[42] Copyright 2025, American Chemical Society.[43] Copyright 2025, Wiley-VCH.[46] Copyright 2025, Tsinghua University Press.

2. What is SiC aerogel?

Aerogels are widely regarded as the ultimate thermal insulation materials owing to their exceptionally low TC[51, 52], as illustrated in Figure 2a. Nevertheless, conventional oxide aerogels, such as SiO_2 and aluminum oxide (Al_2O_3), suffer from sintering, phase transitions, and structural shrinkage at elevated temperatures, which severely compromises their thermal insulation performance (Figure 2b)[53]. In contrast, carbon-based aerogels are prone to oxidation in oxygen rich environments, limiting their applicability under extreme conditions[54, 55]. To address these challenges,

increasing attention has been directed toward SiC, a material that combines the high temperature stability of ceramics with the functional characteristics of semiconductors, thereby enabling the emergence of SiC aerogels[56]. Distinct from merely porous SiC materials, SiC aerogels represent a new class of porous solids that retain the 3D nanoscale network architecture characteristic of traditional aerogels, with SiC constituting the primary skeletal framework (Figure 2c and 2d). Owing to this unique structural and compositional synergy, SiC aerogels exhibit significant promise as high efficiency thermal insulation materials (Figure 2e) and as advanced EMW absorbing materials (Figure 2f)[57].

2.1 The unique characteristics of SiC aerogels

The exceptional performance of SiC aerogels stems from the synergistic coupling between the intrinsic properties of SiC and their highly porous architecture, which enables functionalities that go beyond a simple additive combination of the two components. SiC is an ultrahigh-temperature ceramic characterized by an extremely high melting point of approximately 2700°C. It maintains structural and chemical stability at temperatures exceeding 1600°C in inert atmospheres and up to 1000 to 1200°C in air, where a dense and protective SiO_2 layer forms on the surface, as illustrated in Figure 2g and 2h[58]. This outstanding thermal stability enables SiC aerogels to operate in ultra-high temperature environments that are inaccessible to conventional SiO_2 aerogels, which typically fail above approximately 800°C, and carbon aerogels, which undergo rapid oxidation in air at around 400°C, as shown in Figure 2i and 2j[59]. In addition to their exceptional thermal resistance, SiC aerogels exhibit markedly improved mechanical performance compared with brittle oxide aerogels, as summarized in Table 1. The nanoscale SiC framework possesses a higher elastic modulus and fracture toughness, allowing the material to withstand larger mechanical loads and severe thermal stresses, as demonstrated in Figure 2k and 2l. As a result, SiC aerogels are less susceptible to pulverization and structural degradation, leading to enhanced durability and extended service lifetimes under extreme operating conditions[60]. Furthermore, SiC aerogels retain and even amplify the inherent thermal insulation characteristics of aerogels. Their nanoscale pore network effectively confines

gas molecules, nearly suppressing convective heat transfer and reducing gaseous TC to ultralow levels. At elevated temperatures above 800°C, radiative heat transfer becomes the dominant heat transport mechanism. Owing to its nature as a wide bandgap semiconductor, SiC exhibits strong absorption and scattering of infrared radiation, thereby functioning as an intrinsic and highly efficient radiative shielding medium, as shown in Figure 2m[61]. Consequently, unlike most oxide aerogels, SiC aerogels do not require additional incorporation of external shading agents. Their intrinsic composition and hierarchical nanostructure provide excellent high temperature radiation blocking capability, effectively suppressing radiative heat transfer under extreme thermal conditions[62].

Table 1. Comparison of mechanical properties for different types of SiC-based aerogel materials.

Aerogel Materials	**Additive**	**Structure**	**Mechanical properties**	**Ref.**
SiC	SiO_2	Dual-network	Compressive strength = 2551.5 kPa	[63]
SiC nanofibrous	---	Thin-wall network	Specific modulus = 13.2 $kN \cdot m \cdot Kg^{-1}$	[64]
C/SiC/SiBCN composite ceramic	PSNB	3D network	Compressive strength = 0.48 MPa	[65]
ZnO/SiC nanowire	PVA	3D layer	Compressive modulus = 565.9 MPa	[66]
SiC nanowire	SiO_2	Programmed geometries	Young's modulus = 5.8 MPa	[67]
Paraffin@SiC nanowire/ sheet	Paraffin	Dual nano-network	Maximum compression stress remained 508.34 kPa	[68]
SiC nanofiber	---	3D network	Young's modulus = 28.75 kPa	[69]
SiC-SiO_x nanowire	SiO_2/SiO	3D layer	Compressive stress = 1255 ± 116.3 kPa	[70]
SiC-CNT-SiC/ANF	ANF	3D layer	Compressive strength = 113.83 kPa	[71]
Super-elastic SiC	---	3D network	Maximum stress of 17.0 kPa at 80 % strain	[72]
SiC_{nw}/SiC_{nf} composite	SiO_2	Multi-scale	Retains 99% of its maximum	[73]

			stress after 100 cycles	
Carbonaceous SiC	CNTs	Core-shell	Young's modulus = 45.2 MPa	[74]

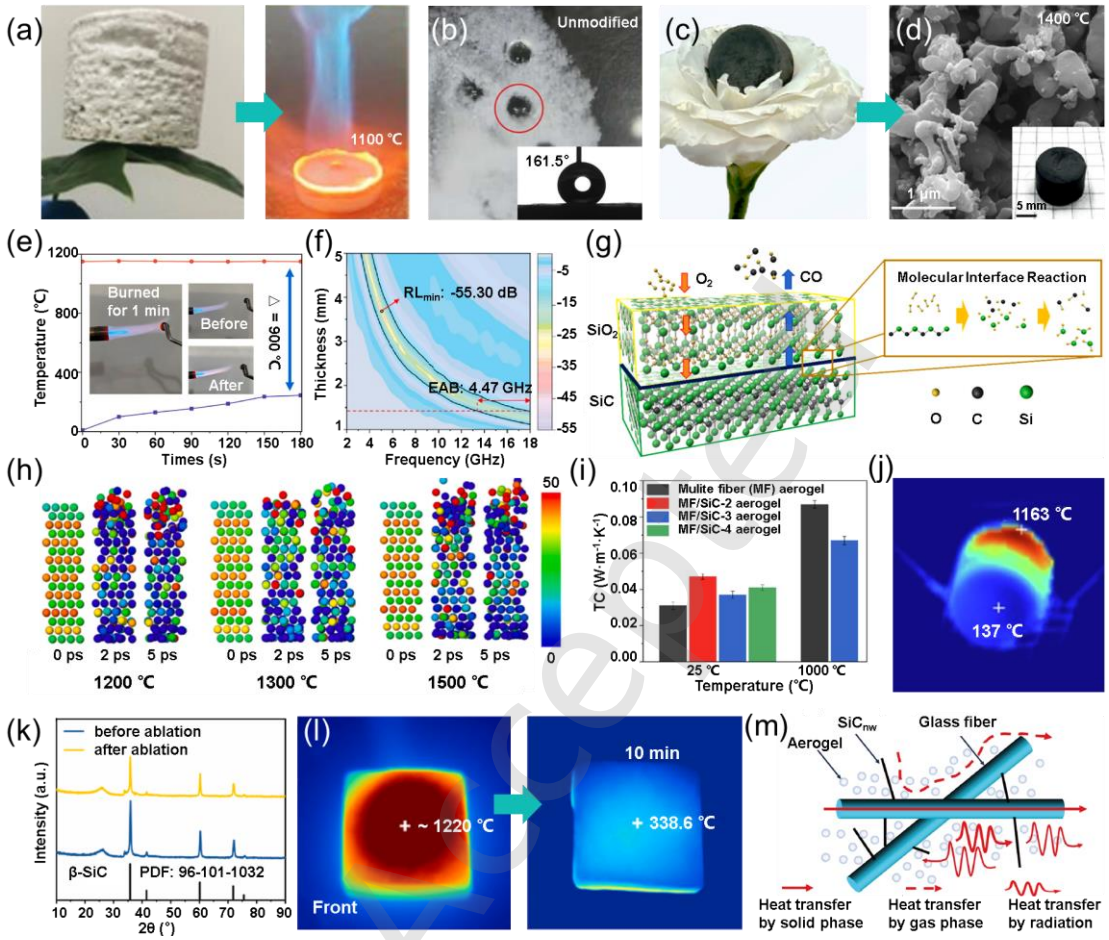

Figure 2. Structure, properties, and advantages of SiC aerogels. (a) Optical photograph of a dual-network nanofibrous-granular composite aerogel and its thermal insulation performance. Reproduced with permission.[51] Copyright 2024, Springer Nature. (b) Surface hydrophobic properties of SiO_2 aerogel powders. Reproduced with permission.[54] Copyright 2025, Elsevier. (c) Photographs of Fe_3Si-encapsulated SiC aerogels placed on a flower petal, (d) SEM and optical images, (e) Thermal insulation performance, and (f) EMW absorption performance of Fe_3Si-encapsulated SiC aerogels. Reproduced with permission.[57] Copyright 2026, Elsevier. (g) SiC oxidation and interfacial reaction processes, and (h) Cloud maps of the oxidation process at 1200℃, 1300℃, and 1400℃. Reproduced with permission.[58] Copyright 2025, Elsevier. (i) TC diagram, and (j) Infrared thermography of mullite fibers/SiC aerogel. Reproduced with permission.[59] Copyright 2025, Springer Nature. (k) XRD spectra of

CF@SiC/SiC_{nw} before and after high temperature ablation. (l) Infrared images obtained from the front and back side of CF@SiC/SiC_{nw} exposed to butane flames at varying durations. (k-l) Reproduced with permission.[60] Copyright 2025, Elsevier. m) Thermal insulation mechanism of a novel aerogel composite multiscale-reinforced by glass fiber felt with SiC_{nw} (AFS). Reproduced with permission.[61] Copyright 2023, Springer Nature.

2.2 Common methods for preparing SiC aerogels

Compared with conventional aerogels, the fabrication of SiC aerogels is considerably more challenging, primarily due to the difficulty in constructing a continuous, homogeneous, and nanoscale SiC framework. Among the various strategies reported to date, sol-gel processing coupled with carbothermal reduction has emerged as one of the most widely adopted and effective approaches. In this route, carbon and silicon containing organic precursors, such as resorcinol formaldehyde and silica sol or tailored organosilicon compounds, are employed to form a uniform organic inorganic hybrid gel via a sol gel reaction, as schematically illustrated in Figure 3a and 3b[75]. Following gelation, the liquid phase within the pore network is removed by freeze drying, as shown in Figure 3c and 3d[76], or by supercritical drying, as shown in Figure 3e[77]. These drying techniques effectively suppress capillary stresses and prevent collapse of the delicate pore structure, thereby yielding a highly porous precursor aerogel. The precursor is subsequently subjected to high temperature heat treatment in an inert atmosphere, typically argon, at temperatures of approximately 1200 to 1500°C. During this process, a carbothermal reduction reaction occurs between silica and carbon within the framework according to the reaction $SiO_2 + 3C \rightarrow SiC + 2CO$, leading to complete conversion of the aerogel skeleton into SiC, as depicted in Figure 3f[78]. Alternatively, SiC aerogels can be fabricated via a template assisted strategy. In this approach, a porous material with a 3D nanostructure serves as a sacrificial template, onto which a conformal SiC layer is deposited by CVI, as shown in Figure 3g. Subsequent removal of the template by chemical etching or thermal decomposition yields a SiC aerogel that faithfully replicates the original template architecture[79, 80]. In addition, commercially available SiC nanowires or nanoparticles may be directly

employed as building blocks. These nanoscale units are interconnected through physical or chemical cross linking to form a 3D network, followed by drying to obtain SiC aerogels, as shown in Figure 3h and 3i[81].

In summary, fabrication strategies for SiC aerogels exhibit distinct characteristics in structural controllability, processing complexity, and scalability. The sol–gel and carbothermal reduction method provides high compositional homogeneity and continuous frameworks but involves complex drying and high-temperature conversion processes. The templating method (e.g., CVI with template removal) enables improved control over pore architecture and structural replication, albeit with additional template-related steps. Additionally, assembly strategies based on SiC nanowires or nanoparticles offer simpler processing routes, while structural continuity and uniformity require further optimization. Therefore, the selection of fabrication strategy should be guided by specific application requirements. SiC-based aerogel materials obtained through these strategies consistently feature an ultra-low-density, highly interconnected 3D porous architecture, which constitutes their defining structural characteristic (Table 2). This fundamental architecture constitutes the physical basis for their exceptional performance, endowing the materials with ultralight weight, superior high-temperature thermal insulation, and effective microwave absorption capabilities.

Table 2. Comparison of density for different types of SiC-based aerogel materials.

Aerogel Materials	**Preparation methods**	**Forms**	**Density (mg/cm^3)**	**Ref.**
SiC@SiO_2 nanowire	Directional freeze casting	Monoblock	6.5	[81]
SiC nanowire	Template method	Monoblock	55 ± 5	[82]
SiC nanowire	CVD	Paper-like	~5	[83]
SiC foam	Template sacrifice method	Monoblock	26	[84]
Mullite fiber/SiC nanowire	Vacuum impregnation and high-temperature pyrolysis	Monolithic preform	220 ± 20	[85]
SiC whisker/mullite whisker/Al_2O_3	Vacuum freeze-drying	Monoblock	95	[86]
SiC nanowire/CNTs	Freeze-drying and heat treatment	Monoblock	4.9	[87]

SiC nanowire/SiOC composite	Sol-gel and high-temperature treatment	Monoblock	200	[88]
Nanowire-filled layered SiC	In situ transformation with induced growth	Layered structure	18.71	[89]
SiC/SiO_2 nanofibrous composite	Agarose-assisted directional freeze-drying	Biomimetic labyrinth-structure	5.66	[90]
SiC nanofibrous aerogels	CVD	Monoblock	4.2	[64]
SiC	Electrospinning and high-temperature treatment	Film	8	[91]

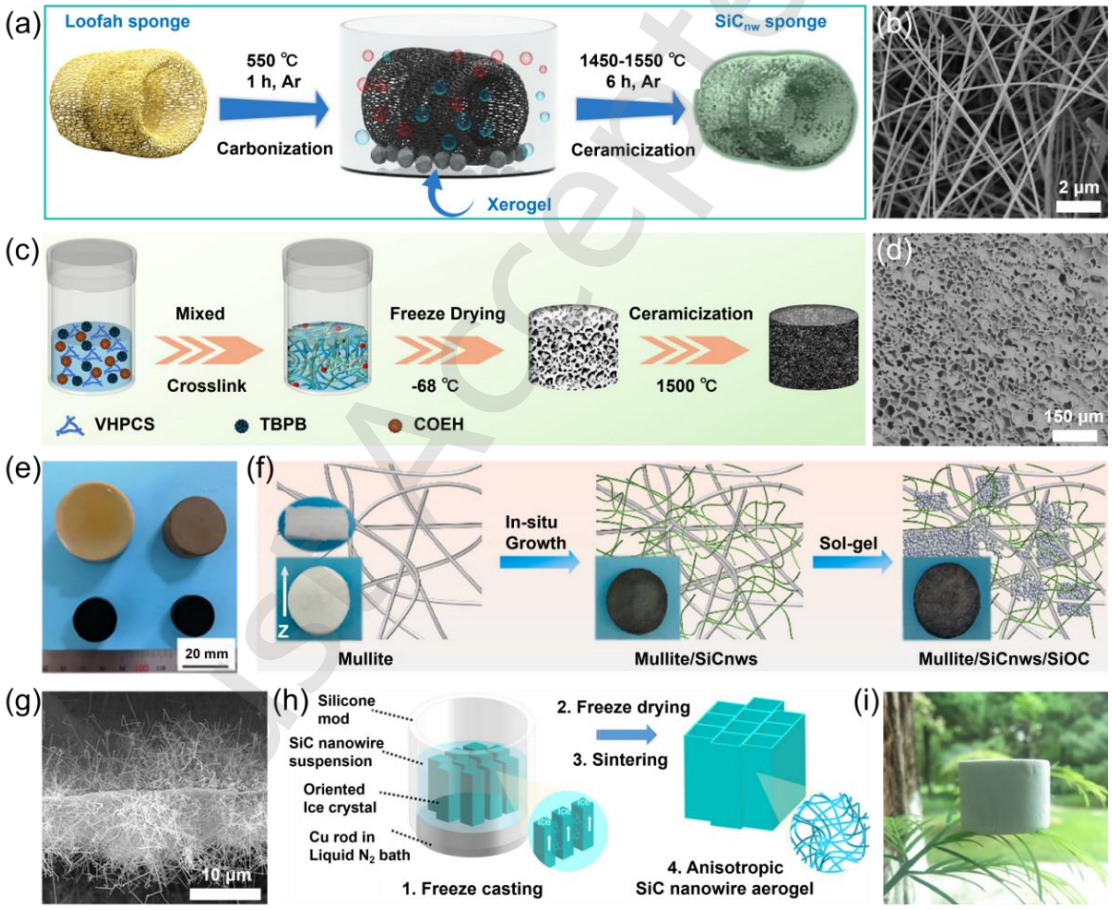

Figure 3. Fabrication strategies of SiC aerogels. (a) Schematic diagram of the preparation process, and (b) SEM image of single-crystal SiC_{nw} prepared from the natural loofah sponge by carbothermal reduction. Reproduced with permission.[75] Copyright 2023, American Chemical Society. (c) Preparation process, and (d) SEM image of SiC ceramic aerogel. Reproduced with permission.[76] Copyright 2025, American Chemical Society. (e) Photographs of aerogel composites at different stages:

wet gel, CF/SiO_2 aerogel, C/SiO_2/SiC aerogel, and SiC_w-C/SiO_2/SiC aerogel. Reproduced with permission.[77] Copyright 2019, Springer Nature. (f) Schematic showing the fabrication process of the mullite/SiC/SiOC composite aerogel. Reproduced with permission.[78] Copyright 2025, Elsevier. (g) SEM image of SiC nanowires grown on the surface of a graphene sheet in the SiC_{nw}/graphene aerogel. Reproduced with permission.[80] Copyright 2018, Elsevier. (h) Fabrication process, and (i) Photograph of a piece of the anisotropic and hierarchical SiC@SiO_2 nanowire aerogel with a volume of ~15 cm^3 standing on a leaf, indicating its ultralow density. Reproduced with permission.[81] Copyright 2020, American Association for the Advancement of Science's.

2.3 Applications and prospects of SiC aerogels

SiC aerogels exhibit remarkable application potential across a broad range of advanced technological and industrial domains due to its three dimensional porous architecture and the intrinsic excellence of SiC. This class of materials not only preserves the hallmark attributes of conventional aerogels, including ultralow density, high specific surface area, and low TC, but also integrates the outstanding high temperature oxidation resistance, chemical inertness, mechanical robustness, and favorable dielectric properties of SiC ceramics. The resulting synergy enables a substantial enhancement in both functionality and performance beyond that of traditional aerogel systems.

For aerospace and extreme thermal protection applications, SiC aerogels are widely recognized as promising candidates for next-generation thermal protection systems in hypersonic vehicles and reusable launch vehicles. As illustrated in Figure 4a and 4b[82], their nanoscale pore networks effectively suppress gaseous conduction and convection, endowing the materials with exceptional thermal insulation capability. Consequently, SiC aerogels can withstand severe aerodynamic heating exceeding 1000°C during atmospheric reentry while maintaining structural integrity, thereby providing reliable protection for critical components. In high temperature industrial energy conservation, SiC aerogels have been explored as advanced insulation materials for furnaces and kilns in sectors such as metallurgy, chemical processing, and glass

manufacturing(Figure 4c and 4d)[92]. Compared with conventional ceramic fiber insulation, SiC aerogels offer higher service temperature limits and lower heat loss, leading to markedly improved thermal efficiency, reduced energy consumption, and extended equipment lifetimes. These advantages directly support the green and low carbon transformation of industrial processes. SiC aerogels also demonstrate significant promise in nuclear energy systems, where materials must endure high temperatures and intense radiation fields. Their excellent thermal and structural stability enables their use as insulation components in advanced nuclear reactors, ensuring reliable operation under extreme conditions and contributing to enhanced safety and system reliability, as shown in Figures 4e-g[83]. In catalysis and chemical engineering, the high specific surface area and interconnected mesoporous and macroporous framework of SiC aerogels provide abundant and well dispersed anchoring sites for active species. Coupled with the superior chemical inertness and TC of SiC, these characteristics render SiC aerogels ideal catalyst supports for harsh reaction environments, including high temperature and corrosive conditions, thereby significantly improving catalytic activity and long term stability, as illustrated in Figures 4h-j[93].

Furthermore, SiC aerogels exhibit unique advantages in multifunctional composite materials. Their 3D porous network facilitates multiple reflections, scattering, and absorption of incident waves, which, when coupled with the tunable dielectric loss characteristics of SiC, enables efficient electromagnetic attenuation[94]. SiC aerogels can simultaneously achieve lightweight construction, high temperature resistance, thermal insulation, and EMW absorption, enabling integrated thermal management and wave absorption designs. Such multifunctionality meets the stringent demands of military and aerospace applications for stealth, thermal control, and electronic protection, as shown in Figures 4k-o[95]. In summary, SiC aerogels have evolved from simple super insulating materials into versatile multifunctional platforms tailored for extreme environments, with their application landscape continuing to expand toward increasingly demanding high technology fields.

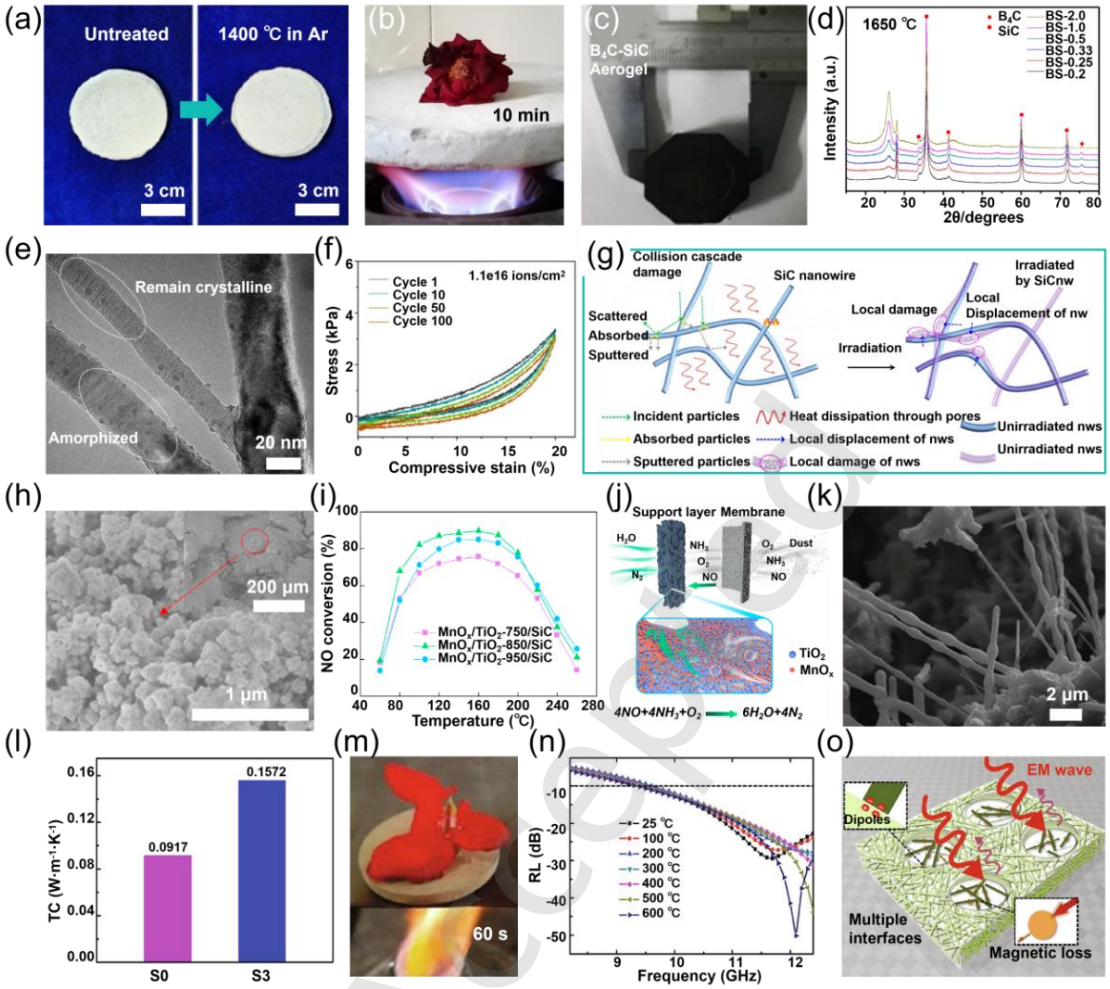

Figure 4. Applications and challenges of SiC aerogels. (a) Photographs of the SiC nanowire aerogel before and after heating at 1400°C, and (b) Evolution of a fresh petal heated by natural gas and protected by a piece of SiC nanowire aerogel. Reproduced with permission.[82] Copyright 2021, Elsevier. (c) Optical images, and (d) XRD patterns of B_4C-SiC aerogels heat-treated at 1650°C. Reproduced with permission.[92] Copyright 2021, Springer Nature. (e) Microstructural evolution of SiC nanowire aerogels under ion irradiation showing localized damage within specific regions of a nanowire. (f) Cyclic stress-strain curves at 20% strain for the irradiated SiC nanowire aerogel. g) Schematic illustration of the radiation resistance mechanism. (e-g) Reproduced with permission.[83] Copyright 2025, American Chemical Society. (h) SEM image, (i) NO conversion rate, and j) schematic diagram illustrating NO removal and dust filtration of the MnO_x/TiO_2/SiC catalytic membrane. Reproduced with permission.[93] Copyright 2020, Elsevier. (k) SEM image of binary porous SiC, (l) Thermal conductivities of the porous SiC skeleton and binary porous SiC, (m) Heat-

resistant properties, (n) RL versus frequency plots at the optimal thickness under different temperatures, and o) Schematic illustration of the EMW attenuation mechanism of binary porous SiC. Reproduced with permission.[95] Copyright 2020, Elsevier.

3. Thermal insulation mechanisms of SiC aerogel

SiC aerogels achieve outstanding thermal insulation through a synergistic combination of their hierarchical porous architecture and the intrinsically superior physicochemical properties. Rather than relying on a single dominant mechanism, thermal insulation in SiC aerogels is achieved through the simultaneous suppression of the three fundamental heat transfer pathways, namely solid-state thermal conduction, gaseous thermal convection, and thermal radiation. The deliberate construction of effective barriers along these pathways enables stable and efficient thermal insulation across an exceptionally wide temperature window, extending from ambient conditions to ultra-high temperatures, as illustrated in Figure 5a[84, 96]. From a mechanistic perspective, the thermal insulation behavior of SiC aerogels can be regarded as a multilevel protective framework composed of three mutually reinforcing defense layers against heat transport. This integrated strategy underpins their exceptional and durable insulation performance under extreme thermal environments.

3.1 Extreme weakening of solid-state thermal conduction in SiC aerogels

Solid-state thermal conduction describes heat transfer through the continuous solid framework of a material. In SiC aerogels, this pathway is effectively inhibited by a deliberately engineered nanoscale architecture. As a structural extension of conventional aerogels, SiC aerogels retain and further refine the characteristic 3D nanonetwork. Their skeletal framework consists of nanoscale SiC particles, fibers, or their hybrids, which assemble into a highly interconnected yet structurally disordered network with pronounced tortuosity, as shown in Figure 5b. During heat transport, phonons, which are the primary carriers of thermal energy in solids, are forced to propagate through elongated and highly convoluted pathways. This markedly increases the effective thermal resistance and substantially reduces the rate of heat conduction, as illustrated in Figure 5c[97]. Moreover, the junctions, often referred to as necks,

between adjacent SiC nano building blocks are typically narrow. These constricted contact regions introduce pronounced interfacial thermal resistance, further impeding phonon transport, as depicted in Figure 5d. At the nanoscale, phonon boundary scattering becomes increasingly dominant. The abundance of internal interfaces, including grain boundaries and particle boundaries, acts as efficient scattering centers that disrupt coherent phonon propagation and suppress directional heat flow, as shown in Figure 5e[98]. In addition, SiC aerogels typically exhibit porosities exceeding 95%, resulting in an extremely low volume fraction of solid material. Consequently, the continuous solid phase available for heat conduction is intrinsically limited. Although bulk SiC possesses high intrinsic TC, the contribution of solid-state heat conduction is reduced to a minimal level within this highly porous and sparsely connected nanostructure.

3.2 Gas thermal convection almost completely suppressed in SiC aerogel

Gaseous heat transfer comprises both thermal conduction mediated by gas molecules and convective heat transport associated with macroscopic gas flow. In SiC aerogels, this heat transfer pathway is effectively suppressed by the characteristic nanoscale pore architecture, as illustrated in Figure 5f. The pore diameters of SiC aerogels are predominantly distributed in the range of 2 to 100 nm, with a large fraction of pores smaller than the mean free path of air molecules under ambient pressure, which is approximately 70 nm[99]. Under these conditions, gas transport within the pores enters the Knudsen diffusion regime, in which gas molecules collide with the pore walls far more frequently than with neighboring molecules. As a result, energy transfer via intermolecular collisions is severely hindered, leading to a pronounced reduction in gaseous TC. Simultaneously, the extremely small pore dimensions prevent the formation of continuous gas pathways required for macroscopic convection. The gas phase is effectively partitioned into numerous isolated nanoscale cavities, thereby losing its ability to transport heat through bulk flow, as schematically shown in Figure 5g and 5h[100]. Consequently, SiC aerogels exhibit a gaseous heat transfer behavior analogous to that of a vacuum environment under atmospheric conditions, yet without the need for vacuum encapsulation. This unique feature endows the material with highly

stable and reliable thermal insulation performance across a wide range of operating environments.

3.3 SiC efficient intrinsic thermal radiation shielding

At ambient temperatures exceeding 800 °C, thermal radiation becomes the dominant mode of heat transfer. Infrared radiation can penetrate conventional materials, directly transporting thermal energy, which is a primary factor underlying the performance degradation of traditional insulation systems. SiC aerogels, however, are particularly effective in mitigating radiative heat transfer. The electronic structure of SiC confers strong absorption and scattering capabilities for specific infrared wavelengths, as shown in Figure 5i[85]. At the microscopic level, the infrared attenuation of SiC at elevated temperatures originates from multiple intrinsic mechanisms, including thermally activated free carrier absorption, multi-phonon scattering, and defect-state related electronic transitions, which collectively provide fundamental absorption channels for infrared energy dissipation. Notably, these absorption bands coincide with the peak emission region of thermal radiation from high-temperature objects. Consequently, the SiC aerogel framework functions as an intrinsically distributed "built-in shading network". Incoming infrared radiation is repeatedly absorbed, scattered, and partially re-emitted by the nanostructured framework. The energy of the radiation is effectively attenuated and trapped within the porous network and is eventually dissipated through the highly inefficient solid-state conduction pathways, as illustrated in Figures 5j-l[86]. This intrinsic radiative shielding obviates the need for additional scattering or shading agents, such as carbon black or titanium dioxide, which are typically required in oxide aerogels (Figure 5m)[101]. Moreover, when the characteristic dimensions of the aerogel's nanoscale framework and pores are comparable to infrared wavelengths, pronounced Mie scattering is induced. Building on this size-matching effect, the multiscale pore structure further promotes multiple scattering and reflections, thereby enhancing the attenuation and redistribution of thermal radiation and ultimately suppressing radiative heat transfer[102].

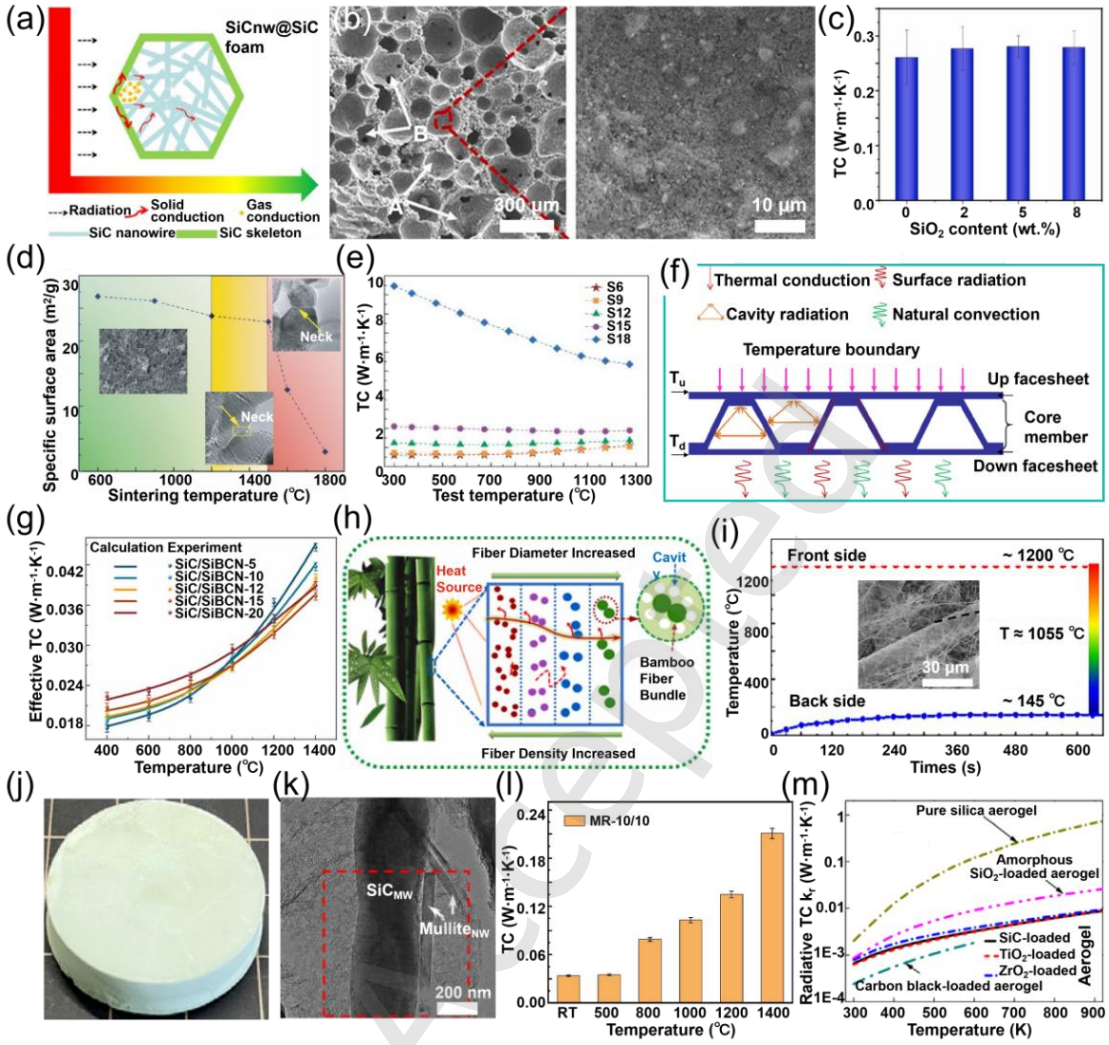

Figure 5. Thermal insulation mechanisms of SiC aerogels. (a) Schematic diagram of the heat insulation mechanism for the SiC_{nw}@SiC foam. Reproduced with permission.[84] Copyright 2021, American Chemical Society. (b) SEM images of the SiC_b-ZrB_2 porous ceramics prepared at 1573 K/3 h with 5 wt.% content, and (c) TC of SiC_b-ZrB_2 porous ceramics depending on SiO_2 content. Reproduced with permission.[97] Copyright 2023, Elsevier.(d) BET surface area of porous SiC ceramics as a function of sintering temperature, with inset images corresponding to SEM and TEM micrographs, and (e) thermal conductivities of porous nano-SiC at elevated temperatures. Reproduced with permission.[98] Copyright 2016, Taylor & Francis. (f) Radiative heat transfer from up facesheet to down facesheet of C/SiC composite corrugated lattice core sandwich panel. Reproduced with permission.[99] Copyright 2021, Elsevier.(g) Effective TC of SiC/SiBCN ceramic hybrid aerogel, and (h)

Schematic diagram of the thermal insulation mechanism of a bamboo-like structure. Reproduced with permission.[100] Copyright 2023, Elsevier. (i) The highest backside temperature of mullite fiber/SiC nanowire composite aerogels during the heating process, with inset SEM image. Reproduced with permission.[85] Copyright 2022, MDPI. (j) Photograph, and (k) TEM image, and (l) High temperature TC of the bimodal-scale whisker-reinforced alumina (SiC_{MW}/$Mullite_{NW}$/Al_2O_3) aerogel sample prepared via a VFD method: reinforced with 10 wt.% of Mullite (MR-10/10). Reproduced with permission.[86] Copyright 2025, Wiley-VCH. (m) Effects of the opacifier type on the radiative TC: same opacifier volume fraction. Reproduced with permission.[102] Copyright 2013, Elsevier.

4. EMW absorption mechanisms of SiC aerogel

SiC aerogels, as an emerging multifunctional material, have demonstrated significant potential in EMW absorption applications, as illustrated in Figures 6a-c[87, 103]. Fundamentally, their absorption performance originates from the synergistic interplay between impedance matching and multiple loss mechanisms, where appropriate matching ensures efficient incident wave coupling, while various dissipation pathways dominate energy attenuation. The absorption mechanism is not governed by a single process but arises from the synergistic interplay between the intrinsic semiconductor properties of SiC and its 3D porous network, which collectively form an effective “energy trap” capable of capturing and dissipating incident electromagnetic radiation, as shown in Figure 6d[88]. Fundamentally, this process involves the conversion of EMW energy into other energy forms, predominantly thermal energy, through multiple physical pathways, followed by its gradual dissipation within the aerogel framework, as schematically depicted in Figure 6e[104].

4.1 SiC semiconductor intrinsic dielectric loss

The intrinsic electrical properties of SiC form the fundamental basis for its EMW absorption performance. SiC is a wide-bandgap semiconductor with electrical conductivity intermediate between that of a conductor and an insulator. This moderate electrical conductivity is pivotal to efficient EMW absorption. Upon irradiation, incident EMW induce localized microcurrents within the interconnected SiC network,

thereby promoting effective electromagnetic energy dissipation. Owing to its inherent electrical resistance, these currents dissipate energy according to Joule's law, converting incident electromagnetic energy into heat, this mechanism referred to as conductive loss, as illustrated in Figure 6f[105]. By contrast, a perfect conductor would reflect incident waves entirely, whereas a perfect insulator would generate negligible currents[106]. The semiconductor nature of SiC thus positions it in an optimal regime for simultaneously coupling electromagnetic energy into the material and efficiently dissipating it, as shown in Figures 6g and 6h[107]. In addition, the nanoscale architecture of SiC aerogels, along with inherent structural defects, impurities, and dangling bonds, provides abundant trapping sites for charge carriers. Under an alternating electromagnetic field, these bound charges undergo delayed rearrangement and migration in response to the field, producing a hysteresis effect known as interfacial polarization, or Maxwell-Wagner polarization, as depicted in Figures 6i and 6j. The subsequent relaxation of this polarization process effectively dissipates electromagnetic energy, a mechanism termed relaxation loss[108]. The extremely high specific surface area of SiC aerogels further amplifies this effect by generating a vast network of interfaces and active sites (Table 3), thereby enhancing the overall EMW attenuation capability.

Table 3. Specific surface areas of different types of SiC-based aerogel materials.

Aerogel Materials	**Microstructure types**	**Forms**	**Specific surface areas (m^2/g)**	**Ref.**
B_4C-SiC composite	Nanoparticles	Monoblock	692.81	[92]
SiC/SiBCN ceramic hybrid	Nanofibers	3D layer	380	[100]
Nanowire-filled layered SiC	Nanowires	3D layer	16.3	[89]
SiC nanofiber composite	Nanofibers	3D layer	12.74	[109]
SiCBN/SiC aerogel	Nanoparticles	Monoblock	292.56	[110]
SiC-SiO_x nanowire	Nanowires	Paper-like	29.1	[70]
SiC/C	Nanoparticles and nanowires	Monoblock	1155.01	[111]

SiC/HfC composite	Nanoparticles	Monoblock	279.75	[112]
SiC nanofiber aerogel	Nanofibers	Paper-like	17.58	[113]
SiC@SiO_2 nanofiber	Nanofibers	Paper-like	185.3	[114]
Coral-like SiC aerogel	Nanoparticles	Powder	1099	[115]
ZrO_2-interface-engineered SiC nanofiber	Hybrid nanofibers	Fiber mat	70.3	[116]
SiC	Nanosheets	3D network	135.2	[117]
SiC/SiO_2 composite foam	Nanoparticles and nanofibers	Monoblock	81.125	[118]
SiC	Hollow microtubes	3D network	11.9234	[119]

4.2 Synergistic enhancement of EMW absorption by 3D porous networks

If the intrinsic properties of SiC are considered the "active ingredient" for EMW absorption, then the 3D porous architecture of the aerogel serves as an "efficient delivery system", significantly enhancing its absorption performance[120]. Upon transitioning from free space into an absorbing medium, EMW experiences an abrupt discontinuity in wave impedance. This mismatch at the interface leads to substantial reflection of the incident waves, thereby hindering their penetration into the material and limiting subsequent energy dissipation[121]. SiC aerogels exhibit a continuous variation in porosity and density from the surface to the interior. Their macroscopic structure can be regarded as a continuous gradient layer, transitioning from air with an impedance of approximately 1 to dense SiC with a much lower impedance, as shown in Figure 6k[122]. This gradient enables EMW to enter the material gradually rather than being abruptly reflected at the surface, thereby improving the incidence efficiency and creating favorable conditions for subsequent energy absorption. This process is analogous to light slowly penetrating the deep ocean rather than being reflected at the water surface.

Once inside the aerogel, incident EMW undergo numerous scattering, refraction, and reflection events within the complex 3D nano-network framework. This structure forms an "optical labyrinth", which greatly extends the propagation path of the waves

within the material, as illustrated in Figure 6l[123]. The extended propagation path increases the number of interactions and the duration of contact between the waves and the SiC framework, allowing the energy to be repeatedly and efficiently dissipated[124]. In contrast, conventional high-performance wave-absorbing materials such as ferrites are often dense and heavy, which limits their application in weight-sensitive fields including aerospace[125]. SiC aerogels, by virtue of their extremely high porosity, function as ultralightweight absorbers. Through careful optimization of their structural and compositional features, they achieve excellent EMW absorption at very low density, thus realizing a combination of lightweight and high-performance properties, as shown in Figures 6m and 6n[126].

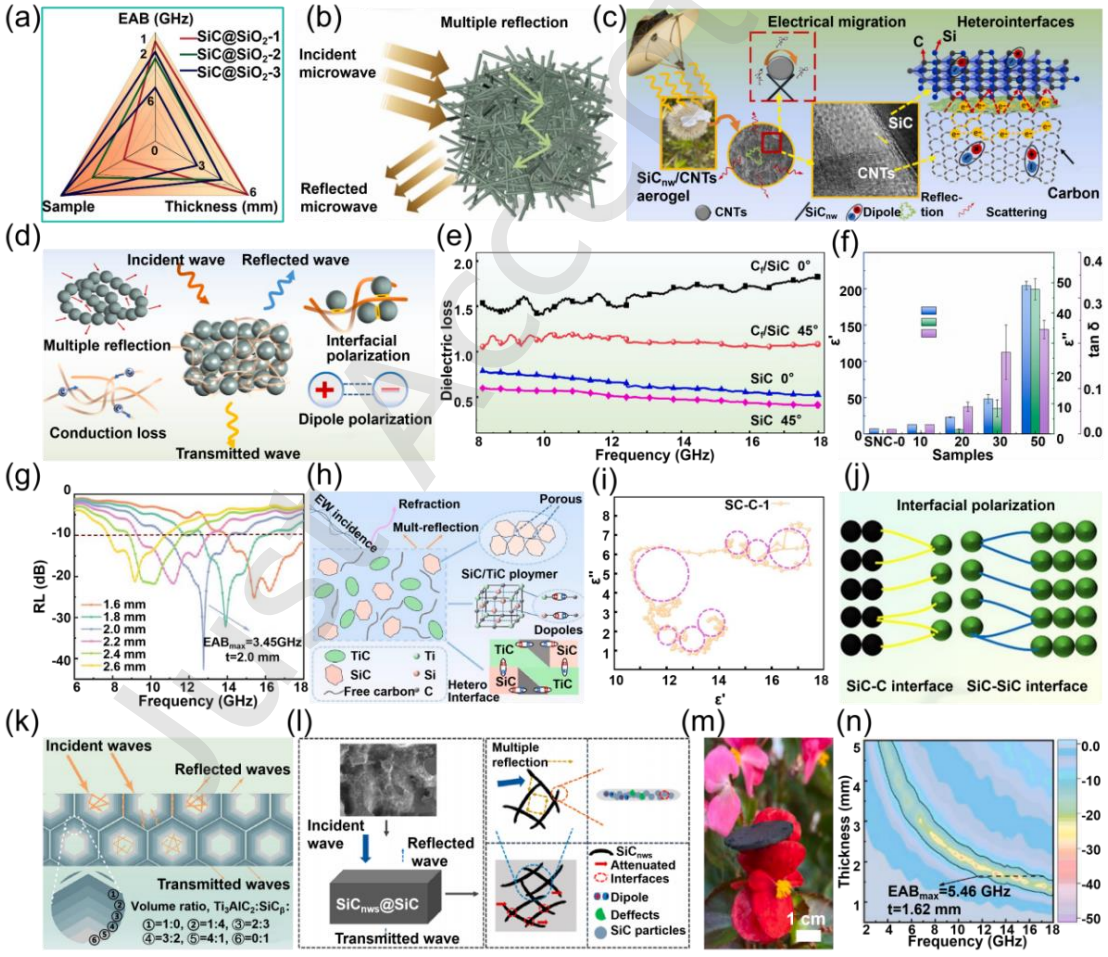

Figure 6. EMW absorption mechanisms of SiC aerogels. (a) Comparison of EAB for SiC@SiO_2-1200-0.5 nanocomposites with different filling contents, and (b) EMW absorption mechanism for SiC@SiO_2 nanocomposites. Reproduced with permission.[103] Copyright 2024, Elsevier. (c) Schematic of the microwave dissipation

mechanism of SiC_{nws}/CNTs aerogels. Reproduced with permission.[87] Copyright 2024, Elsevier. (d) Schematic illustration of EMW absorption mechanisms for SiC_{nw}/SiOC composite aerogel. Reproduced with permission.[88] Copyright 2024, Elsevier. (e) The dielectric loss of C_f/SiC composite and SiC microtube ceramic. Reproduced with permission.[104] Copyright 2024, Elsevier. (f) The mean electromagnetic parameter of the Si_3N_4/SiC composite ceramics in the X-band. Reproduced with permission.[105] Copyright 2025, Elsevier. (g) Minimum RL plots at different thicknesses, and (h) EMW absorption mechanism of SiC/TiC ceramics. Reproduced with permission.[107] Copyright 2025, Elsevier. (i) Cole-Cole curve, and (j) EMW absorption mechanism diagram of porous SiC/C composite. Reproduced with permission.[108] Copyright 2025, Elsevier. (k) Schematic representation of the EMW shielding mechanism of porous gradient composites. Reproduced with permission.[122] Copyright 2023, American Chemical Society. (l) EMW absorption mechanism of SiC_{nws}@SiC composite ceramics. Reproduced with permission.[123] Copyright 2025, MDPI. m) Optical photograph, and (n) EMW absorption properties at different thicknesses of SiC nanowires-carbon composite. Reproduced with permission.[126] Copyright 2025, Elsevier.

4.3 Designability and synergistic strategies of SiC aerogels

As a class of advanced porous ceramics, the EMW performance of SiC aerogels is inherently tunable, stemming from the highly synergistic and tailorable coupling among their composition, structural characteristics, and dielectric properties. As shown in Figures 7a-d, precise control over the intrinsic electrical properties of the SiC lattice can be achieved through atomic-level doping, such as the introduction of elements including nitrogen and aluminum. Doping not only modifies crystallinity and defect types but also effectively regulates carrier concentration, positioning the material's conductivity within an optimal range that enhances dielectric loss and impedance matching. This, in turn, promotes strong polarization relaxation and conductive loss within specific frequency bands, thereby increasing absorption intensity[127-129].

Furthermore, constructing multi-component heterogeneous composites enables significant enhancement in performance and strategic extension of the absorption

frequency range. Combining SiC aerogels with carbon materials or dielectric and magnetic nanoparticles generates a high density of nanoscale interfaces and barriers at heterogeneous boundaries, as illustrated in Figures 7e-g. These interfaces serve as multiple scattering centers for EMW and simultaneously induce pronounced interfacial polarization. Under an alternating electromagnetic field, accumulated space charges at these heterogeneous interfaces undergo periodic rearrangement and relaxation, dissipating substantial electromagnetic energy. Additionally, synergistic loss mechanisms can arise between different components, providing complementary and enhanced dielectric and magnetic loss capabilities[130-132].

The central merit of this synergistic strategy is that it enables coordinated regulation of the complex permittivity and permeability, thereby improving impedance matching and promoting the transmission of EMW into the material instead of being reflected at the interface. Simultaneously, the coupling of multiple loss mechanisms effectively broadens the absorption frequency range, particularly extending performance into the low-frequency region. This addresses the critical requirements of modern stealth technologies for electromagnetic absorbers that are thin, lightweight, wide-band, and highly efficient. Consequently, the designable SiC aerogel framework, when combined with multi-component composite strategies and interface engineering, provides a versatile platform for developing the next generation of high-performance, wide-band EMW absorbing materials.

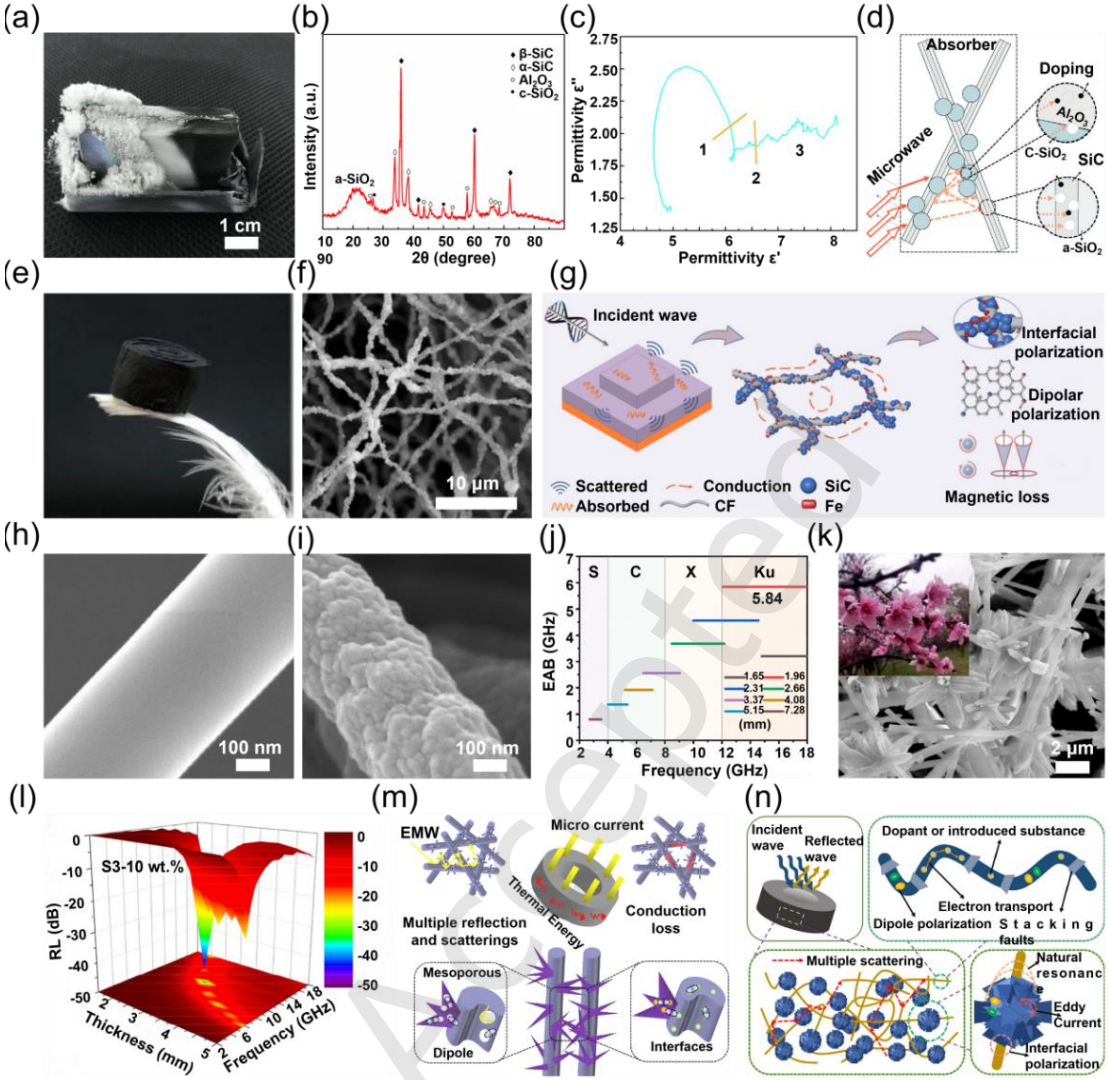

Figure 7. Designable EMW absorption strategies of SiC aerogels. (a) The photograph, and b) XRD pattern, (c) Typical Cole-Cole semicircle, and (d) Schematic representation of microwave absorbing mechanism of nitrogen and aluminum co-doped SiC@SiO_2 core-shell nanowires. Reproduced with permission.[128] Copyright 2020, Wiley-VCH. (e) Photograph, (f) SEM image, and (g) Schematic diagram of microwave dissipation mechanism of the Fe/SiC-C fibrous metastructure. Reproduced with permission.[129] Copyright 2023, Elsevier. SEM images of (h) SiC/C-0 NFs, (i) SiC/C-1 NFs. (j) EAB at different thickness of SiC/C-1 NFs/paraffin. h-j) Reproduced with permission.[130] Copyright 2025, Elsevier. (k) SEM images, (l) RL value 3D maps, and m) Schematic diagram of the microwave absorption mechanism of the flower branch-like TiO_2@SiC/C nanofibers. Reproduced with permission.[131] Copyright 2021, Elsevier. (n) Schematic illustration of the EMW absorption mechanism of flower-like Ni/SiC

nanowires. Reproduced with permission.[132] Copyright 2023, Elsevier.

5. Research progress of thermal insulation and EMW absorption for SiC aerogel materials

5.1 Research status of SiC aerogel materials in thermal insulation

5.1.1 SiC aerogel microstructure design and thermal insulation performance

The exceptional thermal insulation performance of ceramic aerogels originates from their highly tailorable microstructures. Through precise control over pore architecture, interfacial characteristics, and characteristic length scales, the three fundamental heat transfer pathways, namely solid phase heat conduction, gas phase conduction, and radiative heat transfer, can be effectively suppressed. Extensive studies have demonstrated that the construction of hierarchical pore structures represents one of the most effective strategies for achieving ultra-low TC. As shown in Figure 8a, a ZrC/SiBCN aerogel exhibits an extremely low TC of 0.024 W/(m·K) at room temperature (Figure 8b), which is attributed to its well-defined hierarchical pore network comprising micropores, mesopores, and macropores, together with an ultrahigh porosity of up to 97.5%. More importantly, the in situ formed ZrC@SiC core shell structure effectively suppresses SiC grain growth at elevated temperatures, enabling the aerogel to maintain structural integrity after extreme heat treatment at 1800°C, with only a slight increase in TC to 0.029 W/(m·K)[133]. It should also be noted that under long-term high-temperature exposure, SiC aerogels may undergo grain coarsening, pore structure collapse, and interfacial degradation, which can gradually deteriorate their properties. Therefore, enhancing interfacial stability and structural robustness is critical for ensuring long-term service reliability under extreme environments. A similar structure driven thermal insulation mechanism is observed in hollow porous MHP-SiC-CA ceramic fiber aerogels fabricated via electrospinning. As illustrated in Figure 8c, the presence of dense circular and spindle shaped surface pores significantly enhances resistance to thermal shrinkage. The enlarged gas solid interfacial area promotes multiple reflection and refraction of thermal radiation, while the hollow fiber architecture and internal nanopores synergistically suppress solid phase heat conduction and gas convection. Consequently, the aerogel maintains ultra low TC

and excellent thermal stability even at 1300°C[134]. Furthermore, layered SiC aerogels reinforced with nanowires, as shown in Figure 8d, exhibit a TC as low as 0.023 W/(m·K) in the direction perpendicular to the layered structure at room temperature, which is lower than that of static air. This outstanding performance arises from the cooperative effects of the layered framework and the embedded nanowires, which collectively inhibit solid phase heat conduction, gas phase heat conduction, and radiative heat transfer[89].

From the standpoint of compositional engineering and heterogeneous interface design, the intentional incorporation of multiple constituents to construct diverse interfaces has become an effective strategy for further improving high-temperature stability and thermal insulation performance. A biomimetic maze structure reinforced SiO_2 nanofiber aerogel incorporating SiC whiskers was fabricated via agar assisted directional freeze drying, as shown in Figure 8e and 8f. This aerogel exhibits an ultralow TC of 0.0208 W/(m·K) at 25°C and 0.0633 W/(m·K) at 800°C. Notably, after calcination in a butane flame at 1050°C for 60 minutes, a temperature difference as high as 991°C is achieved between the hot and cold surfaces, while the overall structure remains intact, demonstrating excellent thermal shielding capability and structural robustness (Figure 8g)[90]. Similarly, as illustrated in Figure 8h, a SiC/SiO_2 composite aerogel with an interpenetrating double network architecture exhibits a low TC of 0.023 W/(m·K) at room temperature and 0.08 W/(m·K) at 1000°C. Under flame heating at 1100°C, a temperature difference approaching 1000°C is observed across a 1 cm thick sample, highlighting its outstanding thermal insulation efficiency under extreme conditions[63]. In addition, for CF-SC aerogels, the SiC content increases markedly with increasing sintering temperature, which effectively enhances the thermal stability of the material. Combined with a typical porous architecture and an ultralow density of 0.027 g/cm^3, this aerogel exhibits favorable thermal insulation performance[135].

The construction of 3D networks based on nanofibers and nanowires represents another important strategy for advancing the thermal insulation performance of ceramic aerogels. By engineering a SiBCN@SiC dual network architecture, the thermal insulation capability of ceramic composite aerogels is markedly enhanced. The

resulting material exhibits a room temperature TC as low as 0.0316 W/(m·K), which is attributed to the synergistic coupling between the 3D porous SiC fiber skeleton and the infiltrated SiBCN aerogel matrix (Figure 8i). This interconnected architecture effectively suppresses solid phase heat conduction and convective heat transfer[136]. In a representative example, a SiC nanofiber aerogel prepared using melamine foam as a sacrificial template exhibits an ultralow density of 4.2 mg/cm^3 and a room-temperature TC as low as 0.0213 W/(m·K). The highly porous architecture, coupled with a continuous nanofiber network, effectively suppresses heat transfer, thereby conferring outstanding thermal insulation performance (Figure 8j)[64]. Furthermore, 3D network SiC/Si_3N_4 nanowire aerogels demonstrate outstanding thermal insulation characteristics. Owing to their ultrahigh porosity of up to 99.79% and a hierarchical porous architecture formed by interwoven nanowires, these aerogels exhibit a TC as low as 0.02319 W/(m·K) (Figure 8k). Notably, the material is capable of maintaining a back surface temperature of approximately 200°C under an external temperature as high as 1088°C, underscoring its exceptional thermal shielding capability[137].

In addition, specially engineered 3D network architectures exhibit distinct advantages in thermal insulation performance. The C/SiC/SiBCN composite ceramic aerogel displays a TC as low as 0.049 W/(m·K). This low value primarily originates from the internal 3D porous network (Figure 8l and 8m), which effectively suppresses heat conduction and convective heat transfer[65]. Similarly, a ZnO/SiC_{nw} aerogel fabricated via a combination of hydrolysis reaction and directional solidification followed by thermal annealing exhibits an ultralow density of only 0.167 g/cm^3 and a room temperature TC of 0.056 W/(m·K) (Figure 8n)[66]. Furthermore, the SiC/PTFE/SiO_2 aerogel composite prepared by the sol gel method and atmospheric pressure drying demonstrates excellent thermal insulation capability, with a TC as low as 0.052 W/(m·K). After thermal treatment at 300°C for 30 minutes, the back surface temperature of the material remains as low as 118.1°C, highlighting its effective thermal shielding performance[138].

These findings collectively demonstrate that heat transfer pathways in ceramic aerogels can be systematically regulated through the rational construction of

hierarchical pore architectures, heterogeneous interfaces, and 3D networks composed of low dimensional nano units. Through multiscale structural engineering, heat transfer via solid conduction, gas conduction, and thermal radiation at elevated temperatures can be concurrently suppressed, leading to excellent high temperature stability and long-term thermal durability. In addition, a variety of fabrication strategies such as biomimetic structuring and directional freezing enable precise and flexible control over pore size distributions and interfacial architectures. As a result, ceramic aerogels are able to maintain ultralow TC across an exceptionally broad temperature window ranging from room temperature to 1800°C, underscoring their remarkable structural tunability and significant potential as next generation high efficiency thermal insulation materials.

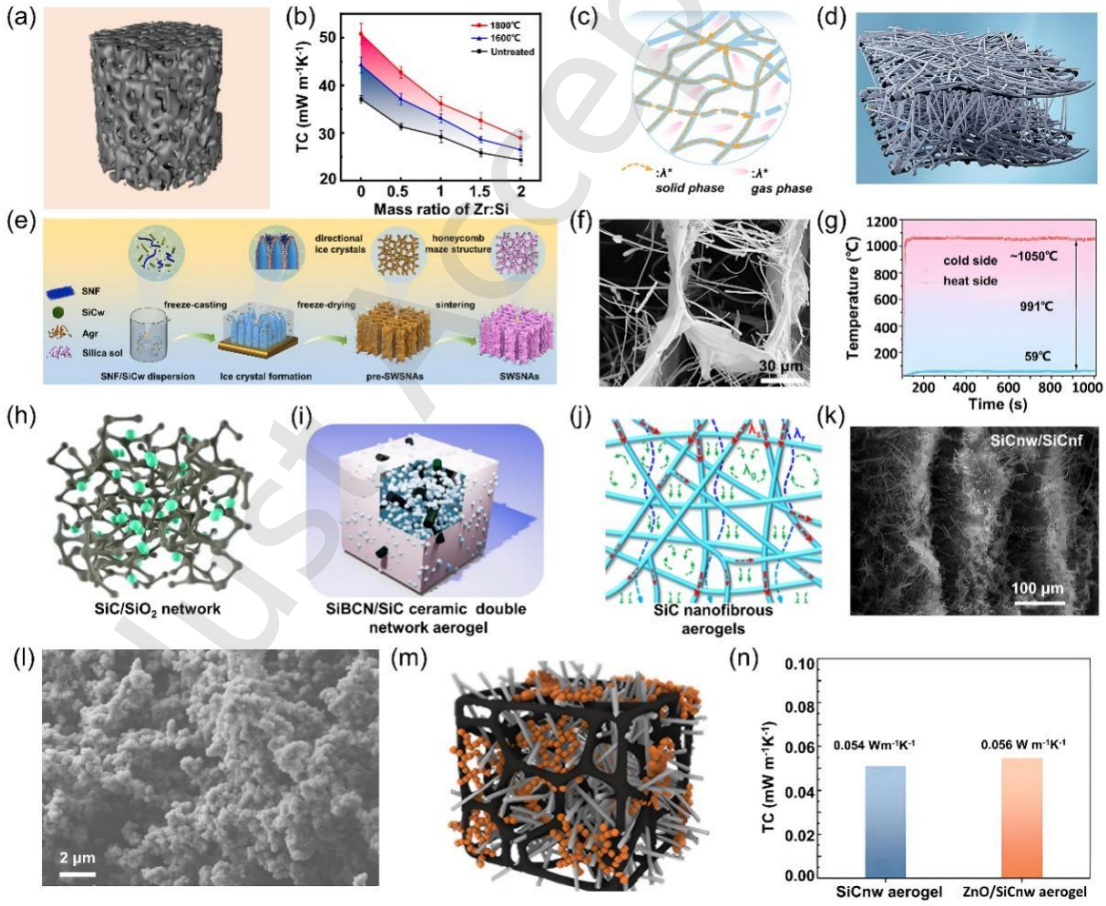

Figure 8. Microstructure design and thermal insulation performance. (a) and (b) Schematic diagram and the TC of ZrC/SiBCN aerogel. Reproduced with permission[133], Copyright 2024, Elsevier; (c) Mechanism of gas-solid thermal transport in SiC aerogel. Reproduced with permission[134], Copyright 2024, Elsevier.

(d) Schematic diagram of nanowire-filled layered SiC aerogel. Reproduced with permission[89], Copyright 2025, Elsevier; (e) The preparation process for SiC whisker-reinforced SiO_2 nanofibrous aerogels; (f) SEM image of SWSNAs; (g) Temperature variation curves of the hot and cold surfaces of SWSNAs. Reproduced with permission[90], Copyright 2025, Elsevier; (h) Schematic diagram of the fabrication of the SiC/SiO_2 composite aerogels. Reproduced with permission[63], Copyright 2024, Elsevier; (i) Schematic diagram of SiBCN/SiC double network ceramic aerogel. Reproduced with permission[136], Copyright 2024, Elsevier; (j) Thermal insulation mechanism of SiC nanofibrous aerogels. Reproduced with permission[64], Copyright 2025, American Chemical Society; (k) SEM of SiCnw/SiCnf composite aerogel. Reproduced with permission[137], Copyright 2024, Elsevier; (l) and (m) Schematic diagram and SEM images of the C/SiC/SiBCN composite aerogel. Reproduced with permission[65], Copyright 2025, Elsevier; (n) Thermal conductivities of ZnO/SiC_{nw} aerogel, SiCnw aerogel. Reproduced with permission[66], Copyright 2025, Elsevier.

5.1.2 SiC aerogel mechanical enhancement and functional integration strategy

Maintaining excellent thermal insulation while improving mechanical robustness and enabling multifunctional integration is essential for the practical deployment of ceramic aerogels. In this context, a variety of mechanical reinforcement strategies have been proven to be highly effective. For example, a SiC nanowire composite aerogel incorporating a mullite fiber skeleton, fabricated via a micromechanical design strategy (Figure 9a), exhibits a room temperature TC as low as 0.026 W/(m·K). Owing to its skeleton reinforced porous architecture, the aerogel retains structural integrity even under direct butane flame exposure at 1300°C (Figure 9b)[139]. Inspired by the hierarchical structure of palm bark, a SiC aerogel assembled through a biomimetic link assembly approach features a layered framework interconnected by elastic links (Figure 9c). This material achieves a TC of 0.027 W/(m·K) at room temperature and only 0.054 W/(m·K) at 1000°C (Figure 9d), while simultaneously exhibiting superelastic behavior and excellent fatigue resistance[140]. In addition, a SiC/Si_3N_4 nanowire composite aerogel fabricated via a one-step precursor pyrolysis route (Figure 9e) demonstrates excellent thermal insulation performance, with a room temperature TC as low as 0.064

W/(m·K). During high temperature spray gun testing at 1300°C, the back surface temperature increases to only 217.4°C (Figure 9f), and the material is capable of sustaining a pronounced temperature gradient under transient radiative heating at 1200°C[141].

A range of composite aerogel systems with tailored functionalities has been developed with respect to integrated functional design. Flexible and recoverable SiC nanofiber aerogels fabricated via electrospinning followed by freeze drying exhibit an extremely low density from 0.039 g/cm^3 to 0.041 g/cm^3 and a high porosity of approximately 98.7%. These materials demonstrate outstanding thermal insulation performance, with room temperature TC values as low as 0.025 to 0.031 W/(m·K). The interconnected 3D nanofiber network effectively restricts solid phase heat conduction and gas convection, thereby minimizing overall heat transfer (Figure 9g)[142]. Ultralight SiC nanowire aerogels prepared by CVI, as shown in Figure 9h, achieve a remarkably low density of only 5.82 mg·cm^{-3}. These aerogels maintain excellent thermal insulation performance at elevated temperatures, exhibiting TC values of 0.063 W/(m·K) at 100°C and 0.243 W/(m·K) at 900°C[143]. Furthermore, a SiBCN/SiC_{nw} composite ceramic aerogel synthesized through in situ growth of SiC nanowires via catalyst assisted annealing possesses a low density of 0.142 g/cm^3 and a TC as low as 0.052 W/(m·K). Beyond thermal insulation, this material exhibits excellent EMW absorption capability. After annealing at 1400°C, the minimum reflection loss (RL_{min}) reaches −50.1 dB (Figure 9i), highlighting its strong potential for multifunctional thermal protection and EMW absorption applications[144].

Multilayer architectures and gradient structural designs constitute another effective strategy for simultaneously improving thermal protection, oxidation resistance, and structural stability. In this context, a multilayer SiC nanofiber composite aerogel felt was rationally engineered to integrate a $ZrO_2/ZrSiO_4$ ablation layer, a SiC-TiO_2 light-shielding layer, and a SiC nanowire-based thermal insulation layer. Owing to this functional layering, the oxidation resistance temperature is increased to 1500°C, and the back surface temperature is reduced to only 130°C under butane flame ablation (Figure 9j), which is 178°C lower than that of a single layer SiC aerogel felt[109].

Similarly, a SiC-SiO_2 gradient ceramic coating fabricated on the surface of a low-density carbon-based aerogel composite via an in situ SiO ceramicization strategy remains structurally stable after ablation at 1850℃ for 600 s. The coating exhibits a pronounced through thickness temperature gradient of 117℃/mm, together with a low linear ablation rate of 0.315 μm/s and a low shrinkage rate of 0.61%, demonstrating its excellent resistance to extreme thermal environments[145]. Furthermore, an ultralight gradient C_6/(CrZrHfNbTa)C-SiC composite material (Figure 9k), prepared using a biomimetic capillary adsorption and transport strategy, achieves a low density of only 0.74 g/cm³ and a TC as low as 0.202 W/(m·K). When subjected to front side heating at 1300℃, the back surface temperature remains below 152℃, highlighting the effectiveness of gradient design in thermal management under severe heat flux conditions[146].

Recent advances in manufacturing technologies have further expanded the design space available for performance optimization of ceramic aerogels. For example, a SiC/SiO_2 aerogel composite sandwich structure fabricated by selective laser sintering (SLS) 3D printing combined with a sol gel process exhibits markedly improved thermal protection and mechanical strength. When the hot surface is maintained at 1000℃ for 1500 s, the back surface temperature of the single layer and double layer sandwich configurations decreases by 69.15℃ and 112.73℃, respectively, accompanied by a substantial enhancement in compressive strength[147]. In addition, a tough SiC nanowire aerogel produced via additive manufacturing, as shown in Figures 9l and 9m, demonstrates a low TC ranging from 0.046 to 0.0545 W/(m·K). Owing to the high precision of the fabrication process, the aerogel can be architected into complex geometries and maintains excellent structural stability over an exceptionally wide temperature range from −196 to 1100℃[67]. Furthermore, a mullite reinforced SiC based aerogel composite prepared through 3D printing followed by high temperature sintering achieves an ultralow TC between 0.016 W/(m·K) and 0.025 W/(m·K), together with a high porosity of up to 90%. This material uniquely integrates robust mechanical properties, including a Young's modulus of 24.4 MPa and a compressive strength of 1.65 MPa, with outstanding high temperature stability, remaining resistant

to temperatures as high as 1200℃[148].

The overall performance improvement of ceramic aerogels arises from the synergistic coupling of three key aspects, namely mechanical reinforcement, functional integration, and structural innovation. Through biomimetic design and nanonetwork architectures, ultralow TC can be maintained while simultaneously achieving enhanced mechanical robustness and excellent high temperature resistance. Functional integration further expands the material's versatility by combining efficient thermal insulation with EMW absorption, ultralow density, and mechanical flexibility. Multilayer gradient architectures and surface coating strategies optimize ablation resistance and thermal management, enhancing performance under extreme conditions. Moreover, advanced fabrication techniques such as additive manufacturing facilitate precise control over complex geometries and microstructural features, propelling ceramic aerogels toward multifunctional platforms that simultaneously achieve lightweight construction, high strength, thermal insulation, and high temperature stability. Collectively, these design and processing strategies establish a foundation for deploying ceramic aerogels in demanding environments, including aerospace and other extreme applications.

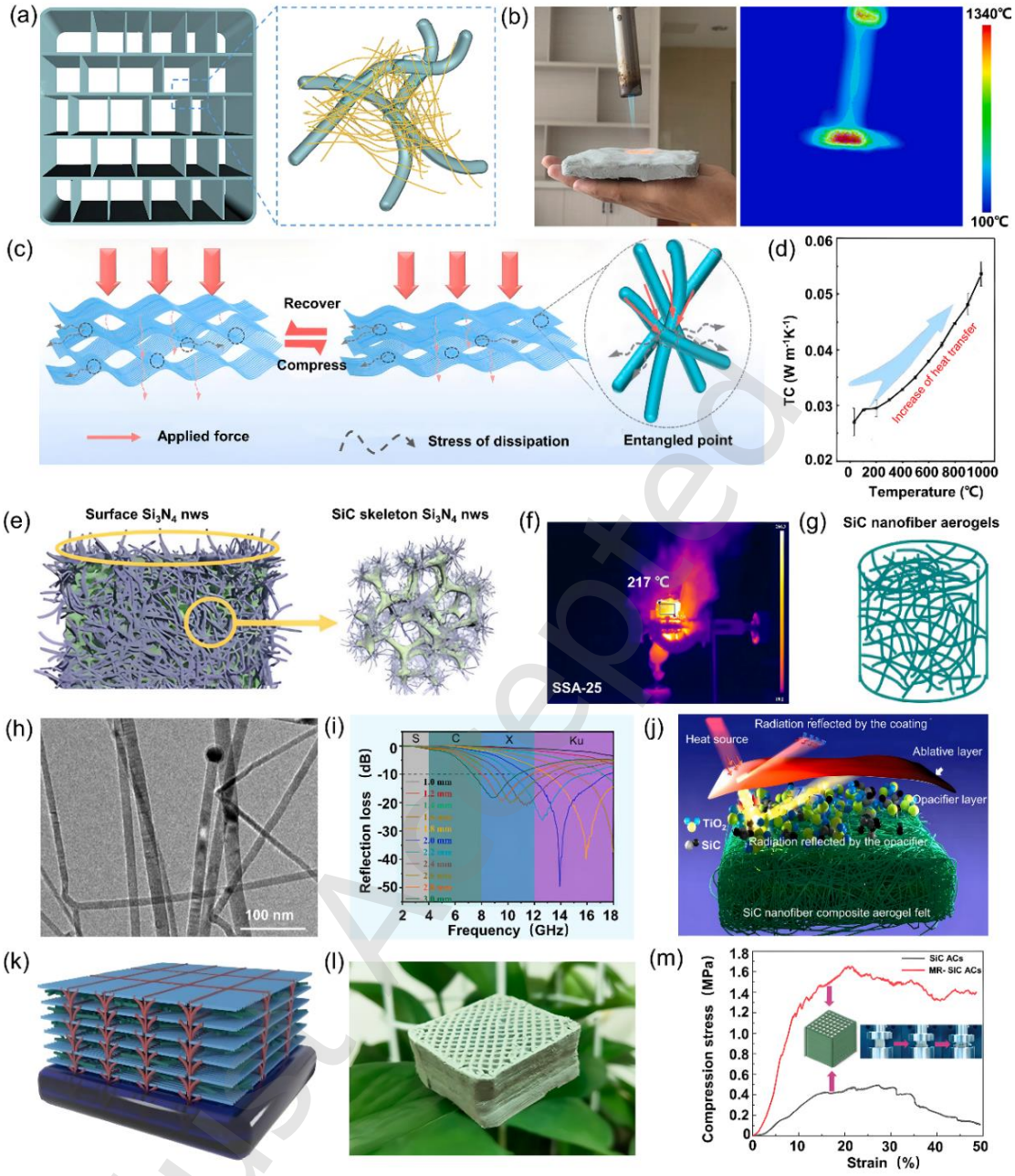

Figure 9. Mechanical enhancement and functional integration. (a) Schematic illustration of the preparation of the SMCAs; (b) Photograph and infrared images of SMCAs for thermal protection. Reproduced with permission[139], Copyright 2023, Elsevier. (c) and (d) Schematic illustration of super-elasticity and the thermal conductivities bioinspired SiC aerogels; Reproduced with permission[140], Copyright 2023, Elsevier;(e) Schematic of the SSA/SiC composite structure with Si_3N_4 nanowires (surface and interior). (f) The back stable thermal infrared temperature of SSA. Reproduced with permission[141], Copyright 2026, Elsevier; (g) Schematic diagram of

preparation process of SiC nanofiber aerogels; Reproduced with permission[142], Copyright 2019, Elsevier; (h) TEM image of SiCNW aerogel. Reproduced with permission[143], Copyright 2023, Springer Nature; (i) The microwave absorption performance of SiBCN/SiC nanowire composite aerogel. Reproduced with permission[144], Copyright 2024, Elsevier; (j)The schematic diagram of radiant heat transfer. Reproduced with permission[109], Copyright 2025, Elsevier; (k) Schematic diagram of the C_f/(CrZrHfNbTa)CSiC gradient composite. Reproduced with permission[146], Copyright 2025, Elsevier; (l) Photograph of the SiC nanowire aerogel lattice; Reproduced with permission[67], Copyright 2022, American Chemical Society (m) Compressive stress–strain curves of SiC ACs and MR-SiC ACs. Reproduced with permission[148], Copyright 2024, Wiley-VCH.

5.1.3 SiC aerogel performance optimization and exploration for specific application scenarios

Performance optimization of ceramic aerogels is progressively oriented toward application driven design, where specific service environments dictate distinct property requirements. For instance, in aerospace thermal protection and hypersonic vehicle applications, materials must not only tolerate extreme temperatures but also integrate multiple functional capabilities. For instance, a SiBCN/SiC/IP ceramic fiber aerogel (Figure 10a), fabricated via electrospinning followed by precursor impregnation and pyrolysis, can reduce a hot surface temperature of 1600 to 75℃ with a thickness of only 2 cm. At 1600℃, its TC is as low as 0.036 W/(m·K) (Figure 10b), infrared transmittance reaches merely 18%, and the mass gain after 12 hours of cyclic isothermal oxidation is only 5.17%[110]. Subcrystalline zirconium nanofiber aerogels exhibit a room temperature TC of 0.026 W/(m·K) (Figure 10c). Their near-zero Poisson's ratio and minimal thermal expansion confer exceptional thermal stability, with strength degradation below 1% even after 10,000 thermal shock cycles (Figures 10d and 10e)[149]. Additionally, a SiC aerogel featuring a directional layered architecture (STISA), prepared via an air suction-induced alignment strategy (Figure 10f), demonstrates a radial TC of only 0.019 W/(m·K) at room temperature. Its superior thermal insulation arises from the synergistic effect of its layered structure and

mesoporous network, which effectively compartmentalizes space and suppresses both air convection and solid heat conduction. Remarkably, even at 1000℃, the radial TC remains as low as 0.086 W/(m·K)[150].

In the domain of new energy safety and thermal management, ceramic aerogels have demonstrated significant application potential. The SiC nanowire aerogel layer within a Paraffin@SiC nanowire/aerogel (PA@SAS) sheet exhibits an ultralow TC of 0.0214 W/(m·K) at room temperature, which increases only slightly to 0.0419 W/(m·K) at 600℃. Remarkably, a 2 mm thick PA@SAS can generate a temperature gradient of 602℃, effectively inhibiting the propagation of battery thermal runaway (Figures 10g and 10h)[68]. SiC doped SiO_2 aerogel composites fabricated via sol-gel impregnation followed by supercritical drying maintain thermal conductivities in the range of 0.021 to 0.045 W/(m·K) at 600–1200℃ (Figure 10i). Their performance remains stable under combined mechanical stress (0.01–0.9 MPa) and elevated temperatures, and a thickness of 2.35 mm is sufficient to suppress the spread of thermal runaway in lithium batteries[151]. Furthermore, a SiC nanofiber aerogel spring prepared via a thermochemical route (Figure 10j) exhibits a room temperature TC of only 0.029 W/(m·K) (Figure 10k), coupled with an ultrahigh porosity of approximately 99.5% and excellent stability across both high and low temperature regimes (Figure 10l). Its hierarchical nanofiber network efficiently reflects mid-infrared radiation, making it a promising material for personal thermal energy management and advanced thermal insulation applications[69].

Within the domains of building energy efficiency and industrial thermal insulation, silica aerogels and their composites have demonstrated significant application potential. Characterized by ultralow TC in the range of 0.012 to 0.025 W/(m • K), silica aerogels also feature low density and partial light-transmitting properties. These materials can be synthesized via sol-gel processes and incorporated into boards, mortars, concrete, and glass window systems (Figure 10m)[152]. Environmentally friendly thermal insulation coatings have been developed by incorporating silica aerogel and other fillers into a styrene-acrylic emulsion matrix. When the coating surface is maintained at 351℃, the back surface temperature remains as low as 188℃, corresponding to a temperature

difference of 163℃, and the TC is only 0.05748 W/(m·K)[153]. Moreover, the thermal insulation performance of silica aerogel composites fabricated with a polyurethane foam skeleton can be further optimized by the addition of TiO_2, GO, and SiC as infrared shielding agents. Optimal performance is achieved with 1.0 wt.% TiO_2 and 0.2 wt.% SiC (Figure 10n), effectively suppressing radiative heat transfer and enhancing overall thermal insulation efficiency[154].

Across specialized environments and emerging application domains, ceramic aerogels exhibit distinct and notable advantages. A SiC-SiO_x bicrystalline nanowire ceramic aerogel demonstrates a low TC of 0.0284 W/(m·K) at room temperature, combined with exceptional mechanical performance, including high compressibility with 80% strain reversibility and tensile strength accommodating 20% strain without fracture. The material remains stable over a wide temperature range from −196 to 1200℃[155]. 3D network aerogels composed of ultra-long SiC nanowires exhibit a TC of 0.03 W/(m·K) at room temperature, increasing only to 0.23 W/(m·K) at 900℃. This ultralow TC is attributed to the highly porous 3D nanowire network, which effectively restricts gas convection and solid heat conduction. The aerogel also possesses excellent high-temperature stability, with an initial oxidation temperature of 750℃, and retains structural integrity after prolonged exposure to an alcohol lamp flame, exhibiting both non-combustibility and fire resistance[156]. A layered SiC-SiO_x nanowire aerogel, fabricated via capillary force-induced self-assembly, exhibits a low room temperature TC of 0.0393 W/(m·K). Its anisotropic layered structure suppresses heat flux perpendicular to the layers, thereby enhancing directional thermal management[70]. Additionally, a three-layer solar evaporator employing silica aerogel as a thermal insulation layer benefits from the aerogel's porous architecture and ultralow TC, which effectively trap heat and minimize energy loss. As a result, the evaporation enthalpy is reduced to 0.8118 MJ/kg, and the evaporation efficiency reaches 94.94% under one sun irradiation[157].

In addition, recent studies have explored new avenues for optimizing the performance of ceramic aerogels through the combination of numerical simulations and innovative fabrication techniques. Numerical investigations of hollow SiC fiber-doped

SiO_2 aerogel composites revealed that a hollow ratio of 0.6 reduces the composite density by 11.45% compared with solid fiber-doped counterparts over the temperature range of 300–1300 K, while maintaining comparable effective TC, highlighting the potential of structural tailoring for lightweight thermal insulation[158]. SiC aerogels synthesized via rapid combustion methods achieve ultralow densities of 6.4–12 mg/cm^3 and room temperature thermal conductivities of 0.023–0.027 W/(m·K). These materials exhibit stability across a wide temperature window from −196 to 1700°C, negative Poisson's ratio behavior, and are produced with high efficiency and low cost, demonstrating the advantages of scalable synthesis approaches[159]. Additionally, multilayer SiC-CNT-SiC/ANF aerogels fabricated by stacking-assisted cryogenic casting exhibit a low density of 0.04711 g/cm^3. The synergistic combination of a highly porous architecture and SiC nanofiller effectively suppresses heat transfer, while conferring both flame retardancy and high compressive strength of 113.83 kPa, illustrating the potential of hierarchical composite design for multifunctional thermal insulation applications[71].

Overall, the development of ceramic aerogels is increasingly guided by application-oriented requirements spanning aerospace, energy safety, building energy conservation, and emerging technological fields. In aerospace applications, rational compositional and structural design strategies enable ultralow TC as well as exceptional stability under extreme high-temperature conditions. In the energy sector, these materials act as critical thermal barriers to suppress battery thermal runaway. In building applications, silica-based aerogels achieve an optimal balance of ultralow TC, optical transparency, and processability. Beyond these domains, their wide-temperature stability and mechanical deformability extend their utility to emerging scenarios, including extreme thermal management and solar evaporation. Furthermore, the integration of numerical simulations and innovative fabrication strategies is accelerating the translation of ceramic aerogels from laboratory research to practical engineering applications. The fundamental physical origin underpinning these promising applications lies in the intrinsically ultra-low TC of SiC-based aerogels, as summarized in Table 4.

Table 4. Thermal conductivities of different types of SiC-based aerogel materials.

Aerogel Materials	Forms	Structure	TC (W/(m·K))	Ref.
Polymer-derived SiBCN/SiC nanowire	Monoblock	3D network	0.052	[144]
SiC nanowire	Monoblock	Programmed geometries	0.046	[67]
Mullite-reinforced SiC	Monoblock	Programmed geometries	0.021	[148]
SiC nanofiber	Paper-like	3D network	0.029	[69]
SiC-SiO_x bicrystal nanowires	Paper-like	3D network	0.0284	[155]
SiC	Paper-like	3D layer	0.027 ± 0.002	[159]
Super-elastic SiC aerogels	Monoblock	3D network	0.024	[72]
SiC@SiO_2 nanocable aerogels	Monoblock	3D network	0.035	[160]
Coral-like SiC	Powder	Coral-like	0.0621	[115]
SiC	Monoblock	Core-shell	0.018	[91]
ZrO_2-interface-engineered SiC nanofiber	Fiber mat	3D network	0.02407	[116]
RGO/SiC nanowire	Monoblock	3D network	0.061	[161]
Hierarchical SiC fiber	Fiber mat	3D layer	0.027	[162]
SiC	Monoblock	3D layer	0.05	[163]
SiC	Monoblock	Core-shell	0.028	[119]
C/SiC nanofiber	Monoblock	3D network	0.03	[164]

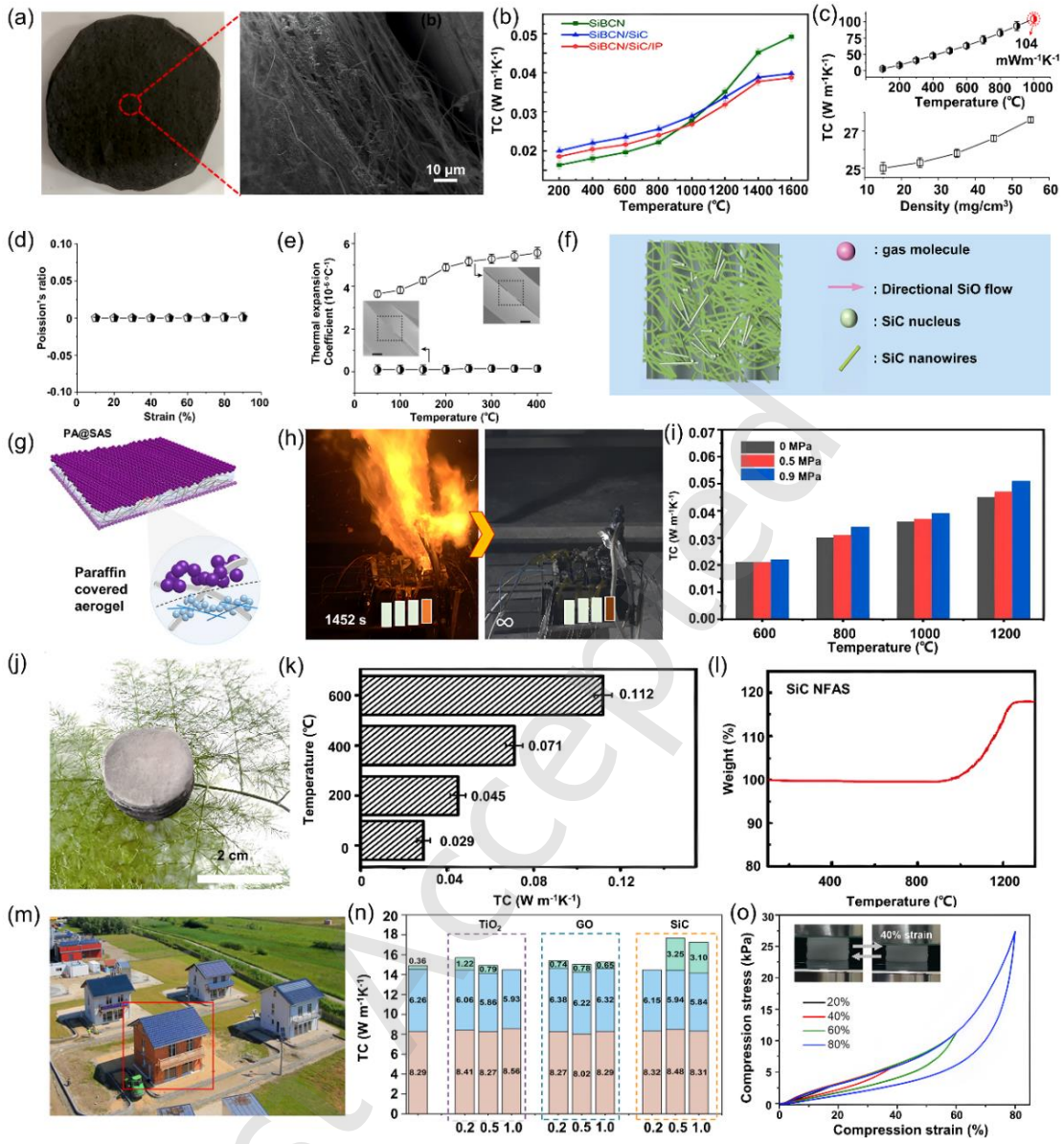

Figure 10. Performance optimization and exploration for specific application scenarios. (a) SEM and macrograph of SiBCN/SiC/IP. (b) TC; Reproduced with permission[110], Copyright 2022, Elsevier; (c)TC of ZAGs as a function of temperature and density; (d) The near-zero ν of ZAGs under different compressive strains.; The near-zero α (black circle) of ZAGs compared with the positive α (white circle) under different temperatures. Reproduced with permission[149], Copyright 2022, Springer Nature. (f) Schematic illustration of the fabrication of the super thermally insulating SiC aerogel; Reproduced with permission[150], Copyright 2022, Wiley-VCH. (g) Schematic illustration of the fabrication of Paraffin@SiC nanowire/aerogel. (h) The thermal runaway behaviors of LIB with Paraffin@SiC nanowire/aerogel. Reproduced

with permission[68], Copyright 2025, Elsevier; (i) thermal conductivities of SAC-SiC. Reproduced with permission[151], Copyright 2025, Elsevier; (j) SiC nanofiber aerogel spring; (k) and (l) TC and TGA curve of SiC nanofiber aerogel spring; Reproduced with permission[69], Copyright 2022, springer; (m) INES experimental platform and the experimental test house in red. Reproduced with permission[152], Copyright 2015, Elsevier; (n) TC contributions for all the specimens. Reproduced with permission[154], Copyright 2055, Elsevier; (o) Uniaxial compression of CSCSNW aerogel; Reproduced with permission[155], Copyright 2021, American Chemical Society.

5.2 Research status of SiC aerogel materials in EMW absorption

5.2.1 SiC aerogel advanced preparation process and multifunctional integrated application

The fabrication of high-performance SiC-based EMW absorbing materials relies critically on advanced preparation techniques. CVD and related methodologies play a central role, particularly in the formation of 1D nanowires and 3D network architectures. SiC nanowire aerogels (Figure 11a)[165] and SiC/SiO_2 nanowire aerogel composites[166] can be directly synthesized via a straightforward CVD route. The integration of CVD with 3D printing enables precise control over macroscopic geometries while simultaneously tuning microscopic properties, facilitating the fabrication of SiC-based composite materials with 3D porous network architectures (Figure 11b)[167] as well as SiC@C nanowire aerogels[168]. Moreover, CVI allows in situ growth of SiC nanowire networks within the 3D interconnected porous carbon skeleton derived from melamine foam carbonization, yielding a hierarchical double-network structure (Figure 11c)[169].

Owing to their low cost, wide availability, and excellent ability to replicate complex natural architectures, template-assisted fabrication strategies, particularly those utilizing biomass templates, have attracted considerable attention. Porous aerogels with in situ grown SiC nanowires can be directly synthesized from eggplant-derived carbon through carbonization and carbothermal reduction, exhibiting excellent EMW absorption performance with a maximum effective absorption bandwidth (EAB_{max}) of 4 GHz[170]. By utilizing biomass-derived carbon microtubes as the

conductive network, SiC nanowires as the dielectric units, and Ni nanoparticles as magnetic components, a CMT@SiCNW/Ni aerogel featuring a 3D hierarchical network was fabricated via a two-step pyrolysis method (Figure 11d)[171]. Similarly, rice husks have been employed as precursors to produce SiC/C composite materials through magnesium thermal reduction, demonstrating the feasibility of large-scale, cost-effective EMW absorbing material production[172]. Furthermore, porous carbon derived from apple was used as a framework for the in situ growth of SiC nanowires via a catalyst-free gas-solid phase process, yielding a composite aerogel with a two-level hierarchical architecture[173].

A classical and highly effective strategy for producing aerogels with high porosity and ultralow density is the combination of sol–gel chemistry with freeze-drying or supercritical drying. Carbon fiber-reinforced C/SiOC aerogel composites, prepared via a sol-gel process followed by atmospheric pressure drying and optimized impregnation (Figure 11e), exhibit an RL_{min} of −65.45 dB at a thickness of 2.91 mm[174]. A SiC/C composite aerogel with a 3D nanonetwork was fabricated using the sol-gel method combined with supercritical CO_2 drying and carbothermal reduction, yielding worm-like SiC nanostructures within the network[111]. Freeze-drying techniques, particularly directional freezing (ice-templating), enable the construction of anisotropic channels that are critical for controlling EMW propagation. This strategy has been successfully applied to produce SiC/SiO_2 composite aerogels with anisotropic porous architectures (Figure 11f)[175] and SiC_{nws}/CNFs/SiC composite aerogels featuring a 3D interpenetrating network (Figures 11g and 11h)[176].

Precursor conversion and polymer-derived ceramic (PDC) approaches offer a versatile route to fabricate SiC-based ceramics with precisely tunable compositions. For example, coating a SiO_2 aerogel precursor with a silicon-containing aryl acetylene resin, followed by carbothermal reduction and PDC treatment, yields honeycomb-like SiC/C aerogels (Figure 11i). The synergistic interaction between SiC and carbon phases endows these materials with outstanding EMW absorption properties, achieving an EAB_{max} of 6 GHz[177]. SiC ceramic aerogels can also be synthesized directly from silicon-containing polymers via sol-gel processing, freeze-drying, and pyrolysis (Figure

11j), with their performance tunable by adjusting the pyrolysis temperature[178]. Additionally, carbon foams derived from melamine foam pyrolysis, when combined with SiC, SiO_2, or other components, have proven to be an effective platform for producing lightweight and high-performance EMW absorbing materials[179, 180].

Ultimately, these advanced fabrication strategies are directed toward achieving the multifunctional integration of SiC-based aerogels to satisfy the demands of complex application scenarios. In addition to excellent EMW absorption performance, many SiC-based aerogels simultaneously exhibit low density, high mechanical strength, super elasticity, thermal insulation, and high-temperature stability[72, 112, 181-183], rendering them highly promising for thermal–electromagnetic integrated protection in aerospace applications[184]. Notably, the SiC_n@MXene/SiOC composite superstructure, fabricated via 3D printing, extends the operational frequency range into the terahertz regime while incorporating electrothermal conversion functionality, highlighting its potential for future communication and stealth technologies[185]. Similarly, the SiC@reduced graphene oxide/epoxy (SiC@RGO/EP, SCGE) composite demonstrates both ultrahigh electromagnetic attenuation (−85.92 dB) and effective TC (0.93 W/(m·K)), illustrating its dual capability to address electromagnetic compatibility and heat dissipation challenges in high-performance electronic devices[186].

The fabrication of high-performance SiC-based EMW absorbing materials critically depends on the precise control of multi-level processes. CVD and its derivatives serve as the cornerstone for constructing intricate architectures, including 1D nanowires and 3D networks, and their integration with 3D printing enables coordinated macro- and micro-scale structural design. Biomass template strategies offer an environmentally friendly route for large-scale production of hierarchical porous materials. The combination of sol-gel chemistry with freeze-drying or supercritical drying represents a classical approach for generating high-porosity aerogels, where directional freezing can further create anisotropic channels to modulate EMW propagation. Precursor conversion and PDC techniques provide precise compositional and structural control. Collectively, these advanced fabrication methods propel the development of multifunctional SiC-based materials that combine low density, high

mechanical strength, thermal insulation, and high-temperature stability, fulfilling the demanding requirements of thermo-electromagnetic synergistic protection, terahertz communication, and thermal management in high-performance electronic devices.

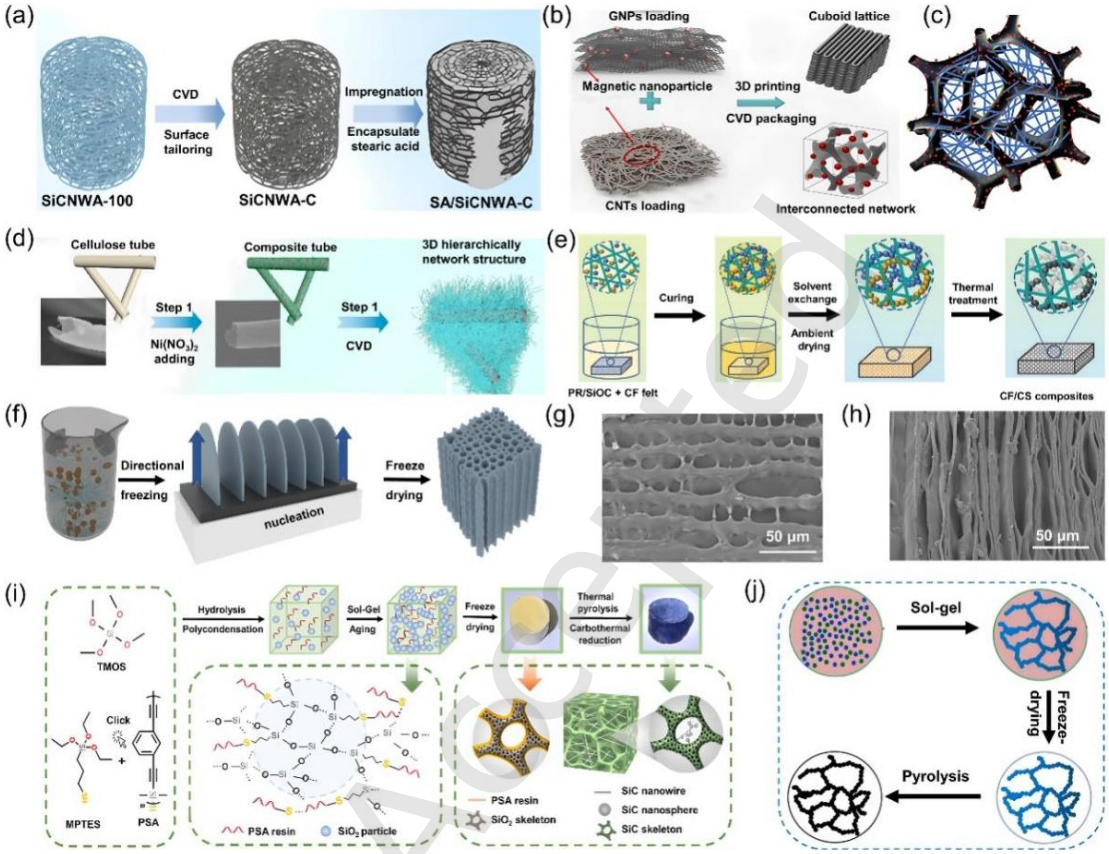

Figure 11. Advanced preparation process. (a) Preparation process of SiCNWA-based composite PCMs by CVD. Reproduced with permission[165], Copyright 2021, American Chemical Society. (b) Schematic diagram of the preparation of FGCS composites by 3D printing combined with CVD. Reproduced with permission[167], Copyright 2024, Elsevier; (c) Schematic diagram for SiC_{nw}/CF composite. Reproduced with permission[169], Copyright 2018, Royal Society of Chemistry; (d) Schematic illustration of the formation process of CMT@SiC_{NW}/Ni aerogel. Reproduced with permission[171], Copyright 2022, Elsevier; (e) Schematic illustration of the preparation for CF/CS composites. Reproduced with permission[174], Wiley-VCH. (f) Schematic diagram of the preparation of SiC/SiO_2 aerogel by ice-templating Reproduced with permission[175], Copyright 2022, Elsevier; (g) and (h) Axial and Radia SEM image of SiC/SiO_2 aerogel. Reproduced with permission[176], Copyright 2022, Elsevier; (i) Schematic diagram of the SiC/C aerogel preparation by PDC. Reproduced with

permission[177], Copyright 2025, Elsevier; (j) Schematics of the sol-gel and transformation process of SiC Cas. Reproduced with permission[178], Copyright 2022, Elsevier.

5.2.2 SiC aerogel multi-component composite materials and composition regulation

The EMW absorption performance of SiC-based aerogels and their composites is primarily governed by compositional design and synergistic interactions among different components. By integrating SiC with materials of distinct electrical properties, both the dielectric constant and magnetic permeability can be effectively regulated, thereby enabling optimized impedance matching and significantly enhanced attenuation capability. Among these strategies, SiC/carbon composites represent a classic and highly effective approach. Using ice-templating and carbothermal reduction, ultralight carbon-doped SiC aerogels with densities below 4 mg/cm^3 were fabricated, exhibiting an EAB_{max} of 5.5 GHz across the 2–18 GHz range, an RL_{min} value of −15 dB, and favorable impedance matching. This outstanding wave absorption arises from the 3D porous architecture, abundant heterogeneous interfaces (3C/2H-SiC), and defect-induced dipole polarization (Figure 12a)[187]. Furthermore, CVI of SiC nanowires into graphene aerogels (GA) enabled the construction of robust 3D conductive networks (Figure 12b), achieving an EAB_{max} of 6.5 GHz at a thickness of 2.0 mm (Figure 12c)[188]. SiC nanowire-reinforced SiC/carbon foam composite aerogels, prepared using melamine foam templates via carbonization, CVD, and CVI (Figure 12d), demonstrated exceptional electromagnetic performance, with an RL_{min} of −31.216 dB and an EAB_{max} of 4.1 GHz at a thickness of 1.5 mm (Figure 12e)[189].

In recent years, two-dimensional MXene materials have emerged as highly promising building blocks for high-performance EMW absorbers, owing to their exceptional electrical conductivity and rich surface functionalization. Notably, a composite aerogel comprising SiC particles and $Ti_3C_2T_x$ (Figure 12f) at a 1:1 mass ratio exhibits an ultralow density of 8.8 mg·cm^{-3}, achieving an RL_{min} of -54.5 dB at a thickness of 2.04 mm, alongside an EAB_{max} of 5.4 GHz (Figure 12g)[190]. Further advancement is realized through a $Ti_3C_2T_x$/SiC nanowire composite aerogel, fabricated

via electrostatic self-assembly and directional freeze-drying, which attains an ultralight density of 0.0197 g cm^{-3} and extends the EAB_{max} to 9.5 GHz at a mere thickness of 1.25 mm[191]. Moreover, integrating these SiC-based composite aerogels into flexible poly(vinylidene fluoride) (PVDF) films broadens their applicability in flexible electronic devices, while preserving excellent EMW absorption performance, with an RL_{min} of -45.5 dB[192].

Incorporating metals or metal oxides with magnetic loss capabilities to establish a dielectric–magnetic synergistic mechanism represents an effective strategy to enhance EMW absorption[193, 194]. For instance, by modifying the surface of SiC nanowire-reinforced SiC aerogels with nickel-terminated CNTs via metal-organic CVD, a 3D hierarchical SiC_mw@SiC-Ni@CNT composite was constructed (Figure 12h), exhibiting an EAB_{max} of 8.96 GHz (9.04–18.0 GHz)[195]. Similarly, employing biomass templates, NiCo alloy nanoparticles were introduced through electroless plating to fabricate NiCo-SiC aerogels, which also realize dielectric–magnetic synergy, achieving an EAB_{max} of 7.6 GHz at a thickness of 3 mm (Figures 12i and 12j)[196]. Moreover, the growth of Fe-CNTs on SiC aerogels via CVD markedly improves the magnetic loss performance, reaching an RL_{min} of -49.6 dB[197]. Therefore, the incorporation of magnetic components not only enhances electromagnetic energy dissipation via magnetic loss, but also regulates impedance matching through the coupled variation of complex permittivity and permeability.

Significant advances have been achieved in tailoring the overall dielectric properties and optimizing impedance matching through the integration of additional ceramic components such as Si_3N_4, BN, and SiO_2. For instance, a hierarchical 3D reduced graphene oxide/BN/SiC (3D-rGO/BN/SiC) composite aerogel was fabricated by sequentially depositing BN and SiC coatings onto a porous 3D-rGO scaffold, prepared via a combination of 3D printing and freeze-casting self-assembly followed by CVI. This composite exhibited an EAB_{max} of 5.90 GHz at a thickness of 2.8 mm, with an RL_{min} of –37.8 dB (Figure 12k)[198]. Similarly, an ultralight SiC/Si_3N_4 aerogel with a density of only 8.67 mg·cm^{-3} was successfully synthesized via freeze-drying and carbothermal reduction. This material achieved an RL_{min} of –25 dB at 3.97 mm

thickness, corresponding to an EAB_{max} of 4.3 GHz (6.1–10.4 GHz). Its exceptional wave-absorbing performance arises from the porous network and abundant heterogeneous interfaces formed by SiC and Si_3N_4 nanowires, which significantly enhance interfacial polarization and dipolar relaxation losses. Moreover, the incorporation of Si_3N_4 improves impedance matching, facilitating EMW penetration and dissipation (Figure 12l)[199]. In carbonaceous SiC/mullite aerogels, both amorphous carbon and SiC act as dielectric loss-type absorbers, attenuating EMW through resistive loss and polarization relaxation mechanisms. The addition of mullite and SiO_2 further tunes the composite's impedance, mitigating wave reflection[200]. Notably, the incorporation of SiC nanoparticles into a novel high-entropy ceramic matrix achieved an ultralow RL_{min} of –54.28 dB, attributed to pronounced interfacial and defect polarization effects (Figure 12m)[201]. Therefore, in heterointerface engineering, interfacial polarization and conductivity modulation not only optimize impedance matching but also synergistically enhance dielectric loss.

Collectively, these findings indicate that the performance of SiC (SiC)-based wave-absorbing aerogels is governed by the synergistic interplay of multi-component design and complementary loss mechanisms. The roles of different composite strategies in electromagnetic response are not single-dimensional; instead, they achieve a dynamic balance between attenuation capability and impedance matching through tailored regulation of electromagnetic parameters[202, 203]. Incorporation of carbonaceous materials enables the formation of 3D conductive networks, enhancing resistive loss and interfacial polarization to achieve broadband absorption. The introduction of 2D MXenes overcomes the intrinsic trade-off between high conductivity and ultralow density, facilitating the development of ultrabroadband absorbers. Incorporating magnetic constituents establishes dielectric–magnetic synergistic loss, effectively extending the low-frequency absorption range[204]. Integration with additional ceramic phases allows precise tuning of the dielectric constant, optimizing impedance matching and promoting interfacial polarization. Collectively, these strategies, implemented within porous hierarchical architectures, enable the concurrent optimization of impedance matching and electromagnetic energy

dissipation through multi-component, multi-scale integration, driving the materials toward comprehensive performance characterized by "strong, broad, thin, light, and stable" attributes.

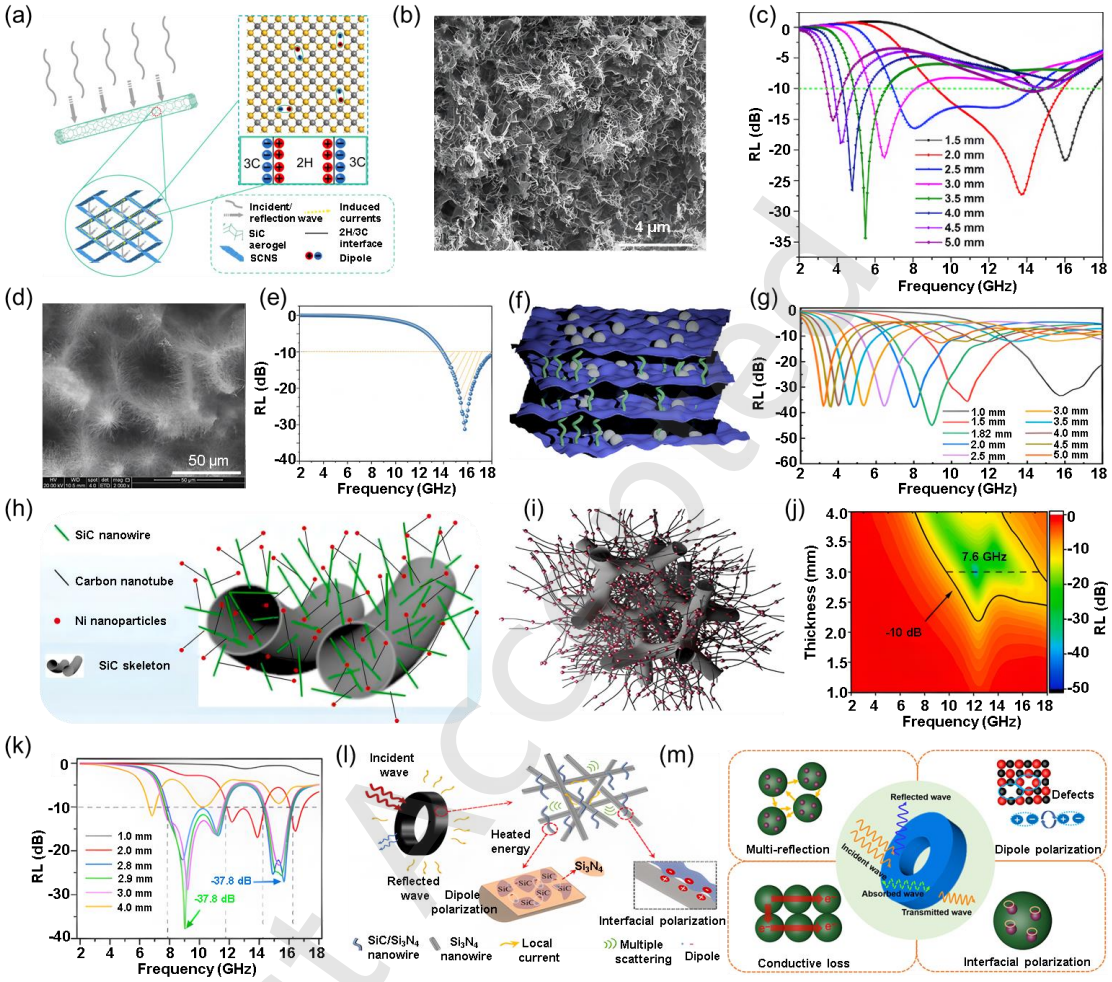

Figure 12. Multi-component composite materials and composition regulation. (a) Microwave attenuation mechanism for the SiC aerogel. Reproduced with permission[187], Copyright 2022, Elsevier; (b) and (c) SEM image and RL of SiCnw/GA–S composite. Reproduced with permission[188], Copyright 2018, Elsevier; (d) SEM images and EMW RL of SiC nanowire-reinforced SiC/carbon foam composites. Reproduced with permission[189], Copyright 2020, Elsevier; (f) Schematic illustration of SiC particles/$Ti_3C_2T_x$ aerogel. (g) RL of $Ti_3C_2T_x$/SiCnw hybrid aerogel. Reproduced with permission[190], Copyright 2024, Elsevier; (h) Schematic illustration of the SiCnw@SiC-Ni@CNT composite. Reproduced with permission[195], Copyright 2023, Elsevier; (i) and (j) Schematic illustration and RL of NiCo-SiC aerogel. Reproduced with permission[196], Copyright 2022, Elsevier; (k)

RL curves of 3D-rGO/BN/SiC. RL curves of 3D-rGO/BN2h/SiC, Reproduced with permission[198], Copyright 2023, Elsevier; (l) Schematic illustration of the EM wave absorption mechanisms of SiC/Si_3N_4 aerogel; Reproduced with permission[199], Copyright 2022, Elsevier; (m) EMW absorption mechanism for HEC–SiC composites. Reproduced with permission[201], Copyright 2023, Elsevier;

5.2.3 SiC aerogel multi-level micro/nano structure design

Rather than relying solely on compositional hybridization, tailoring the microstructural architecture plays a pivotal role in optimizing EMW absorption performance[205]. In particular, porous frameworks, especially 3D interconnected networks, can effectively prolong the propagation pathways of incident waves through multiple reflections and scattering processes, thereby significantly enhancing energy dissipation efficiency. SiC/SiOC aerogels with tunable microstructures were synthesized by controlling the heat-treatment temperature between 1100 and 1700°C (Figures 13a and 13b). With increasing temperature, SiC nanocrystals gradually precipitated, forming a conductive network of disordered carbon and markedly improving dielectric loss. The sample treated at 1700°C exhibited optimal performance, with an RL_{min} of –53.5 dB and an EAB_{max} of 6 GHz. This enhancement is attributed to the synergistic effects of interfacial polarization within the SiC@C core–shell structure, conductive and defect polarization from the nanocrystalline carbon network, and the multiple scattering and impedance matching facilitated by the porous architecture[206]. Similarly, SiC nanofiber aerogel felt, prepared using chopped carbon fiber felt as a template and possessing a density of only 5.29 $mg \cdot cm^{-3}$, demonstrated pronounced wave-absorption potential due to the combined effect of high-aspect-ratio nanofibers and porous morphology[113]. 3D SiC@C composite aerogels doped with metal ions (Fe, Ni, Al) were fabricated using sodium alginate as a carbon precursor and SiC nanowhiskers as reinforcement via ionic crosslinking followed by high-temperature pyrolysis (Figure 13c). Among these, the SiC@C-Fe aerogel exhibited an RL_{min} of –49.2 dB and an EAB_{max} of 3.6 GHz at a thickness of 2.0 mm[207].

Expanding upon 1D nanostructures, the construction of core–shell architectures has become an effective strategy for introducing abundant heterogeneous interfaces and

strengthening interfacial polarization. Core–shell SiC@C nanowires (Figure 13d), synthesized via surface carbonization of SiC nanowires, allowed optimization of dipolar and interfacial polarization by tuning the carbon shell thickness. At a thickness of 2.69 mm, the EAB_{max} reached 7.20 GHz, with an RL_{min} of –56.34 dB (Figure 13e)[208]. Ultralight (~12 $mg \cdot cm^{-3}$) multifunctional SiC nanowire aerogels fabricated by CVD (Figure 13f) exhibited an RL_{min} of –50.6 dB at 16.9 GHz and an EAB_{max} of 7.7 GHz at a thickness of 3.04 mm (Figure 13g), spanning nearly half of the X-band and the entire Ku-band[209]. Likewise, lightweight porous SiC/Si_3N_4 composite nanowires were prepared via electrospinning followed by heat treatment under a nitrogen atmosphere (Figures 13h and 13i). Optimal EMW absorption was achieved at a carbothermal reduction temperature of 1500 °C. With a filling fraction of only 15 wt% and a thickness of 2.1 mm, the material exhibited an EAB_{max} of 7.12 GHz (10.88–18 GHz) and an RL_{min} of –48 dB at 6.5 GHz[210].

Hollow structural design is an effective strategy to reduce the effective dielectric constant of a material, thereby optimizing impedance matching. β-phase hollow SiC spheres, fabricated using yeast as a biological template (Figure 13j), leverage their hollow architecture to improve impedance matching while simultaneously introducing additional interfacial polarization (Figure 13k), achieving an EAB_{max} of 6.05 GHz at a thickness of 4.0 mm[211]. Double-interconnected network hollow SiC foams, prepared via CVD followed by oxidation (Figures 13l and 13m), integrate hollow and porous architectures to realize superior wave absorption performance (RL_{min} of –50.75 dB) while maintaining low density (11.56 $mg \cdot cm^{-3}$) and high compressive strength (1.409 MPa) (Figure 13n)[212]. Furthermore, gradient multilayer $SiC@SiO_2$ nanowire aerogels achieve ultrabroadband and highly efficient EMW absorption. The optimized architecture comprises a low-dielectric outer layer, alternating transparent/attenuating intermediate layers, and a high-loss inner layer, delivering near-complete absorption across the 2–18 GHz frequency range and achieving an RL_{min} of –45.6 dB at a thickness of 10 mm (Figure 13o)[213].

The construction of hierarchically ordered and oriented architectures enables precise regulation of EMW propagation and attenuation. A vertically aligned SiC

nanowire/boron nitride cellulose aerogel network, fabricated via ice-templating and subsequently composited with epoxy resin, exhibits not only superior thermal management owing to its oriented structure but also enhanced wave absorption performance by extending the EMW reflection pathways (Figure 13p)[214]. Similarly, a SiC/SiO_x micro-nanofiber sponge with a hierarchical hollow architecture was prepared via template-assisted CVD, demonstrating excellent EMW absorption with an RL_{min} of −51.8 dB and an EAB_{max} of 8.6 GHz. The hollow structure effectively optimizes impedance matching, lowers the overall dielectric constant, and promotes multiple reflections and scattering of EMW (Figure 13q)[215]. Additionally, a sponge-like graphene@SiC aerogel, fabricated through directional freeze-casting followed by thermal reduction, possesses a hierarchically ordered structure that synergistically enhances interfacial polarization, conductive loss, and multiple scattering, thereby improving energy attenuation efficiency[216].

The rational design of microstructures is crucial for enabling high-efficiency EMW absorption in SiC-based aerogels. 3D porous networks effectively prolong the propagation pathways of EMW through multiple reflection and scattering events, thereby enhancing attenuation efficiency. Meanwhile, the introduction of core-shell and hollow architectures in nanowires or nanosheets significantly intensifies interfacial polarization and dipolar relaxation processes. At the macroscopic level, the construction of gradient, oriented, or hierarchically ordered structures enables active control over wave propagation and impedance matching, with vertically aligned arrays optimizing absorption of vertically incident waves and gradient multilayer designs promoting broadband performance. By integrating these multi-scale structural strategies with tailored component design, the effective dielectric constant can be precisely tuned, impedance matching optimized, and internal energy dissipation maximized, collectively advancing the performance of SiC-based absorbers toward ultrabroad bandwidths, enhanced attenuation, reduced thickness, and ultralight characteristics, as summarized in Table 5.

Table 5. EMW absorption performances of different types of SiC-based aerogel materials.

Aerogel Materials	RL_{min} (dB)	Thickness at RL_{min} (mm)	EAB_{max} (GHz)	Ref.
Eggplant-derived SiC	−43	2	4	[170]
SiC/C	−52.6	2.25	6	[177]
C/SiC@SiC	−53.8	2.35	6.06	[182]
SiC nanowires/graphene	−54.8	2	6.5	[188]
$Ti_3C_2T_x/SiC_{nw}$ hybrid	−44.9	1.25	9.5	[191]
NiCo-SiC	−44.5	3	7.6	[196]
Bone-like graphene@SiC	−47.3	3	4.7	[216]
$SiC@SiO_2$ nanocable	−56.6	2.55	10.2	[160]
$SiC@SiO_2$ nanofiber	−50.36	1.6	8.6	[114]
Si_3N_4/SiC	−45	3.2	8.4	[217]
SiC/Si_3N_4	−48.6	2	7.4	[218]
RGO/SiC nanowire	−42.23	2.5	7.47	[161]
Carbonaceous SiC	−66.01	1.5	6.76	[74]
MOF-derived $Co@SiC_{nw}$	−61.4	2.64	7.44	[219]
SiC/SiO_2 composite	−64.86	1.46	13.2	[118]
SiOC/SiC	−30.23	4	5.4	[220]

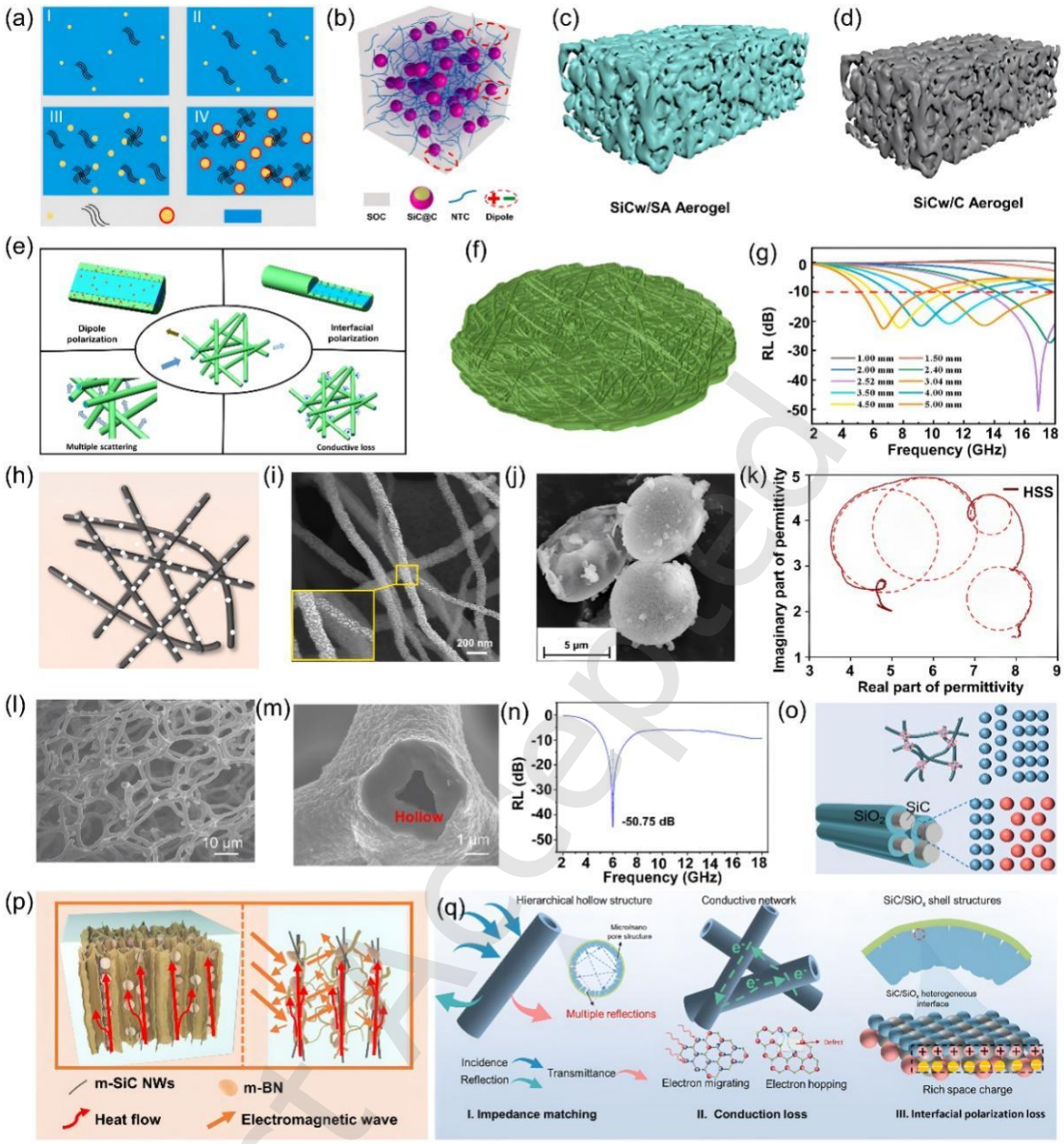

Figure 13. Multi-level micro/nano structure design. (a) Schematic diagram of the microstructure evolution mechanism of SiC/SiOC aerogels; (b) Schematic mechanism of dielectric loss. Reproduced with permission[206], Copyright 2023, Elsevier; (c) and (d) SiCw/SA aerogel and SiCw/C aerogel. Reproduced with permission[207], Copyright 2024, Elsevier; (e) Schematic illustration of microwave absorption mechanisms for SiC@C samples. Reproduced with permission[208], Copyright 2024, Elsevier; (f) and (g) Diagrammatic representation and theoretical RL curves of the SNWA. Reproduced with permission[209], Copyright 2024, Elsevier; (h) and (i) Schematic diagram and SEM of SiC/Si_3N_4 NWs. Reproduced with permission[210], Copyright 2023, Elsevier; (j) and (k) SEM image and typical Cole-Cole semicircles of

HSS. Reproduced with permission[211], Copyright 2023, Elsevier; (l) and (m) Microstructure morphologies of SiC/C foam. (n) Minimum RL values of SiC/C foam. Reproduced with permission[212], Copyright 2020, Elsevier; (o) Schematic diagram of SAs-H-H. Reproduced with permission[213], Copyright 2024, Elsevier; (p) Schematic diagram of thermal conduction and EMW absorption mechanisms of CA/m-SiC/m-BN/EP. Reproduced with permission[214], Copyright 2022, Springer. (q) Schematic diagram of EMW absorption mechanism for HHSMSs. Reproduced with permission[215], Copyright 2025, Springer.

5.3 Research status of SiC aerogel materials integrated with thermal insulation and EMW absorption

5.3.1 SiC aerogel porous structure and heterogeneous interfaces synergistic regulation enable efficient energy conversion and barrier functions

The synergistic enhancement of EMW absorption and thermal insulation in SiC-based aerogels relies on the deliberate construction of microstructures capable of simultaneously regulating both electromagnetic and thermal energy. 3D porous networks play a dual role in this regard. At the nanoscale, abundant interfaces and defects promote interfacial polarization and multiple relaxation processes, thereby enhancing dielectric loss[221]. At the microscale, the porous network prolongs EMW propagation paths, intensifies multiple scattering, and simultaneously suppresses gaseous heat convection[222]. At the macroscale, the continuous skeletal framework reduces solid-phase TC while ensuring overall structural stability. Such multiscale features collectively enable efficient energy regulation: EMWs are attenuated via extended propagation paths, scattering, and impedance matching modulation, while heat transfer is inhibited through suppressed convection and reduced lattice thermal conduction. These multifunctional characteristics have been achieved through a variety of advanced fabrication strategies. A nanocable aerogel with a SiC@SiO_2 core–shell architecture (Figure 14a), exhibiting a density of only 4 $mg \cdot cm^{-3}$, demonstrates excellent thermal insulation due to its ultra-high porosity of 99.9%, with a room-temperature TC of merely 0.035 W/(m·K). Concurrently, the unique core–shell structure and 3D network deliver an EAB_{max} of 10.2 GHz and an RL_{min} of –55.6 dB at

a thickness of 3.5 mm[160]. Similarly, a 3D porous cross-linked SiC@SiO_2 nanofiber aerogel (Figure 14b) achieves a low TC of 0.027 W/(m·K) and a wide EAB_{max} of 8.6 GHz with an RL_{min} of –50.36 dB, enabled by its 99.6 % porosity (Figures 14c and 14d)[114]. The synergistic enhancement of both thermal and electromagnetic performance is primarily attributed to impedance matching optimization by the SiO_2 shell, strong interfacial polarization at the SiC/SiO_2 heterointerface, and the multiple reflection effects facilitated by the porous architecture.

The coral-like SiC aerogel exhibits a high specific surface area of 1099 $m^2 \cdot g^{-1}$ and a low TC of 0.0621 W/(m·K) (Figure 14e). Its intricate pore architecture simultaneously optimizes impedance matching and enhances interfacial polarization, resulting in an RL_{min} of –46.30 dB (Figure 14f)[115]. A SiC_{nw}/SiC_{nf} composite aerogel, constructed via an in-situ free-carbon conversion strategy, forms a hierarchical multi-level network (Figure 14g). This structure not only imparts excellent flexibility and a low TC of 0.053 W/(m·K) but also achieves an ultrawide EAB_{max} of 8.81 GHz at a thickness of 2.94 mm (Figure 14h)[73]. An even more extreme example is a SiC aerogel with an ultralow density of 0.008 $g \cdot cm^{-3}$, exhibiting a room-temperature TC of only 0.018 W/(m·K), alongside outstanding elastic recovery and efficient EMW absorption performance[91]. Collectively, these materials highlight the fundamental role of porous architectures in synergistically enhancing both EMW absorption and thermal insulation.

Introducing secondary or multiple ceramic phases to generate heterogeneous interfaces within porous architectures is a key strategy for enhancing interfacial polarization loss while simultaneously improving high-temperature stability and thermal insulation. A representative example is the alternating multilayer Si_3N_4/SiC aerogel inspired by the lobster shell structure. In this architecture, Si_3N_4 serves as a transparent layer to optimize impedance matching, whereas SiC functions as an absorbing layer to provide dielectric loss. The multilayer-induced "reflection–absorption–zigzag reflection" mechanism synergizes with the porous network (Figure 14i), yielding a wide EAB_{max} of 8.4 GHz and an RL_{min} of –45 dB at room temperature, while maintaining excellent performance at 1000 °C, with the back-surface temperature stabilizing around 300°C (Figures 14j and 14k), thereby demonstrating superior thermal

protection[217]. Similarly, SiC/Si_3N_4 composite aerogels exploit the bicontinuous network formed by the two components to achieve low TC of 0.03 W/(m·K) and high-temperature stability at 1000°C, alongside an EAB_{max} of 7.4 GHz and an RL_{min} of –48.6 dB[218]. The incorporation of ZrO_2 has also proven effective for interfacial engineering. ZrO_2/SiC composite nanofiber aerogels exhibit an ultralow density of 6.6 $mg \cdot cm^{-3}$, a TC of only 0.024 W/(m·K), and achieve an RL_{min} of –53.1 dB with an EAB_{max} of 6.4 GHz, owing to the abundant heterogeneous interfaces[116]. Collectively, these studies demonstrate that the synergistic design of porous architectures and heterogeneous interfaces establishes highly efficient pathways for electromagnetic energy dissipation and thermal management.

The synergistic enhancement of EMW absorption and thermal insulation fundamentally relies on the construction of multifunctional microstructures. 3D high-porosity networks provide the structural foundation, simultaneously suppressing heat conduction and extending the propagation path of EMW, thereby achieving both low TC and optimized impedance matching. The introduction of heterogeneous interfaces within this framework is critical, as these interfaces not only enhance interfacial polarization to improve electromagnetic energy dissipation but also act as phonon scattering centers, impeding heat transfer and enhancing high-temperature stability. This integrated strategy, combining macroscopic porous architectures with microscopic interfacial engineering, establishes the fundamental principles and material basis for the design of advanced thermal-EMW absorption materials suitable for extreme environments. Multiscale architectures synergistically regulate polarization behavior, energy transport pathways, and heat conduction processes across different length scales, enabling coupled optimization of electromagnetic attenuation and thermal insulation.

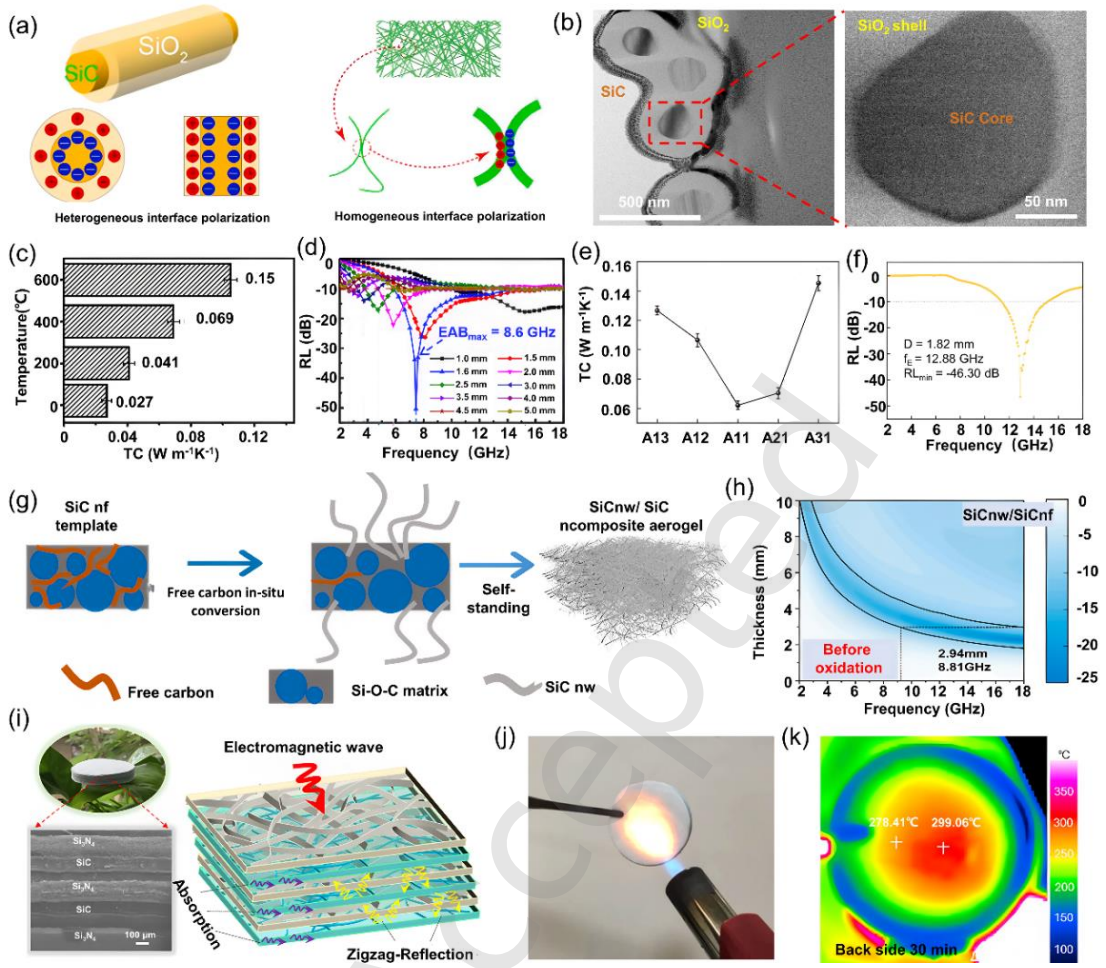

Figure 14. Porous structure and heterogeneous interfaces synergistic regulation enable efficient energy conversion and barrier functions. (a) Schematic of the MA mechanisms for the SNCA. Reproduced with permission[160], Copyright 2024, Elsevier; (b) TEM images of the SiC@SiO_2 nanofibers; (c) and (d) Thermal conductivities and EMW absorption performance of the SiC@SiO_2 NFA. Reproduced with permission[114], Copyright 2021, Springer; (e) and (f) TC and EMW absorption performance of SiC aerogels. Reproduced with permission[115], Copyright 2024, Springer; (g) Schematic diagram of SiC_{nw}/SiC_{nf} composite aerogel. (h) RL of SiC_{nw}/SiC_{nf} before oxidation. Reproduced with permission[73], Copyright 2024, Elsevier; Alternating Multilayered Si_3N_4/SiC Aerogels and the electromagnetic attenuation mechanism. (j) and (k) Optical photograph of the Alternating Multilayered Si_3N_4/SiC Aerogels during ablation and back side thermal infrared images. Reproduced with permission[217], Copyright 2021, American Chemical Society.

5.3.2 SiC aerogel composite materials innovative composition and

multidimensional compounding can expand performance boundaries and application potential

Beyond the construction of ideal microstructures, innovations in composition and the integration of multi-dimensional materials enable the introduction of diverse loss mechanisms, further optimizing overall performance and expanding applicability under demanding conditions. A widely adopted strategy is the incorporation of SiC with carbonaceous materials to enhance conductive loss and interfacial polarization while maintaining low TC. In particular, graphene/SiC nanosheet aerogels combine the high conductivity of graphene with the dielectric nature of SiC, where heterogeneous interfaces and a 3D porous network act synergistically to improve electromagnetic response (Figure 15a). These aerogels exhibit excellent thermal insulation, with a TC of 0.029 W/(m·K), while achieving an ultrahigh RL_{min} of –65.08 dB (Figure 15b)[117]. Similarly, the rGO/m-SiC_{NWs} composite aerogels exploit component synergy (Figure 15c) to attain an RL_{min} of –42.23 dB and an EAB_{max} of 7.47 GHz, while maintaining low TC (0.061 W/(m·K)) and robust thermal stability (Figure 15d)[161]. The incorporation of CNTs further enhances performance. CNT@SiC nanostructure-reinforced SiC aerogels benefit from increased conductive loss and interfacial polarization provided by the CNTs (Figure 15e), achieving an RL_{min} of –66.01 dB and an EAB_{max} of 6.76 GHz, while preserving low TC (0.0582 W/(m·K)) and high-temperature structural stability[74].

Introducing magnetic components to construct a dielectric–magnetic synergistic loss mechanism is an effective strategy for improving low-frequency EMW absorption and optimizing impedance matching. Metal–organic framework-derived Co@SiC nanowire composite aerogels exemplify this approach. Cobalt nanoparticles provide magnetic loss, and their synergy with SiC nanowires and layered porous structures (Figure 15f) enables the material to achieve an RL_{min} of –61.4 dB and an EAB_{max} of 7.44 GHz at a thickness of 2.64 mm. Concurrently, the aerogel maintains self-supporting mechanical properties and excellent thermal insulation performance (Figure 15g)[219]. Similarly, magnetic nickel nanoparticle channels constructed on SiC/SiO_2 foams via electroless plating yield $Ni/SiC/SiO_2$ porous composites that exploit deep

dielectric–magnetic synergy, achieving an RL_{min} of –64.86 dB and an EAB_{max} of 5.12 GHz at a thickness of 1.46 mm, while retaining lightweight and high-temperature-resistant characteristics[118]. This dielectric–magnetic synergistic design not only strengthens electromagnetic energy dissipation but also minimally affects thermal insulation, preserving the material's overall thermal protection functionality.

Driven by the demand for operation in higher-frequency regimes (e.g., the terahertz band) and advanced multifunctional scenarios such as radar–infrared compatible stealth, multidimensional compositional engineering and metamaterial-inspired architectures have emerged as highly promising strategies. In this context, $ZrB_2@SiC_{nw}$ composite aerogels constructed via a 0D/1D/3D dimensional design strategy integrate 0D ZrB_2 nanoparticles with 1D SiC nanowires to build an interconnected 3D network structure (Figure 15h). This architecture enables effective absorption across the entire X-band at 873 K, with an RL_{min} of –61.9 dB, while maintaining excellent thermal insulation properties (Figure 15i)[223]. Sandwich structures, such as SiO_2/C@SiC/SiO_2, represent an effective design for radar–infrared compatible stealth. In this configuration, the central C@SiC layer functions as the primary wave-absorbing medium, whereas the outer SiO_2 aerogel layers provide thermal insulation and optimize impedance matching (Figure 15j). The optimized structure exhibits a surface temperature of only 44°C when exposed to 200°C and delivers effective absorption across the entire X-band[224]. Further, multilayer radar–infrared compatible stealth metamaterials, constructed by integrating a SiC nanowire composite dielectric layer with a frequency-selective surface, achieve effective absorption ($RL < -10$ dB) over an ultra-wide frequency range of 2.42–30 GHz. These materials simultaneously reduce infrared emissivity to 0.292 and exhibit pronounced thermal insulation, making them well-suited for protecting defense equipment under harsh high-temperature conditions (Figure 15k)[225]. Collectively, these macroscopic structural designs transcend the limitations of single-component systems, enabling the integration of wave absorption, thermal insulation, and infrared stealth through the spatial arrangement of functional layers.

Furthermore, biomass-derived templates, such as carbonized silk fibers, as well as

advanced fabrication strategies for constructing hierarchical architectures, have been demonstrated to significantly enhance overall performance. A hierarchical SiC fiber aerogel, prepared using carbonized silk fibers as a template, exhibits an ultralow density of 0.04 $g \cdot cm^{-3}$. Its porous architecture and heterogeneous interfaces act synergistically (Figure 15l), delivering an ultra-low TC of 0.027 W/(m·K) and an exceptional RL_{min} of –68 dB with an EAB_{max} of 7.2 GHz[162]. Similarly, a zirconium-modified hierarchical porous SiC-based nanofiber aerogel, fabricated via electrospinning and carbothermal reduction, incorporates Zr to form a highly conductive ZrC phase, enhancing conductive loss. This design achieves an RL_{min} of –60.72 dB while maintaining ultralow TC in the range of 0.023–0.024 W/(m·K)[226]. These examples demonstrate that through cross-scale structural engineering combined with innovative multi-component composites, the performance limits of SiC-based materials can be continuously advanced in terms of ultralight weight, broadband EMW absorption, and efficient thermal insulation.

Through multidimensional compounding and compositional engineering, SiC-based aerogels evolve into multifunctional systems that integrate efficient electromagnetic energy dissipation with intrinsically low TC. Carbonaceous integration enhances conductive pathways and interfacial polarization, thereby strengthening dielectric loss while generally preserving the ultralow TC enabled by the porous framework. Magnetic component incorporation further introduces dielectric–magnetic synergistic losses that extend low-frequency absorption and improve impedance matching, albeit with carefully balanced effects on thermal transport. At higher complexity levels, multidimensional architectures, sandwich configurations, and metamaterial designs enable spatial decoupling and functional integration, allowing simultaneous optimization of EMW absorption, thermal insulation (ultralow TC), and infrared regulation. Collectively, these cross-scale designs establish a coupled structure–composition–property paradigm that reconciles electromagnetic attenuation with thermal transport suppression, enabling robust performance in extreme thermal–electromagnetic environments.

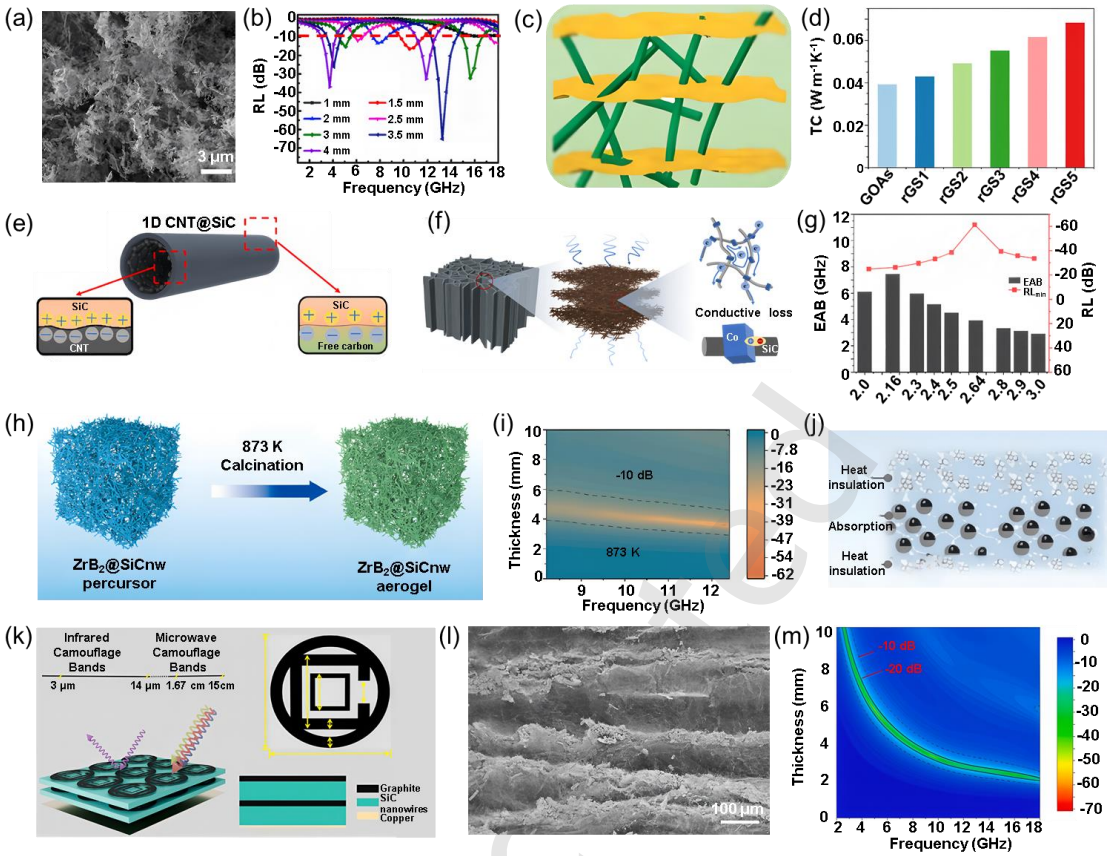

Figure 15. Composites innovative composition and multidimensional compounding. (a) and (b) SEM image and RLs of SiC/G. Reproduced with permission[117], Copyright 2022, Elsevier; (c) Schematic of rGO/m-SiC_{NWs}; (d) Thermal conductivities of GOAs and rGO/m-SiC_{NWs}. Reproduced with permission[161], Copyright 2024, IOP publishing; (e) Schematic illustration of the C@SAs. Reproduced with permission[74], Copyright 2025, Elsevier; (f) Microwave attenuation mechanism of the Co@SiCnw nanocomposite aerogel. (g) RL_{min} and EAB values of the Co@SiC_{nw} sample. Reproduced with permission [219], Copyright 2025, American Chemical Society; (h) and (i) Synthesis process diagram and RL of ZrB_2@SiC_{nw} nanocomposite aerogel. Reproduced with permission [223], Copyright 2025, Elsevier; (j) the sandwich structured SiO_2/C@SiC/SiO_2 composites; Reproduced with permission[224], Copyright 2024, Wiley-VCH. (k) Schematic diagram of HTSM's radar-infrared stealth mechanism. Reproduced with permission [225], Copyright 2024, IOP publishing. (l) and (m) Cross-section SEM image and RL of Hierarchical SiC fiber aerogel. Reproduced with permission [162], Copyright 2022, Elsevier.

5.3.3 SiC aerogel macrostructure design and performance regulation: application-

oriented performance optimization

Moving beyond microscopic components and mesoscopic architectures, sophisticated macroscopic structural design plays a crucial role in achieving synergistic enhancement of EMW and thermal insulation while addressing specific engineering requirements. Through multilayered heterogeneous design, a layered composite aerogel comprising a hollow SiC@SiO_2 fiber framework interwoven with a nanowire network (Figure 16a) was fabricated. This structure delivers excellent wave absorption, exhibiting a wide EAB_{max} of 5.46 GHz and a strong RL_{min} of –67.62 dB (Figure 16b), while also maintaining ultralow TC (0.02 W/(m·K)) and robust thermal insulation at temperatures exceeding 1000 °C[227]. Similarly, a double-layered SiC-reinforced SiO_2 aerogel employs the SiO_2 layer to provide baseline thermal insulation and optimize impedance matching, while the SiC layer serves as the primary electromagnetic loss medium (Figure 16c), achieving an EAB_{max} of 6.8 GHz at a thickness of 4.0 mm (Figure 16d)[228]. The layered porous architecture of an all-ceramic SiC aerogel (Figure 16e) contributes to a low TC of 0.049 W/(m·K), and, owing to optimized impedance matching and heterogeneous interfaces, enables effective attenuation across the entire X-band from room temperature to 400 °C at a thickness of 3.3 mm, with an RL_{min} of –64.4 dB (Figure 16f), demonstrating substantial potential for wide-temperature range applications[163].

The core–shell architecture represents a highly effective strategy for achieving functional integration at the nano and micro-scale. By precisely controlling the oxidation of SiC nanowires, an amorphous SiO_2 sheath of defined thickness is formed on their surface, yielding a SiC@SiO_2 core–shell structure. Samples oxidized for 30 minutes exhibit optimal performance, with the SiO_2 shell effectively tuning impedance matching and enhancing defect-induced polarization (Figure 16g), resulting in an RL_{min} of –57.22 dB and an EAB_{max} of 9.4 GHz (Figure 16h). Simultaneously, the material maintains ultrahigh porosity and a room-temperature TC below 0.020 W/(m·K)[229]. This core–shell design strategy has also been extended to nanofibers. SiC@SiO_2 core–shell nanofibers fabricated via CVD followed by controlled oxidation (Figure 16i) demonstrate excellent wave absorption (RL_{min} of –

53.09 dB, EAB_{max} of 8.85 GHz) while preserving strong thermal insulation performance[230]. At the particle scale, porous heterogeneous SiC/SiO_2 microspheres further illustrate the potential for functional synergy. Their abundant heterogeneous interfaces and internal porosity enable an ultrawide EAB_{max} of 8.49 GHz and an RL_{min} of –54.68 dB at a low filler loading of only 10 wt%, while also offering promise as thermal insulation fillers[231].

The design of hollow and hierarchical pore architectures can further optimize impedance characteristics, enhance multiple reflections of EMW, and maintain superior thermal insulation. Aerogels featuring a hollow SiC microtubule framework, with their distinctive hollow structure and synergistic SiC-SiO_2 heterointerfaces (Figure 16j), achieve an EAB_{max} of 6.7 GHz and an ultralow TC of 0.028 W/(m·K) at a porosity of 98.1 % and a density of only 0.06 g·cm^{-3} (Figure 16k)[119]. SiC aerogels with tunable nanopores (SC-1550) display continuous dual-peak absorption arising from the overlap of the SiC-dominated primary absorption peak and a secondary peak induced by dielectric resonance within the nanopores. This results in an EAB_{max} of 6.24 GHz at a thickness of 3.59 mm, fully covering the Ku band, while retaining a lightweight structure (36.8 mg·cm^{-3}) and excellent thermal insulation[232]. SiOC/SiC foams composed of SiOC flakes interwoven with SiC nanowires leverage their 3D porous network and synergistically optimized properties to achieve densities of 0.07–0.13 g·cm^{-3}, TC as low as 0.028 W/(m·K) at 23 °C, and sustained thermal insulation at 1000 °C, while simultaneously providing an EAB_{max} of 5.4 GHz[220].

In function-oriented macroscopic structural design, synergistic optimization of EMW absorption and thermal insulation can be achieved through the construction of hierarchical porous architectures. Employing an in situ CVD strategy with a carbon foam template, a three-dimensional network was constructed in which SiC nanofibers were grown within the carbon framework and subsequently coated with polypyrrole. This conductor-semiconductor-conductor multi-interface design markedly enhances interfacial polarization and conductive loss, enabling the material to achieve a strong RL_{min} of –60.31 dB and a wide EAB_{max} of 4.88 GHz at an ultralow density of 0.013 g·cm^{-3}. Concurrently, the nanofiber network and microporous structure

synergistically suppress heat conduction and convection, yielding an ultralow TC of 0.03 W/(m·K) and a thermal insulation temperature difference exceeding 759 °C under high-temperature flames (Figure 16l)[164]. Similarly, SiC foams featuring hierarchical micro–nano pores, prepared via biomass templating and carbothermal reduction, combine mechanical robustness, with a micron-sized framework supporting compressive strengths up to 9.8 MPa, and enhanced electromagnetic performance through extended heat transfer paths and multiple reflections within the nanopores. These materials exhibit low TC of 0.02 W/(m·K) and efficient electromagnetic shielding, with a specific shielding effectiveness exceeding 24.8 $dB \cdot cm^3 \cdot g^{-1}$ at 72.8 % porosity[233]. Collectively, these examples demonstrate that the synergistic integration of macroscopic porous frameworks and microscopic nanonetworks enables lightweight systems to simultaneously achieve superior wave absorption and thermal insulation, providing critical guidance for the design of high-temperature stealth and thermal protection materials.

Macroscopic structural engineering plays a pivotal role in achieving the synergistic combination of EMW absorption and thermal insulation in SiC-based aerogels. By introducing multilayer heterogeneous architectures, impedance matching can be effectively optimized, while electromagnetic attenuation is spatially orchestrated through functional partitioning. At the nanoscale, core-shell structures integrate impedance control and interfacial polarization, facilitating simultaneous optimization of electromagnetic and thermal properties. Hollow and hierarchical porous architectures further combine lightweight design, mechanical robustness, and thermal–electromagnetic management by extending energy transfer pathways and introducing multiple interfaces to enhance polarization losses. Through these cross-scale strategies, impedance matching, energy dissipation mechanisms, and heat transport are systematically coordinated, allowing the material to concurrently achieve ultralow TC, broadband strong absorption, and environmental stability within a single system. This framework establishes a foundation for the development and component-level application of next-generation integrated protective materials.

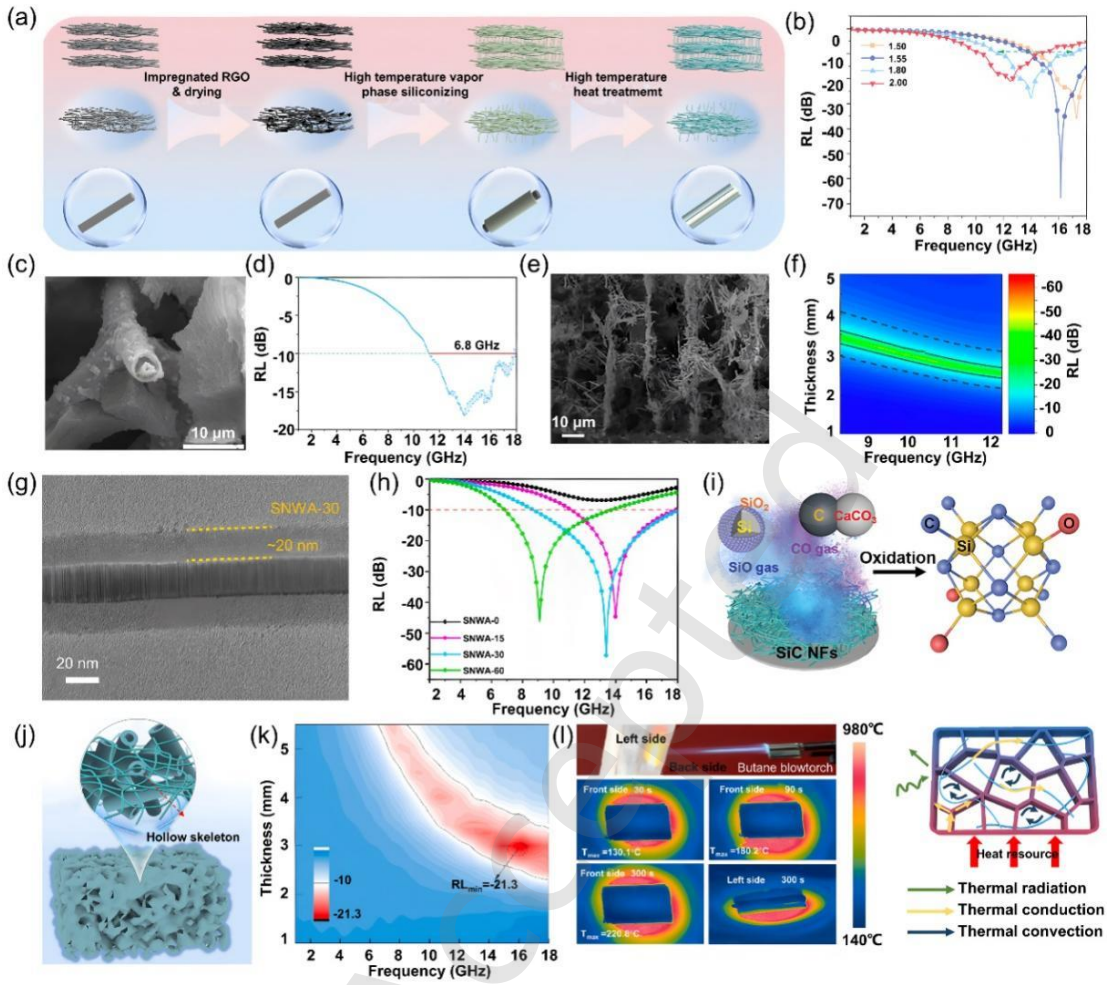

Figure 16. Macrostructure design and performance regulation: application-oriented performance optimization. (a) and (b) Schematic representation and RL of the layered hollow fiber skeleton based SiC@SiO_2 nanowire aerogel. Reproduced with permission[227], Copyright 2022, Elsevier; (c) and (d) SEM and RL of double-layered SiC aerogel. Reproduced with permission[228], Copyright 2023, Elsevier ; (e) and (f) SEM and RL of SiC ceramic aerogel**.** Reproduced with permission[163], Copyright 2022, American Chemical Society; (g) and (h) SEM and RL of SiC nanowire aerogels. Reproduced with permission[229], Copyright 2024, Elsevier; (i) Schematic of SiC@SiO_2 NFs synthesis. Reproduced with permission[230], Copyright 2024, Wiley-VCH. (j) and (k) Schematic diagram andRL of SAs-H-H. Reproduced with permission[119], Copyright 2022, Elsevier; (l) The thermal infrared images and the thermal insulation mechanism of C/SiC nanofiber aerogel. Reproduced with permission[164], Copyright 2024, Elsevier.

6. Conclusions and outlook

6.1 Conclusions

This article provides a comprehensive review of SiC aerogels as a novel multifunctional material that integrates the intrinsic superior properties of SiC with the unique 3D porous architecture of aerogels. The development of SiC aerogels addresses the limitations of conventional oxide aerogels, which suffer performance degradation at elevated temperatures due to sintering and phase transitions, as well as carbon-based aerogels, which are prone to oxidation. SiC exhibits ultrahigh temperature stability, withstanding 1000 to 1200 °C in air, along with high mechanical strength and wide bandgap semiconductor characteristics. When incorporated into the highly porous, low-density network of aerogels, these properties combine synergistically to produce a "1+1>2" effect, enabling the material to perform thermal insulation and EMW absorption under extreme high-temperature conditions.

The exceptional performance of SiC aerogels arises from the synergy between their refined microstructure and intrinsic material properties. Thermal insulation is achieved through the construction of a triple-barrier system. The nano-labyrinthine framework elongates phonon pathways and enhances interfacial scattering, thereby suppressing solid-state heat conduction. Pore sizes smaller than the mean free path of air molecules confine the gas within the nanopores, effectively eliminating gas conduction and convection. Furthermore, the SiC framework itself functions as an intrinsic shading agent, strongly absorbing and scattering infrared radiation at temperatures above 800°C, providing efficient high-temperature radiative shielding. EMW absorption is derived from the combination of intrinsic dielectric loss, including resistive and relaxation loss, and the 3D porous structure. The hierarchical porosity optimizes impedance matching, facilitating wave entry, while multiple scattering and reflection events within the nanonetwork extend the wave propagation path, allowing repeated energy dissipation and simultaneously achieving ultralightweight absorption.

Through rational microstructural design, including hierarchical pores, core-shell, and layered or hollow architectures, as well as component compounding with carbon, magnetic, or other ceramic materials and macroscopic configuration control, such as multilayered and gradient structures, the thermal, dielectric, and mechanical properties

of SiC aerogels can be precisely tuned. Recent studies have demonstrated SiC-based composite aerogels exhibiting ultralow TC, typically below 0.03 W/(m·K), and strong EMW absorption, with RL_{min} reaching below -50 dB and effective absorption bandwidths spanning several gigahertz or even ultra-wide bands. These materials maintain stable thermal insulation from room temperature to over 1000°C and integrate multifunctional capabilities, including wave absorption, thermal insulation, mechanical reinforcement, and infrared stealth. Such properties highlight their substantial potential for applications in aerospace thermal protection, military stealth technologies, thermal management of advanced batteries, and electromagnetic compatibility and heat dissipation in high-end electronic devices. In summary, the unique and highly designable structure and composition of SiC aerogels position them as a highly promising advanced material platform for addressing the dual challenges of thermal management and EMW control in extreme environments.

6.2 Outlook

SiC aerogels, as advanced multifunctional materials integrating ultralow TC, high-temperature stability, lightweight yet high mechanical strength, and efficient EMW absorption, have demonstrated significant application potential in a range of cutting-edge fields. However, their further development still faces several critical challenges. First, in terms of fabrication techniques, existing approaches such as sol-gel processing, carbothermal reduction, and chemical vapor deposition are generally associated with complex procedures, high costs, and limited control over the uniformity and reproducibility of microstructures. Therefore, there is an urgent need to develop efficient, controllable, low-cost, and scalable fabrication strategies suitable for large-scale production. On this basis, particular attention should also be paid to the coordinated control of structural consistency and performance stability during scale-up processes, while exploring feasible routes such as low-cost precursor design, process simplification, and rapid drying techniques.

Second, from the perspective of performance optimization, key challenges remain in simultaneously maintaining ultralow TC while further enhancing mechanical properties, especially toughness, achieving more stable and efficient EMW absorption

over broad temperature and frequency ranges, and realizing precise multi-performance synergy and balance through cross-scale structural design. In addition, the intrinsic stability of dielectric properties of SiC aerogels under high-temperature conditions, as well as their correlation with structural evolution, still requires further elucidation to provide a more reliable theoretical foundation for regulating their electromagnetic response.

Furthermore, for extreme service environments such as thermal protection systems for hypersonic vehicles, thermal insulation in advanced nuclear energy systems, and electromagnetic compatibility in high-frequency communication devices, it is necessary to conduct in-depth investigations into long-term stability, failure mechanisms, and lifetime prediction under complex multi-field coupled conditions involving stress, heat, and radiation. In particular, the structural evolution behavior under sustained high-temperature and complex loading conditions, and its impact on overall performance, deserves special attention.

Finally, to facilitate the transition of SiC aerogels from laboratory research to engineering applications, their compatibility with existing material systems, processability, and integration strategies must be further strengthened, along with the establishment of standardized performance evaluation protocols and application databases. At the same time, a systematic development pathway should be constructed to address key bottlenecks such as scalable fabrication, cost control, and structural stability. Looking forward, through the deep integration of materials science, chemistry, physics, and engineering disciplines, SiC aerogels are expected to achieve broader and more profound breakthroughs in key fields such as aerospace, defense technology, new energy, and electronic information.

Acknowledgements

This work was financially supported by the National Natural Science Foundation of China (52502079 and 52503085), China Postdoctoral Science Foundation (2024M760816), Henan Province Science and Technology Research Project (252102231066 and 252102320354), the Key Research and Development Project of Henan Province (241111231600), the Basic Scientific Research Project of Henan

Academy of Sciences (20250643001 and 20250643002), the Scientific Research Startup Project of Henan Academy of Sciences (20251843001 and 20251843002), Joint Fund of Research and Development Program of Henan Province (235200810089 and 245200810064), the Natural Science Foundation of Henan Province (252300423415), 2025 Special Project for Enhancing the Basic Disciplinary Innovation Capacity of Zhengzhou University of Aeronautics (XKZX25100).

Declaration of competing interest

The authors have no competing interests to declare that are relevant to the content of this article.

References

[1] Wang D, Song C, Dang S*, et al.* High-entropy ceramic aerogel with ultrahigh thermomechanical properties. *ACS Appl Mater Interfaces* 2025, 17: 18636-18644.
[2] Xu Z, Liu Y, Xin Q*, et al.* Ceramic meta-aerogel with thermal superinsulation up to 1700°C constructed by self-crosslinked nanofibrous network via reaction electrospinning. *Adv Mater* 2024, 36: 2401299.
[3] Wu L, Zhang H, Li J*, et al.* A superelastic polymeric aerogel with ultrahigh fire resistance for thermal insulation in a harsh environment. *J Mater Chem A* 2025, 13: 33855-33865.
[4] Chen Y, Song C, Chen L*, et al.* Scalable multi-stage spinning of weavable high temperature resistant SiNAFs@PSO/Aramid composite aerogel fibers. *J Colloid Interface Sci* 2025, 700: 138437.
[5] Niu Z, Qu F, Chen F*, et al.* Multifunctional integrated organic-inorganic-metal hybrid aerogel for excellent thermal insulation and electromagnetic shielding performance. *Nano-Micro Lett* 2024, 16: 200.
[6] Wang X, Li H, Li H*, et al.* Coaxial porous SiBCN/SiCN ceramic fiber aerogels with reduced shrinkage and low thermal conductivity. *Chem Eng J* 2024, 501: 157621.
[7] Wang R, Wang F, Zhu Y*, et al.* Polysilazane hybrid phenolic resin ceramic aerogels with excellent electromagnetic wave absorption performance. *J Am Ceram Soc* 2024, 107: 1170-1184.
[8] Xu B, Wang F, Yang X*, et al.* Bioinspired fabrication of lightweight gradient ceramizable phenolic aerogel composites with exceptional ablation resistance and thermal insulation for superior thermal protection system. *Corros Sci* 2026, 258: 113382.
[9] Tang J, Wei X, Liu W*, et al.* Lightweight and elastic ceramic nanofiber aerogels designed by enhancing interfacial compatibility for thermal superinsulation in extreme conditions. *ACS Appl Mater Interfaces* 2025, 17: 38357-38366.
[10] Liu Y, Zhang L, Xiao C*, et al.* Thermal insulating Si_3N_4@SiO_2 nanowire aerogel with excellent mechanical performance at high-temperatures up to 1300°C. *Nano Res* 2025, 18: 94907008.

[11] Yang L, Xie J, Wu Q*, et al.* Ultralow thermal conductivity and excellent gamma-radiation resistance of a novel boron-doped silica aerogel for thermal protection in nuclear applications. *ACS Sustain Chem Eng* 2025, 13: 4535-4547.
[12] Wu K, Zhou Q, Cao J*, et al.* Ultrahigh-strength carbon aerogels for high temperature thermal insulation. *J Colloid Interface Sci* 2022, 609: 667-675.
[13] Zhou P, Cheung C F. Temperature dependence of two-dimensional structural evolution of monocrystalline 6H-SiC with vacancy and processing defects. *Ceram Int* 2025, 51: 9176-9188.
[14] You J, Wang Y, Wang H*, et al.* Structural control and mechanical properties optimization of porous SiC foams with three-dimensional network structure. *Mater Today Commun* 2024, 39: 108817.
[15] Song L, Fan B, Chen Y*, et al.* Multifunctional SiC nanofiber aerogel with superior electromagnetic wave absorption. *Ceram Int* 2022, 48: 25140-25150.
[16] Cai Z, Su L, Niu M*, et al.* Ultralight and resilient bicontinuous Si_3N_4/SiC nanowire network for tunable and highly efficient electromagnetic wave absorption in extreme conditions. *Adv Mater Interfaces* 2022, 9: 2201553.
[17] Liu J, Xu L, Yue W*, et al.* Preparation of β-SiAlON/SiC composite ceramic foam filters and their oxidation resistance. *Ceram Int* 2024, 50: 38200-38208.
[18] Wu X, Shao G, Shen X*, et al.* Evolution of the novel C/SiO_2/SiC ternary aerogel with high specific surface area and improved oxidation resistance. *Chem Eng J* 2017, 330: 1022-1034.
[19] Cheng Y, Zhang J, Ren C*, et al.* Facile preparation of high-strength SiC/C aerogels from pre-reacted resorcinol-formaldehyde and siloxane. *J Ind Eng Chem* 2024, 134: 75-83.
[20] Cao X, Duan J, Wang C*, et al.* Structure design and tribological properties of Cu-SiC foam ceramic composites. *Ceram Int* 2024, 50: 7366-7373.
[21] Latypova L, Murzakhanov F, Mamin G*, et al.*, Exploring high-spin color centers in wide band gap semiconductors SiC: a comprehensive magnetic resonance investigation (EPR and ENDOR analysis). *Molecules* 2024, 29: 3033.
[22] Tang X-Z, Zhao Z, Chang W*, et al.* Magnetic SiC aerogel with integrated heat insulation and wave absorption. *Ceram Int* 2025, 51: 63054-63062.
[23] Hao-Qiang P, Zeng-Yao L. Experimental investigations on the thermal insulation performance of SiC opacifier doped silica aerogel at large temperature difference. *Int J Therm Sci* 2021, 160: 106681.
[24] Song L, Hu F, Chen Y*, et al.* Heterointerface-engineered SiC@SiO_2@C nanofibers for simultaneous microwave absorption and corrosion resistance. *Adv Sci* 2025, 12: e09071.
[25] Xiang L, Pan D, Lei J*, et al.* Sodium alginate aerogel derived SiC@Co-C 3D network enhances electromagnetic wave absorption and thermal conductivity of PDMS based composite. *Int J Biol Macromol* 2025, 306: 141539.
[26] Ye X, Chen Z, Li M*, et al.* Microstructure and microwave absorption performance variation of SiC/C foam at different elevated-temperature heat treatment. *ACS Sustain Chem Eng* 2019, 7: 18395-18404.
[27] Ye X, Chen Z, Ai S*, et al.* Porous SiC/melamine-derived carbon foam frameworks

with excellent electromagnetic wave absorbing capacity. *J Adv Ceram* 2019, 8: 479-488.
[28] Su K, Dou Q, Wang Y*, et al.* SiC_{nw}@SiC foam prepared based on vapor-solid mechanism for efficient microwave absorption. *Ceram Int* 2023, 49: 450-460.
[29] Huang Y, Yang L, Hou M*, et al.* Low-temperature microwave sintering of foam SiC for mechanical properties and electromagnetic absorption. *Ceram Int* 2024, 50: 55682-55692.
[30] Ding C, Hu D, He X*, et al.* Fabrication and microstructure evolution of monolithic bridged polysilsesquioxane-derived SiC ceramic aerogels. *Ceram Int* 2022, 48: 25833-25839.
[31] Ye X, Chen Z, Ai S*, et al.* Microstructure characterization and thermal performance of reticulated SiC skeleton reinforced silica aerogel composites. *Compos Part B-Eng* 2019, 177: 107409.
[32] Xia Y, Zhang Z, Li K*, et al.* Lightweight and high-strength SiC/MWCNTs nanofibrous aerogel derived from RGO/MWCNTs aerogel for microwave absorption. *Chem Eng J* 2024, 486: 150417.
[33] Jiang J, Yan L, Li J*, et al.* Lightweight and resilient SiBCNa/mullite/SiC_{nw} composite for thermal insulation and electromagnetic wave absorption. *Ceram Int* 2025, 51: 2315-2323.
[34] Zhang B, Duan J, Wu A*, et al.* Hierarchical porous Zr-SiC nanofibrous aerogels for advanced thermal insulation and electromagnetic wave absorption. *Chem Eng J* 2025, 524: 169757.
[35] Han L, Li X, Li F*, et al.* In-situ preparation of SiC reinforced Si_3N_4 ceramics aerogels by foam-gelcasting method. *Ceram Int* 2022, 48: 1166-1172.
[36] Su X, Qi Z, Qu H*, et al.* Effects of pore density on microstructure and mechanical properties of porous SiC ceramic foam/Zr-based metallic glass interpenetrating phase composites. *Intermetallics* 2021, 129: 106964.
[37] Han M, Yin X, Hou Z*, et al.* Flexible and thermostable graphene/SiC nanowire foam composites with tunable electromagnetic wave absorption properties. *ACS Appl Mater Interfaces* 2017, 9: 11803-11810.
[38] Liu Q, Hai W, Li M*, et al.* Synthesis of hierarchical SiC@MA@Ni heterostructure fibers via MXene-reduced Ag NPs activator and electroless Ni deposition for electromagnetic microwaves absorption. *Appl Mater Tody* 2026, 48: 102997.
[39] Gordani G R, Loghman Estarki M R, Kiani E*, et al.* The effects of strontium ferrite micro-and nanoparticles on the microstructure, phase, magnetic properties, and electromagnetic waves absorption of graphene oxide-$SrFe_{12}O_{19}$-SiC aerogel nanocomposite. *J Magn Magn Mater* 2022, 545: 168667.
[40] Yuan K, Han D, Liang J*, et al.* Microwave induced in-situ formation of SiC nanowires on SiCNO ceramic aerogels with excellent electromagnetic wave absorption performance. *J Adv Ceram* 2021, 10: 1140-1151.
[41] Zhang B, Zhi W, Duan J*, et al.* Mechanically robust SiC aerogel with both electromagnetic absorption and pollutant adsorption via microtube/nanowire structure design. *J Adv Ceram* 2025, 14: 9221181.
[42] Ni Z, Lu D, Jia S*, et al.* Gradient impedance all-ceramic aerogels: resolving the

trade-off between broadband and strong microwave absorption. *ACS Appl Mater Interfaces* 2025, 17: 43189-43198.
[43] Zhang H, Deng G, Sun X*, et al.* Interface chemical welding by nanoparticles endow ceramic aerogels with broad-temperature microwave absorption and thermal insulation. *Adv Funct Mater* 2025, n/a: e24866.
[44] Huo Y, Zhao K, Xu Z*, et al.* Ultralight and superelastic polyvinyl alcohol/SiC nanofiber/reduced graphene oxide hybrid foams with excellent thermal insulation and microwave absorption properties. *Ceram Int* 2021, 47: 25986-25996.
[45] Li X, Qi Y, Lu K*, et al.* Simple preparation of SiC@SiO_2 nanofiber with bead-like structure by microwave sintering. *Ceram Int* 2024, 50: 13982-13987.
[46] Wang Y, Han H, Zhang M*, et al.* Biomass-derived carbon-based SiC coral-like nanostructures for electromagnetic wave absorption. *Nano Res* 2025, 18: 94907790.
[47] Huo Y, Tan Y, Zhang F*, et al.* Carbon-ceramic nanofiber embedded with LDHs-derived composites for enhanced electromagnetic wave absorption. *Ceram Int* 2023, 49: 33039-33050.
[48] Xiao S, Mei H, Han D*, et al.* Sandwich-like SiC_{nw}/C/Si_3N_4 porous layered composite for full X-band electromagnetic wave absorption at elevated temperature. *Compos Part B-Eng* 2020, 183: 107629.
[49] Li W, Li C, Lin L*, et al.* All-dielectric radar absorbing array metamaterial based on silicon carbide/carbon foam material. *J Alloy Compd* 2019, 781: 883-891.
[50] Du B, Zhang D, Qian J*, et al.* Multifunctional carbon nanofiber-SiC nanowire aerogel films with superior microwave absorbing performance. *Adv Compos Hybrid Ma* 2021, 4: 1281-1291.
[51] Yang M, Chen Z, Ding Y*, et al.* A lightweight and high compressive resistance thermal insulation material with dual-network structure. *Nano Res* 2024, 17: 4279-4287.
[52] Shao G, Xu R, Chen Y*, et al.* Miniaturized hard carbon nanofiber aerogels: from multiscale electromagnetic response manipulation to integrated multifunctional absorbers. *Adv Funct Mater* 2024, 34: 2408252.
[53] Yu G, Shao G, Xu Z*, et al.* Hierarchical interface-engineered magnetic graphene-SiCN aerogels via a stepwise confinement strategy for low-frequency and broadband microwave absorption. *J Adv Ceram* 2025, 14: 9221187.
[54] Shen W, Tan S, Wang T. Preparation and properties of gypsum-based modified SiO_2 aerogel fire resistive coating. *Constr Build Mater* 2025, 489: 142237.
[55] Luo R, Xie F, Zhang H*, et al.* High-efficiency thermal insulation materials optimization of Al_2O_3f@Al_2O_3/RF/SiO_2. *J Mater Res Technol* 2025, 38: 5135-5145.
[56] Ye X, Xu P, Yu H*, et al.* Preparation and microwave absorption performance of SiC aerogel via sol-gel and carbonization reduction process. *Def Technol* 2024, 42: 73-82.
[57] Xu F, Yang Y, Kong Y*, et al.* Fe_3Si-encapsulated SiC aerogels enable low-frequency electromagnetic wave absorption with extreme-temperature resistance and thermal insulation. *Compos Part B-Eng* 2026, 311: 113204.
[58] Cai X, Lin H, Sun Z*, et al.* Anomalous high-temperature oxidation behavior of SiC coatings on C_f/SiC Composites: degradation mechanisms and microstructural evolution from 1200°C to 1400°C. *Compos Part B-Eng* 2025, 303: 112605.

[59] Liu H, Peng Z, Yuan W, *et al.* Silicon carbide modified mullite fiber ceramic aerogel with high strength and favourable high-temperature infrared shielding capabilities. *J Sol-Gel Sci Technol* 2025, 114: 549-558.
[60] Zheng C, Yu J, Li X, *et al.* Synthesis of carbon fiber reinforced SiC aerogel composites with enhanced mechanical and antioxidant properties for high temperature insulation. *J Mater Res Technol* 2025, 36: 4547-4556.
[61] Wu Q, Yang L, Chen Z, *et al.* SiO_2 aerogel multiscale reinforced by glass fibers and SiC nanowhiskers for thermal insulation. *J Porous Mater* 2023, 30: 1587-1596.
[62] Chen S, Shen K, Chen Z, *et al.* Ultrathin SiO_2 aerogel papers with hierarchical scale enable high-temperature thermal insulation. *Ceram Int* 2024, 50: 17836-17847.
[63] Yan M, Pan Y, He P, *et al.* Hyperelastic and multifunctional SiC/SiO_2 composite aerogels with excellent mechanical, thermal insulation and electromagnetic wave absorbing properties. *Compos Part A-Appl S* 2024, 186: 108408.
[64] Sha R, Wang B, Dai J, *et al.* Ultralight carbon tube foam-derived SiC nanofibrous aerogels with arbitrary shape, excellent rigidity, and resilience for thermal insulation. *ACS Appl Mater Interfaces* 2025, 17: 8209-8218.
[65] Jiang J, Yan L, Song M, *et al.* Thermally insulated C/SiC/SiBCN composite ceramic aerogel with enhanced electromagnetic wave absorption performance. *Ceram Int* 2025, 51: 17-24.
[66] Jin Z, Feng X, Hou Y, *et al.* Lightweight and thermally insulating ZnO/SiC_{nw} aerogel: a promising high temperature electromagnetic wave absorbing material with oxidation resistance. *Chem Eng J* 2024, 498: 155110.
[67] Guo P, Su L, Peng K, *et al.* Additive manufacturing of resilient SiC nanowire aerogels. *ACS Nano* 2022, 16: 6625-6633.
[68] Xiao Y, Mao T, Zhao Z, *et al.* Experimental study of dual nano-network, high-temperature resistant aerogel material as an integration of thermal management functions. *J Energy Chem* 2025, 100: 157-170.
[69] Song L, Fan B, Chen Y, *et al.* Ultralight and hyperelastic SiC nanofiber aerogel spring for personal thermal energy regulation. *J Adv Ceram* 2022, 11: 1235-1248.
[70] Su L, Jia S, Ren J, *et al.* Strong yet flexible ceramic aerogel. *Nat Commun* 2023, 14: 7057.
[71] Wang Z, Zhou Y, Liu J, *et al.* LEGO-inspired fabrication strategy for aramid nanofibers-based multilayer aerogels with tunable multiple functions. *Compos Sci Technol* 2025, 261: 111029.
[72] Yan M, Cheng X, Gong L, *et al.* Growth mechanism and structure regulation of super-elastic SiC aerogels for thermal insulation and electromagnetic wave absorption. *Chem Eng J* 2023, 475: 146417.
[73] Wang T, Feng M, Xiang Z, *et al.* Self-standing and compressible SiC_{nw}/SiC_{nf} composite aerogel via free carbon in-situ transformation mechanism: towards thermal and electromagnetic wave protection. *Compos Part B-Eng* 2024, 279: 111454.
[74] Xu F, Wang Y, Tang F, *et al.* Synergistic enhancement of structure and function in carbonaceous SiC aerogels for improved microwave absorption. *Carbon* 2025, 233: 119854.
[75] Li H, Dong Q, Zheng X, *et al.* Large-scale fabrication of high-performing single-

crystal SiC nanowire sponges using natural loofah. *ACS Sustain Chem Eng* 2023, 11: 2554-2563.
[76] Huang Z, Wang R, Wang Z*, et al.* Preparation and properties of SiC ceramic aerogels with high temperature oxidation resistance. *ACS Appl Eng Mater* 2025, 3: 1834-1843.
[77] An Z, Ye C, Zhang R*, et al.* Multifunctional C/SiO_2/SiC-based aerogels and composites for thermal insulators and electromagnetic interference shielding. *J. Sol-Gel Sci Technol* 2019, 89: 623-633.
[78] Jia X, Wang X, Guo D*, et al.* Lightweight mullite fiber-reinforced SiC_{nw}/SiOC composites for efficient insulation and electromagnetic wave absorption. *Ceram Int* 2025, 51: 12387-12395.
[79] Han D, Mei H, Xiao S*, et al.* Electromagnetic shielding properties of carbon-rich chemical vapor infiltration-prone silicon carbide matrix composites. *J Am Ceram Soc* 2018, 101: 1991-1998.
[80] Cheng Y, Hu P, Zhou S*, et al.* Achieving tunability of effective electromagnetic wave absorption between the whole X-band and Ku-band via adjusting PPy loading in SiC nanowires/graphene hybrid foam. *Carbon* 2018, 132: 430-443.
[81] Su L, Wang H, Niu M*, et al.* Anisotropic and hierarchical SiC@SiO_2 nanowire aerogel with exceptional stiffness and stability for thermal superinsulation. *Sci Adv* 2020, 6: eaay6689.
[82] Liang P, Li H, Wang G*, et al.* Green preparation of 3D large-sized SiC nanowire aerogels. *Mater Lett* 2021, 284: 129014.
[83] Niu M, Fu W, Gao H*, et al.* A nanowire network structure for radiation tolerant ceramic aerogels. *Nano Lett* 2025, 25: 17041-17049.
[84] Su K, Wang Y, Hu K*, et al.* Ultralight and high-strength SiC_{nw}@SiC foam with highly efficient microwave absorption and heat insulation properties. *ACS Appl Mater Interfaces* 2021, 13: 22017-22030.
[85] Xu H, Li X, Tong Z*, et al.*, Thermal radiation shielding and mechanical strengthening of mullite fiber/SiC nanowire aerogels using in situ synthesized SiC nanowires. *Materials* 2022, 15: 3522.
[86] Zhang H, Zhu Z, Ma Y*, et al.* Preparation of bimodal-scale whiskers reinforced alumina aerogel composites via a vacuum freeze-drying process. *J Am Ceram Soc* 2026, 109: e70365.
[87] Wang C, Wang H, Wang B*, et al.* Lightweight broadband electromagnetic wave absorption achieved by a like-clustered CNTs spheres modified SiC nanowires. *Colloid Surface A* 2024, 689: 133756.
[88] Jia X, Zhou Z, Guo D*, et al.* Low-density, large-sized SiC_{nw}/SiOC composite aerogels with excellent thermal insulation, microwave absorption, and thermostability. *Ceram Int* 2024, 50: 33315-33324.
[89] Xia Y, Chen G, Zhang Z*, et al.* Nanowire-filled layered SiC aerogels with excellent thermodynamic properties for thermal insulation at ultrahigh temperatures. *Chem Eng J* 2025, 510: 161479.
[90] Zhang P, Zhao S, Li K*, et al.* Large-scale production of elastic SiC/SiO_2 nanofibrous composite aerogels with a labyrinth structure for high-temperature

insulation, fire prevention, and noise absorption. *Chem Eng J* 2025, 505: 159166.
[91] He P, Pan Y, Yan M*, et al.* Super thermal insulation SiC aerogel with high elasticity and good adsorption performance prepared by constructing coaxial precursor. *Compos Part A-Appl S* 2024, 181: 108153.
[92] Wang W, Zhao Y, Yan W*, et al.* Preparation of the novel B4C-SiC composite aerogel with high compressive strength and low thermal conductivity. *J. Porous Mater* 2021, 28: 703-710.
[93] Pan B, Chen J, Zhang F*, et al.* Porous TiO_2 aerogel-modified SiC ceramic membrane supported MnO_x catalyst for simultaneous removal of NO and dust. *J Membr Sci* 2020, 611: 118366.
[94] Chen Y-T, Peng H, Cai B*, et al.* Synthesis of ultralight hollow SiC/C nanofiber for highly efficient electromagnetic wave absorption. *J Adv Ceram* 2026, 15: 9221225.
[95] Lan X, Li Y, Wang Z. High-temperature electromagnetic wave absorption, mechanical and thermal insulation properties of in-situ grown SiC on porous SiC skeleton. *Chem Eng J* 2020, 397: 125250.
[96] Liang X, Wan P, Wu Z*, et al.* Light and strong nano-SiC foam with extremely low thermal conductivity. *Mater Lett* 2020, 274: 128017.
[97] Zhang X, He J, Han L*, et al.* Foam gel-casting preparation of SiC bonded ZrB_2 porous ceramics for high-performance thermal insulation. *J Eur Ceram Soc* 2023, 43: 37-46.
[98] Wan P, Wu Z, Zhang H*, et al.* Porous nano-SiC as thermal insulator: wisdom on balancing thermal stability, high strength and low thermal conductivity. *Mater Res Lett* 2016, 4: 104-111.
[99] Chen Y, Zhang L, He C*, et al.* Thermal insulation performance and heat transfer mechanism of C/SiC corrugated lattice core sandwich panel. *Aerosp Sci Technol* 2021, 111: 106539.
[100] Zhong Y, Li H, Liu H*, et al.* Bio-inspired gradient multilayer ceramic fiber aerogel loaded with $TaSi_2$ and WSi_2: fabrication, anti-oxidation and thermal insulation. *J Alloy Compd* 2023, 967: 171726.
[101] Uzun S. Comprehensive analysis of nuclear clad materials: neutronics, radiation shielding, and modal assessment. *Nucl Eng Des* 2024, 428: 113510.
[102] Zhao J-J, Duan Y-Y, Wang X-D*, et al.* Optical and radiative properties of infrared opacifier particles loaded in silica aerogels for high temperature thermal insulation. *Int J Therm Sci* 2013, 70: 54-64.
[103] Lei D, Liu C, Wang S*, et al.* Ultrabroad electromagnetic absorbing core-shell $SiC@SiO_2$ nanocomposites derived from in situ oxidation SiC whiskers. *J Alloy Compd* 2024, 994: 174637.
[104] Hou Z, Gao Y, Wang Y*, et al.* Construction of periodic hollow SiC microtube ceramic for synergistic broadband absorption performance at elevated temperatures. *Ceram Int* 2024, 50: 46121-46129.
[105] Sun Y, Zhao L, Hu Y*, et al.* Dense Si_3N_4/SiC composite ceramics with enhanced mechanical and electromagnetic absorption using micron-sized powders via spark plasma sintering. *Ceram Int* 2025, 51: 25673-25680.
[106] Zhao H, Liu W, Liu J*, et al.* Size-dependent electromagnetic wave absorption of

3C-SiC particles. *J Mater Chem C* 2024, 12: 14054-14061.
[107] Yang Y, Huang S, Li J*, et al.* Electromagnetic wave absorption properties and microstructural evolution of TiC-modified polymer-derived SiC ceramics. *Ceram Int* 2025, 51: 15745-15755.
[108] Guo B, Jiang Y, Zhang Y*, et al.* Differentiated electromagnetic wave absorption enabled by load modulation of cross-dimensional SiC nanostructures. *Chem Eng J* 2025, 509: 161364.
[109] Guo J, Chen J, Li J*, et al.* Structural design of the multi-layer SiC nanofiber composite aerogel felt for applications in high-temperature thermal-insulating refractories. *J Eur Ceram Soc* 2025, 45: 117370.
[110] Wang J, Li H, Liu H*, et al.* "Finger coral-like" ceramic fiber aerogels with enhanced high-temperature thermal insulation, anti-oxidation, and mechanical performance. *Compos Sci Technol* 2022, 225: 109515.
[111] Zirakjou A, Kokabi M. SiC/C aerogels from biphenylene-bridged polysilsesquioxane/clay mineral nanocomposite aerogels. *Ceram Int* 2020, 46: 2194-2205.
[112] Wang W, You Q, Wu Z*, et al.* Fabrication of the SiC/HfC composite aerogel with ultra-low thermal conductivity and excellent compressive strength. *Gels* 2024, 10: 292.
[113] Li J, Ahmad Z, Chen J*, et al.* Fabrication of SiC nanofiber aerogel felt with high-temperature thermal insulation performance. *J Eur Ceram Soc* 2024, 44: 1923-1931.
[114] Song L, Zhang F, Chen Y*, et al.* Multifunctional SiC@SiO_2 nanofiber aerogel with ultrabroadband electromagnetic wave absorption. *Nano-Micro Lett* 2022, 14: 152.
[115] Zhang X, Xia C, Liu W*, et al.* Microwave absorption and thermal properties of coral-like SiC aerogel composites prepared by water glass as a silicon source. *Int J Min Met Mater* 2023, 30: 1375-1387.
[116] Zhu H, Weng X, Liao M*, et al.* ZrO_2-interface-engineered SiC nanofiber aerogel with integrated hydrophobicity, thermal insulation, and broadband electromagnetic wave absorption. *Appl Surf Sci* 2025, 711: 164079.
[117] Song L, Chen Y, Gao Q*, et al.* Low weight, low thermal conductivity, and highly efficient electromagnetic wave absorption of three-dimensional Graphene/SiC-nanosheets aerogel. *Compos Part A-Appl S* 2022, 158: 106980.
[118] Xu B, He Q, Wang Y*, et al.* Construction of magnetic nanoparticle channels in SiC/SiO_2 composite foam toward efficient electromagnetic wave absorption. *Appl Surf Sci* 2023, 636: 157839.
[119] Yan M, Pan Y, He P*, et al.* Mechanically strong SiC aerogels with broadband electromagnetic wave absorption enabled by hollow skeleton and interface engineering. *Chem Eng J* 2024, 497: 154556.
[120] Zeng G, Li X, Wei Y*, et al.* Significantly toughened SiC foams with enhanced microwave absorption via in situ growth of Si_3N_4 nanowires. *Chem Eng J* 2021, 426: 131745.
[121] Lv S, Jiang Y, Liu M*, et al.* Vacancy-mediated electromagnetic loss tuning in Cr-doped lanthanum manganite perovskites for broadband and high-intensity microwave absorption. *J Adv Ceram* 2025, 14: 9221202.
[122] Yao P, Li X, Zhang Y*, et al.* Electromagnetic wave absorption and shielding

performances and mechanisms of a porous Ti_3AlC_2/SiC gradient composite. *ACS Appl Electron Mater* 2023, 5: 1558-1565.
[123] Liu J, Li G, Zhao T*, et al.*, The effects of in situ growth of SiC nanowires on the electromagnetic wave absorption properties of SiC porous ceramics. *Materials*, 2025, 18: 1910.
[124] Li H, Deng W, Li T*, et al.* Construction of SiC_{nws}/carbon foam composites with multiple loss mechanisms for excellent electromagnetic wave absorption. *Synth Met* 2022, 291: 117207.
[125] Li L, Liu G, Wei S*, et al.* Facile synthesis of nickel ferrite decorated carbon nanotube/cellulose aerogel for efficient electromagnetic wave absorption. *Small Methods* 2025, 9: 2402260.
[126] Guo X, Li H, Zhang Z*, et al.* In situ formation SiC nanowires on loofah sponge-derived porous carbon for efficient electromagnetic wave absorption. *Vacuum* 2025, 231: 113769.
[127] Shi R, Liu Z, Liu W*, et al.*, Preparation and electromagnetic wave absorption properties of N-doped SiC nanowires. *Materials*, 2023, 16: 5765.
[128] Zhong B, Zhang J, Wang H*, et al.* Fabrication of novel silicon carbide-based nanomaterials with unique hydrophobicity and microwave absorption property. *Int J Appl Ceram Technol* 2020, 17: 2598-2611.
[129] Zhao Y, Chua J W, Zhang Y*, et al.* Development of multiscale Fe/SiC-C fibrous composites for broadband electromagnetic and acoustic waves absorption. *Compos Part B-Eng* 2023, 250: 110454.
[130] Wang Y, Yuan X, Ping Z*, et al.* Structure engineering by Zn sublimation to enhance electromagnetic wave absorption performance of SiC/C nanofibers. *Ceram Int* 2025, 51: 24327-24333.
[131] Huo Y, Zhao K, Miao P*, et al.* Construction of tunable and high-efficiency microwave absorber enabled by growing flower-like TiO_2 on the surface of SiC/C nanofibers. *J Solid State Chem* 2021, 304: 122553.
[132] Wei J, Zhang Y, Li X*, et al.* Multifunctional flower-like Ni particles/silicon carbide nanowires for infrared radar compatible stealth performance. *J Colloid Interface Sci* 2023, 641: 414-427.
[133] Wang H, Hu Z, Su D. Construction of ZrC@SiC shell-core structure in SiBCN aerogel for enhanced thermal stability and thermal insulation. *Chem Eng J* 2024, 499: 156158.
[134] Liu J, Li H, Li H*, et al.* Deep-sea glass sponges-like hollow porous ceramic fiber aerogel: Fabrication, anti-shrinkage and thermal insulation. *Ceram Int* 2024, 50: 37714-37725.
[135] Dai D, Lan X, Wang Z. Hierarchical carbon fiber reinforced SiC/C aerogels with efficient electromagnetic wave absorption properties. *Compos Part B-Eng* 2023, 248: 110376.
[136] Liu H, Pengcheng H, Ying S*, et al.* High thermal insulation and high strength SiBCN@SiC double network ceramic composite aerogel. *Ceram Int* 2023, 49: 38351-38359.
[137] Zhang X, Zhang Y, Qu Y-N*, et al.* Three-dimensional reticulated, spongelike,

resilient aerogels assembled by SiC/Si_3N_4 nanowires. *Nano Lett* 2021, 21: 4167-4175.
[138] Cao Y, Wang L, Wang Z*, et al.* In-situ crosslinked SiC/PTFE/SiO_2 aerogel composite: a multifunctional material with synergistic hydrophobic, flame-retardant, thermal-insulating, and mechanical properties. *Ceram Int* 2025, 51: 51952-51962.
[139] Yan M, Cheng X, Gong L*, et al.* Flexible SiC nanowire/mullite fiber composite aerogel with adjustable strength based on micromechanical design. *Chem Eng J* 2023, 466: 143089.
[140] Yan M, Cheng X, Shi L*, et al.* Bioinspired SiC aerogels for super thermal insulation and adsorption with super-elasticity over 100,000 times compressions. *Chem Eng J* 2023, 455: 140616.
[141] Liu Q, Zhang L, Wan X*, et al.* Robust and thermostable silicon-based aerogels towards highly efficient thermal insulation and microwave absorption. *J Mater Sci Technol* 2026, 257: 222-232.
[142] An Z, Ye C, Zhang R*, et al.* Flexible and recoverable SiC nanofiber aerogels for electromagnetic wave absorption. *Ceram Int* 2019, 45: 22793-22801.
[143] Zhang J-X, Zhang J, Ye X-L*, et al.* Ultralight and compressive SiC nanowires aerogel for high-temperature thermal insulation. *Rare Metals* 2023, 42: 3354-3363.
[144] Jiang J, Yan L, Xue Y*, et al.* Lightweight and thermally insulating polymer-derived SiBCN/SiCnw ceramic aerogel with enhanced electromagnetic wave absorbing performance. *Chem Eng J* 2024, 482: 148878.
[145] Ji M, Hu C, Yan M*, et al.* Novel strategy of in-situ ceramization with SiO for preparing gradient ceramic coatings on low-density C/CA composites for non-ablative thermal protection. *Carbon* 2025, 244: 120707.
[146] Hu Y, Ni D, Chen B*, et al.* Ultra-light gradient C_f/(CrZrHfNbTa)C-SiC composite all-in-one strategy enables efficient thermal insulation, EMI shielding and ablation resistance. *J Mater Sci Technol* 2025, 235: 302-312.
[147] Mei H, Li H, Jin Z*, et al.* 3D-printed SiC lattices integrated with lightweight quartz fiber/silica aerogel sandwich structure for thermal protection system. *Chem Eng J* 2023, 454: 140408.
[148] Miao M, Yin J, Mao Z*, et al.* 3D-printed mullite-reinforced SiC-based aerogel composites. *Small* 2024, 20: 2401742.
[149] Guo J, Fu S, Deng Y*, et al.* Hypocrystalline ceramic aerogels for thermal insulation at extreme conditions. *Nature* 2022, 606: 909-916.
[150] Yan M, Zhang H, Fu Y*, et al.* Implementing an air suction effect induction strategy to create super thermally insulating and superelastic SiC aerogels. *Small* 2022, 18: 2201039.
[151] Liu M, Kong Y, Tang J*, et al.* Structure and performance evolutions with temperature, stress, and thermal-force coupling of the silica aerogel composite for suppressing thermal runaway propagation of LIBs. *Compos Part A-Appl S* 2025, 190: 108692.
[152] Lamy-Mendes A, Pontinha A D R, Alves P*, et al.* Progress in silica aerogel-containing materials for buildings' thermal insulation. *Constr Build Mater* 2021, 286: 122815.
[153] He S, Wu X, Zhang X*, et al.* Preparation and properties of thermal insulation

coating based on silica aerogel. *Energ Buildings* 2023, 298: 113556.
[154] Merillas B, Almeida C M R, Álvarez-Arenas T E G*, et al.* Enhanced thermal insulation performance of silica aerogel composites through infrared opacifier integration for high-temperature applications. *Compos Part C-Open* 2025, 16: 100573.
[155] Su L, Wang H, Jia S*, et al.* Highly stretchable, crack-insensitive and compressible ceramic aerogel. *ACS Nano* 2021, 15: 18354-18362.
[156] Li B, Yuan X, Gao Y*, et al.* A novel SiC nanowire aerogel consisted of ultra long SiC nanowires. *Mater Res Express* 2019, 6: 045030.
[157] Wu L, Guan S, Si W*, et al.* Rational design of high-efficiency interfacial solar evaporator with low evaporation enthalpy based on biomass-derived materials and silica aerogel. *Sep Purif Technol* 2025, 362: 131736.
[158] Ma Y, Tang G H, Hu Y. Modelling of hollow-fiber doping in silica aerogel composites for radiative and conductive insulation under high temperatures. *Appl Therm Eng* 2024, 254: 123917.
[159] Han L, Chen S, Li H*, et al.* Rapid and inexpensive synthesis of liter-scale SiC aerogels. *Nat Commun* 2024, 15: 6959.
[160] Wang Z, Hou Y, Hao H*, et al.* Scalable preparation of SiC@SiO_2 nanocable aerogels for broadband microwave absorption using low-cost carbon source. *Carbon* 2023, 211: 118092.
[161] Wang Z, Li R, Liu H*, et al.* Reduced graphene oxide/SiC nanowire composite aerogel prepared by a hydrothermal method with excellent thermal insulation performance and electromagnetic wave absorption performance. *Nanotechnology* 2024, 35: 135703.
[162] Quan J, Lan X, Lim G J H*, et al.* Hierarchical SiC fiber aerogel toward microwave attenuation and thermal insulation application. *J Alloy Compd* 2022, 911: 165097.
[163] Lan X, Hou Y, Dong X*, et al.* All-ceramic SiC aerogel for wide temperature range electromagnetic wave attenuation. *ACS Appl Mater Interfaces* 2022, 14: 15360-15369.
[164] Song M, Yan L, Li Y*, et al.* Thermal insulated C/SiC nanofiber aerogel with high thermal stability and superior electromagnetic wave absorption performance. *Ceram Int* 2024, 50: 28907-28917.
[165] Peng K, Chen H, Ye J*, et al.* Tailoring SiC nanowire aerogel in phase change composites with multiresponsive thermal energy storage. *ACS Appl Mater Interfaces* 2025, 17: 22871-22881.
[166] Chen B-Y, Chi C-C, Hsu W-K*, et al.* Synthesis of SiC/SiO_2 core-shell nanowires with good optical properties on Ni/SiO_2/Si substrate via ferrocene pyrolysis at low temperature. *Sci Rep* 2021, 11: 233.
[167] You X, Dai G, Deng R*, et al.* Fabrication of high-performance electromagnetic wave absorbing SiC composites reinforced by 3D printed carbon-based nanonetwork with Fe_3O_4 nanoparticles. *Addit Manuf* 2022, 55: 102855.
[168] Guo P, Su L, Jia S*, et al.* Strong SiC@Carbon nanowire aerogel metamaterials for efficient electromagnetic interference shielding. *Carbon* 2024, 229: 119492.
[169] Ye X, Chen Z, Zhang J*, et al.* Double network nested foam composites with tunable electromagnetic wave absorption performances. *Inorg Chem Front* 2019, 6: 1579-1586.

[170] Liang C, Wang Z. Eggplant-derived SiC aerogels with high-performance electromagnetic wave absorption and thermal insulation properties. *Chem Eng J* 2019, 373: 598-605.
[171] Cai Z, Su L, Wang H*, et al.* Hierarchically assembled carbon microtube@SiC nanowire/Ni nanoparticle aerogel for highly efficient electromagnetic wave absorption and multifunction. *Carbon* 2022, 191: 227-235.
[172] Chen Z, Wu Z, Su J*, et al.* Large-scale and low-cost synthesis of in situ generated SiC/C nano-composites from rice husks for advanced electromagnetic wave absorption applications. *Surf Coat Technol* 2021, 406: 126641.
[173] Liu D, Gui K, Wang M*, et al.* A novel hierarchical structure comprised of biomass-derived porous carbon and silicon carbide nanowires for highly efficient microwave absorption. *Ceram Int* 2022, 48: 16033-16041.
[174] Yang D, Dong S, Cui T*, et al.* Multifunctional carbon fiber reinforced C/SiOC aerogel composites for efficient electromagnetic wave absorption, thermal insulation, and flame retardancy. *Small* 2024, 20: 2308145.
[175] Fu M, Wang H, Xu L*, et al.* A compressible, highly elastic anisotropic SiC/SiO_2 composite aerogel for thermal-insulated building materials. *AIP Adv* 2025, 15.
[176] Yang Y, You X, Ouyang H*, et al.* Electromagnetic interference shielding properties of foamed SiC_{nws}/SiC composites reinforced by in-situ grown carbon nanofibers. *J Alloy Compd* 2024, 1008: 176641.
[177] Zhao C, Xia S, Lv Y*, et al.* Preparation of lightweight, honeycomb-like, wideband microwave absorbing SiC/C aerogels via carbothermal reduction. *J Eur Ceram Soc* 2025, 45: 117097.
[178] Liu D, Zhou Z, Wang Y*, et al.* Preparation and characterization of polymer-derived SiC ceramic aerogels toward excellent electromagnetic wave absorption properties. *J Mater Res Technol* 2022, 19: 507-519.
[179] Ye X, Chen Z, Ai S*, et al.* Novel three-dimensional SiC/melamine-derived carbon foam-reinforced SiO_2 aerogel composite with low dielectric loss and high impedance matching ratio. *ACS Sustain Chem Eng* 2019, 7: 2774-2783.
[180] Wang Y, Chen Z, Lu Y*, et al.* A review of application, modification, and prospect of melamine foam. *Nanotechnol Rev* 2023, 12.
[181] Su L, Wang H, Niu M*, et al.* Ultralight, recoverable, and high-temperature-resistant SiC nanowire aerogel. *ACS Nano* 2018, 12: 3103-3111.
[182] Ye X, Zhang H, Yu H*, et al.* Synergistic design of C/SiC@SiC aerogel for enhanced thermal insulation and electromagnetic wave absorption. *Ceram Int* 2024, 50: 43023-43031.
[183] Liang X, Shao Z, Wu Z*, et al.* Flexible SiC nanowire aerogel with excellent thermal insulation properties. *Ceram Int* 2022, 48: 22172-22178.
[184] Zhang X, Yu J, Zhao C*, et al.* Elastic SiC aerogel for thermal insulation: a systematic review. *Small* 2024, 20: 2311464.
[185] Su R, Liu P, Chen J*, et al.* Self-assembly and 3D printing of SiC_w@MXene/SiOC metastructure toward simultaneously excellent terahertz electromagnetic interference (EMI) shielding and electron-to-thermal conversion properties. *Adv Funct Mater* 2025, 35: 2500970.

[186] Luo J, Lv Z, Zhang L*, et al.* Modulation of dielectric behavior in ceramic-based materials for integrated electromagnetic waves absorption and thermal conduction. *Adv Funct Mater* 2025, 35: 2420086.
[187] Wang Z, Zhao H, Dai D*, et al.* Ultralight, tunable monolithic SiC aerogel for electromagnetic absorption with broad absorption band. *Ceram Int* 2022, 48: 26416-26424.
[188] Cheng Y, Tan M, Hu P*, et al.* Strong and thermostable SiC nanowires/graphene aerogel with enhanced hydrophobicity and electromagnetic wave absorption property. *Appl Surf Sci* 2018, 448: 138-144.
[189] Li B, Mao B, Wang X*, et al.* Novel, hierarchical SiC nanowire-reinforced SiC/carbon foam composites: lightweight, ultrathin, and highly efficient microwave absorbers. *J Alloy Compd* 2020, 829: 154609.
[190] Li Y, Xing Y, Yang T*, et al.* SiC particles/$Ti_3C_2T_x$ aerogel with tunable electromagnetic absorption performance in Ku band. *Surf Interfaces* 2024, 49: 104384.
[191] Tang C, Yang J, Deng W*, et al.* Design of ultralight and stable $Ti_3C_2T_x/SiC_{nw}$ hybrid aerogel with hierarchical structure and heterogeneous interface for electromagnetic wave absorption. *Carbon* 2024, 218: 118697.
[192] Zhou Y, Wu M, Jiang J*, et al.* Self-assembling SiC nanoflakes/MXenes composites embedded in polymers towards efficient electromagnetic wave attenuation. *Appl Surf Sci* 2022, 574: 151463.
[193] Huang X, Guan J, Feng Y*, et al.* Mn and O defect modulation in birnessite creates multiplicate polyhedra to improve dielectric and magnetic losses. *Cell Rep Phys Sci* 2025, 6: 102350.
[194] Zhou Y, Zhao B, Yu G*, et al.* Dynamic regulation in electromagnetic shielding properties of three-dimensional elastic magnetic Ni aerogels. *Chem Eng J* 2025, 525: 170666.
[195] He J, Zhang Y, Zhou K*, et al.* A hierarchical SiC_{nw}@SiC aerogel decorated with Ni-capped carbon nanotubes toward high-performance electromagnetic wave absorber. *Results Phys* 2023, 49: 106500.
[196] Zhang Y, He J, Fu Z*, et al.* Lightweight porous NiCo-SiC aerogel with synergistically dielectric and magnetic losses to enhance electromagnetic wave absorption performances. *J Alloy Compd* 2022, 926: 166758.
[197] Lei C, Wang L, Huang X*, et al.* SiC aerogel composites modified by carbon nanotubes encapsulated with Fe nanoparticles for microwave absorption. *J Alloy Compd* 2024, 1005: 175910.
[198] Zhang Q, You X, Tian L*, et al.* Fabrication and efficient electromagnetic waves attenuation of three-dimensional porous reduced graphene oxide/boron nitride/silicon carbide hierarchical structures. *J Mater Sci Technol* 2023, 155: 192-201.
[199] Dai D, Lan X, Wu L*, et al.* Designed fabrication of lightweight SiC/Si_3N_4 aerogels for enhanced electromagnetic wave absorption and thermal insulation. *J Alloy Compd* 2022, 901: 163651.
[200] Xie M, Wu X, Liu J*, et al.* In-situ synthesis and textural evolution of the novel carbonaceous SiC/mullite aerogel via polymer-derived ceramics route. *Ceram Int* 2017, 43: 9896-9905.

[201] Du B, Wang S, Guo L*, et al.* Design and fabrication of $(Hf_{0.25}Zr_{0.25}Ta_{0.25}Nb_{0.25})C$-SiC ceramics with improved microwave absorbing properties via PDC route. *J Adv Ceram* 2025, 14: 9220998.
[202] Zhao P Y, Peng H L, Cai B*, et al.* Mechanism decoupling of impedance matching and attenuation enhancement via spatial distribution of loading components. *Adv Funct Mater* 2025, 36: e18479.
[203] Zeng X, Deng X, Yu Z*, et al.* Evolution of Fe single atom in SiOC ceramic fibers and their high-temperature and ultrathin electromagnetic wave absorption. *Adv Mater* 2026, 38: e21533.
[204] Hu F, Zhang P, Ding P*, et al.* Magnetic-dielectric synergy in one-dimensional metal heterostructures for enhanced low-frequency microwave absorption. *Nano-Micro Lett* 2026, 18: 155.
[205] Zhang Y, Hu P, Zhao P Y*, et al.* Phosphorus vacancy-induced built-in electric field for electromagnetic properties modulation. *Adv Sci* 2025, 12: e02857.
[206] Zhang J, Li Q, Jia Y*, et al.* Effects of microstructure evolution of SiC/SiOC aerogel on electromagnetic wave absorption and infrared stealth properties. *Ceram Int* 2025, 51: 7437-7450.
[207] Ren X, Huang L, Yuan H*, et al.* Sodium alginate derived SiC-carbon composite aerogel for effective microwave absorption. *J Magn Magn Mater* 2024, 596: 171970.
[208] Duan L-q, Xu C, Dai X-q*, et al.* Nano-porous carbon wrapped SiC nanowires with tunable dielectric properties for electromagnetic applications. *Mater Des* 2020, 192: 108738.
[209] Hao H, Wang Z, Zhang Y*, et al.* Multifunctional SiC nanowire aerogels with efficient electromagnetic wave absorption for applications in complex environments. *Carbon* 2024, 230: 119653.
[210] Li X, Lei W, Wei J*, et al.* Synthesis and broadband electromagnetic wave absorption for lightweight porous SiC/Si_3N_4 composite nanowires. *Ceram Int* 2023, 49: 37746-37757.
[211] Zhou J, Wei B, Yao Z*, et al.* Preparation of hollow SiC spheres with biological template and research on its wave absorption properties. *J Alloy Compd* 2020, 819: 153021.
[212] Ye X, Chen Z, Li M*, et al.* Hollow SiC foam with a double interconnected network for superior microwave absorption ability. *J Alloy Compd* 2020, 817: 153276.
[213] Wang Q, Wang G, Lu X*, et al.* Prediction of broadband and highly-efficient electromagnetic wave-absorbing $SiC@SiO_2$ nanowire aerogel by genetic algorithm. *ACS Appl Mater Interfaces* 2024, 16: 57972-57980.
[214] Pan D, Yang G, Abo-Dief H M*, et al.* Vertically aligned silicon carbide nanowires/boron nitride cellulose aerogel networks enhanced thermal conductivity and electromagnetic absorbing of epoxy composites. *Nano-Micro Lett* 2022, 14: 118.
[215] Yan M, Pan Y, He P*, et al.* Flexible hierarchical hollow SiC/SiO_x micro/nanofiber sponges for broadband electromagnetic wave absorption. *Adv Fiber Mater* 2025, 7: 853-863.
[216] Jiang Y, Chen Y, Liu Y-J*, et al.* Lightweight spongy bone-like graphene@SiC aerogel composites for high-performance microwave absorption. *Chem Eng J* 2018,

337: 522-531.
[217] Cai Z, Su L, Wang H*, et al.* Alternating multilayered Si_3N_4/SiC aerogels for broadband and high-temperature electromagnetic wave absorption up to 1000°C. *ACS Appl Mater Interfaces* 2021, 13: 16704-16712.
[218] Wang L, Cai Z, Su L*, et al.* Bifunctional SiC/Si_3N_4 aerogel for highly efficient electromagnetic wave absorption and thermal insulation. *J Adv Ceram* 2023, 12: 309-320.
[219] Hou Y, Wang J, Chen B*, et al.* Self-standing MOF-derived Co@SiC_{nw} nanocomposite aerogel with a hierarchical microstructure for highly effective and wideband electromagnetic attenuation. *ACS Appl Mater Interfaces* 2025, 17: 28503-28513.
[220] Niu M, Wang H, Su L*, et al.* Lightweight and resilient SiOC/SiC foam with efficient electromagnetic wave absorption and high-temperature stability. *J Am Ceram Soc* 2023, 106: 3078-3088.
[221] Wu Z, Huang J, Tan Y*, et al.* Transition/rare earth metal co-modified SiC for low-frequency and high-temperature electromagnetic response. *J Adv Ceram* 2025, 14: 9221164.
[222] Huang X, Cong W, Chen Y*, et al.* Conductive network reconstruction driven by carbonization: enabling the transition of hard carbon from electromagnetic wave absorption to shielding. *Carbon* 2026, 251: 121326.
[223] Zhang H, Meng F, Gao Y*, et al.* Hierarchical ZrB_2@SiC_{nw} nanocomposite aerogel via 0D/1D/3D dimensionality expansion strategy: towards full X-band microwave absorption at high temperature. *Compos Part B-Eng* 2025, 306: 112806.
[224] Liu C, He T, Hu C*, et al.* The optimized design of sandwich structured SiO_2/C@SiC/SiO_2 composites through numerical simulation for temperature-resistant radar and infrared compatible stealth. *Adv Funct Mater* 2025, 35: 2416108.
[225] Wang H, Sun J, Gao Y*, et al.* A radar-infrared compatible stealth metamaterial with high-temperature resistance. *J Phys D: Appl Phys* 2025, 58: 355301.
[226] Zhang B, Tong Z, Wang X*, et al.* Zirconium-modified hierarchical porous SiC-based nanofibrous aerogel with efficient electromagnetic waves absorption and thermal insulation properties. *J Eur Ceram Soc* 2025, 45: 116808.
[227] Xia Y, Yang Z, Zhang Z*, et al.* Heterogeneous multi-scale ceramic aerogel with infrared/radar compatible stealth capability at high temperatures. *Compos Part B-Eng* 2025, 307: 112901.
[228] Mao B, Xia X, Qin R*, et al.* Microstructure evolution and microwave absorbing properties of novel double-layered SiC reinforced SiO_2 aerogel. *J Alloy Compd* 2023, 936: 168314.
[229] Wang Z, Liu J, Hao H*, et al.* Microwave absorption enhancement by SiC nanowire aerogels through heat treatment-based oxidation modulation. *Carbon* 2024, 217: 118622.
[230] Song L, Wang L, Chen Y*, et al.* Engineered core-shell SiC@SiO_2 nanofibers for enhanced electromagnetic wave absorption performance. *Small* 2024, 20: 2407563.
[231] Xiang Z, Wang Y, Yin X*, et al.* Microwave absorption performance of porous heterogeneous SiC/SiO_2 microspheres. *Chem Eng J* 2023, 451: 138742.

[232] Liu J, Wang Z, Hao H*, et al.* Nanopore construction in SiC aerogels for continuous dual-peak electromagnetic wave absorption with full Ku-band coverage. *Carbon* 2024, 224: 119096.
[233] Liang C, Wang Z, Wu L*, et al.* Light and strong hierarchical porous SiC foam for efficient electromagnetic interference shielding and thermal insulation at elevated temperatures. *ACS Appl Mater Interfaces* 2017, 9: 29950-29957.